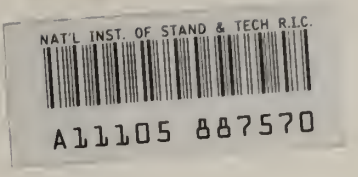

NBSIR 83-2718

A Model of Multiroom Fire Spread

U.S. DEPARTMENT OF COMMERCE
National Bureau of Standards
National Engineering Labora ory
Center for Fire Research
Washington, DC 20234

August 1983

U.S. DEPARTMENT OF COMMERCE
NATIONAL BUREAU OF STANDARDS

NBSIR 83-2718

A MODEL OF MULTIROOM FIRE SPREAD

Takeyoshi Tanaka

Guest Worker
Building Research Institute
Japan

U.S. DEPARTMENT OF COMMERCE
National Bureau of Standards
National Engineering Laboratory
Center for Fire Research
Washington, DC 20234

August 1983

U.S. DEPARTMENT OF COMMERCE, Malcolm Baldrige, *Secretary*
NATIONAL BUREAU OF STANDARDS, Ernest Ambler, *Director*

TABLE OF CONTENTS

LIST OF FIGURES

LIST OF TABLES

LIST OF SYMBOLS

A	Area
a	Thermal diffusivity
AA	Air flow rate through an opening (air to air layer)
AS	Air flow rate through an opening (air to smoke layer)
B	Width
C	Specific heat
C_p	Specific heat at constant pressure
D	Depth of room
F	Configuration factor
f_v	Volume fraction of soot
g	Gravitational acceleration
H	Height
ΔH	Enthalpy difference, Heat of combustion
h	Specific enthalphy
k	Thermal conductivity, Absorption coefficient
L	Heat of gasification, Length
ℓ	Length, Thickness
M	Molecular weight
m	Water content
$\dot{m}$	Mass rate
P	Total pressure, Relative pressure, Partial pressure
Q	Heat per unit mass
$\dot{Q}$	Heat Rate
$\dot{q}''$	Heat Flux
R	Gas constant
r	Specific heat ratio ($r=C_p/C_v$)
s	Mass fraction of original fuel that turns into soot
SS	Hot gas flow rate through an opening (smoke to smoke layer)
SA	Hot gas flow rate through an opening (smoke to air layer)
SA'	Flow rate of gas that enters upper layer through doorjet
SE	Air entrainment rate into a doorjet
T	Temperature
t	Time
u	Specific internal energy
V	Volume
W	Mass fraction of species
w	Mass fraction of original fuel that turns into residual char
X_n	Neutral zone height
x	Distance from the surface of a wall
Y	Mass fraction of a species
Z	Layer thickness, Vertical distance
z	Vertical distance
α	Flow coefficient
γ	Mass generation rate of a species
ε	Emissivity
η	Fraction of carbon that turns into CO
ν	Kinematic viscosity, Stoichiometric coefficient

ρ	Density
σ	Stefan-Boltzmann constant
λ	Fraction of air flow AS that mixes into upper layer

Superscripts

*	complete combustion
$(\dot{})$	per unit time
"	per unit area
$(\hat{})$	vector
n	iteration number
a	air, ambient
p	pyrolyzed fuel

Subscripts

a	lower layer, air, ambient, actual
as	between lower and upper layer
C	convection, carbon
d	discontinuity, decomposition
e	entrainment, effective
ex	experiment
f	fuel
G	hot gas, hot gas layer
g	gas, gasification
H	hydrogen
i	room number, in
j	room number, time step
ij	from i to j, between i and j
k	opening number
l	sill, species
m	mean
O	oxygen
o	original, reference state, out
p	pyrolysis, pyrolyzed fuel, constant pressure
pr	products
R	room
r	reference state
S	upper layer, soot
SS	between the two upper layers
v	vaporization, constant volume
W	wall

A MODEL OF MULTIROOM FIRE SPREAD

T. Tanaka

ABSTRACT

Some refinements have been made on a multi-room fire spread model. The primary improvements are: (a) that a model on excess fuel burning in arbitrary room has been introduced; (b) that a model for the prediction of gas concentrations has been added; (c) that subroutine ABSORB, which was created by Modak, has been introduced to predict the upper layer emissivity; (d) that a new fire plume model developed by McCaffrey has been included to remove the inaccuracy and inplausibility of a vertical point heat source plume model; and (e) that the code has been revised so that it can deal with tall buildings with somewhat less computer memory size.

Also, some sample calculation results with the new code and a documentation of the code have been included.

I. INTRODUCTION

When the previous model for hot gas flow in multi-room structure was devised [10,11], an intention was to use the model to predict or analyze inter-room fire spread in small buildings, particularly residential structures. The previous model had assumed that the combustion of input fuel is completed within the room of origin. But it was soon realized that in order to raise the temperature of an adjacent room high enough to ignite the combustible material in there, quite a big fire is needed in the room of origin. In such cases, it is no longer plausible to assume complete consumption of input fuel within the room of origin and the burning should be sensitive to the air supply into the room. In fact, it is a well known fact that the pyrolysis rate of

an intense fire is almost controlled by the air inflow rate alone. As can be seen when one observes window flames brought forth by a big fire, excess fuel burns outside the room of origin. If this occurs in a room of the structure, it will affect even the flow in the structure, not to speak of the temperature elevation. Therefore, emphasis was placed on the pursuit of modeling the transport of excess fuel in a structure in refining the model. This appears to be indispensable for the purpose of predicting fire spread.

Additional refinements have also been made. First, species conservation equations were introduced to predict the concentration of soot and primary gases in any room in a structure under the condition that their generation rate due to the burning of unit mass of fuel can be specified. The importance of the prediction of the species concentrations in fire growth lies in that it relates the prediction of the burning rate of gaseous fuel and the estimation of the upper layer emissivity. With these predictions, subroutine ABSORB, which is an excellent outcome of Modak's work [7], conveniently provides the layer emissivity. With regard to element process modeling, a major refinement is the replacement of the point heat source fire plume in the former model with McCaffrey's most recent model [6]. Generally, a point heat source model does not provide a good prediction for a fire plume in a room in which our primary concern is the region significantly close to fire base, even if some manipulations such as a virtual point heat source are introduced. McCaffrey's model has an advantage in that it is based on accurate measurements in this region and it accounts for the size effect of the source.

It might seem to some readers somewhat redundant that this paper has duplicated, to some extent, the same discussion already stated in the previous papers [10,11]. This was done partly because it was suspected that some readers may feel it is more convenient to be able to read this article without frequent reference back to the previous papers, and partly because the layer equations were derived in a somewhat different way as based on the derivations of Baum [3], Quintiere [5] and Zukoski [5].

Finally, a documentation of the code, which was revised so that it can deal with tall buildings with less computer memory capacity, has been attached in this paper.

Before proceeding into the details of this report several points should be emphasized about its general applicability and accuracy. Primarily the model and computer code should serve as a framework for multi-room fire growth predictions. But some elements of the model are not accurately and completely formulated because of our current lack of understanding. Therefore these elements or their omission will contribute to uncertainties in the overall results. The weakest element is the transport of gases in vertical shafts. The treatment of this phenomenon as an effective plume in a tall room is not valid once the plume interacts with the walls or with structural elements in the shaft. Pressure drops due to walls and obstacles in vertical shafts and corridors are not taken into account. These phenomena must be accurately modeled before the code is sound. Also the effect of vertical mixing so as to heat the lower layer must be better understood, and the assumption of a cold lower layer must be quantitatively examined. Finally the fuel supply rate by the fire must be specified in this model. For building design purposes that may be sufficient; however, a model for combustion efficiency will be needed to predict multi-room fire growth. Despite these limitations, thoughtful use of this code should give insight into a variety of fire growth problems.

II. THEORY

1. Conceptual Model

The problem considered here is the motion and state of the hot gas, which is generated by a fire and considered to be responsible both for human casualties and property damage.

A fire usually starts from the ignition of a combustible item in a room. The ignited item emits pyrolyzed fuel into the air, which, by reacting with the oxygen, releases heat and combustion products. The heat and combustion products are pumped up through the buoyant plume induced above the fire, entraining more air as they rise to form a hot gas layer of mixture of the combustion products and fresh air under the ceiling. This layer may contain even unburnt fuel as well when the fuel input rate is so large that it cannot be completely burnt with the oxygen available in the room.

At the very early stage immediately after the start of a fire, the hot gas layer will descend simply pushing only air out of the room openings because the gas at high temperature expands to displace the cold air that has occupied the upper part of the room. But before long, the hot gas layer will drop below the soffits of the openings, which of course allows the hot gas to flow out of the room of origin into the adjacent rooms to form other hot gas layers there. Those upper layers will behave basically in the same way as that of the room of origin, thereby reproducing the similar filling process and spreading the hot gas throughout the structure. Thus, a fire in an arbitrary structure at an arbitrary elapsed time after ignition may be illustrated as in Fig. 2.1. In such situations, the behavior of the fire depends on the conditions of the structure and the fire source. The mathematical zone modeling approach will be a useful approach for predicting the fire behavior in such complex structures and can be a viable alternative to expensive and time consuming full scale fire experiments. To formulate

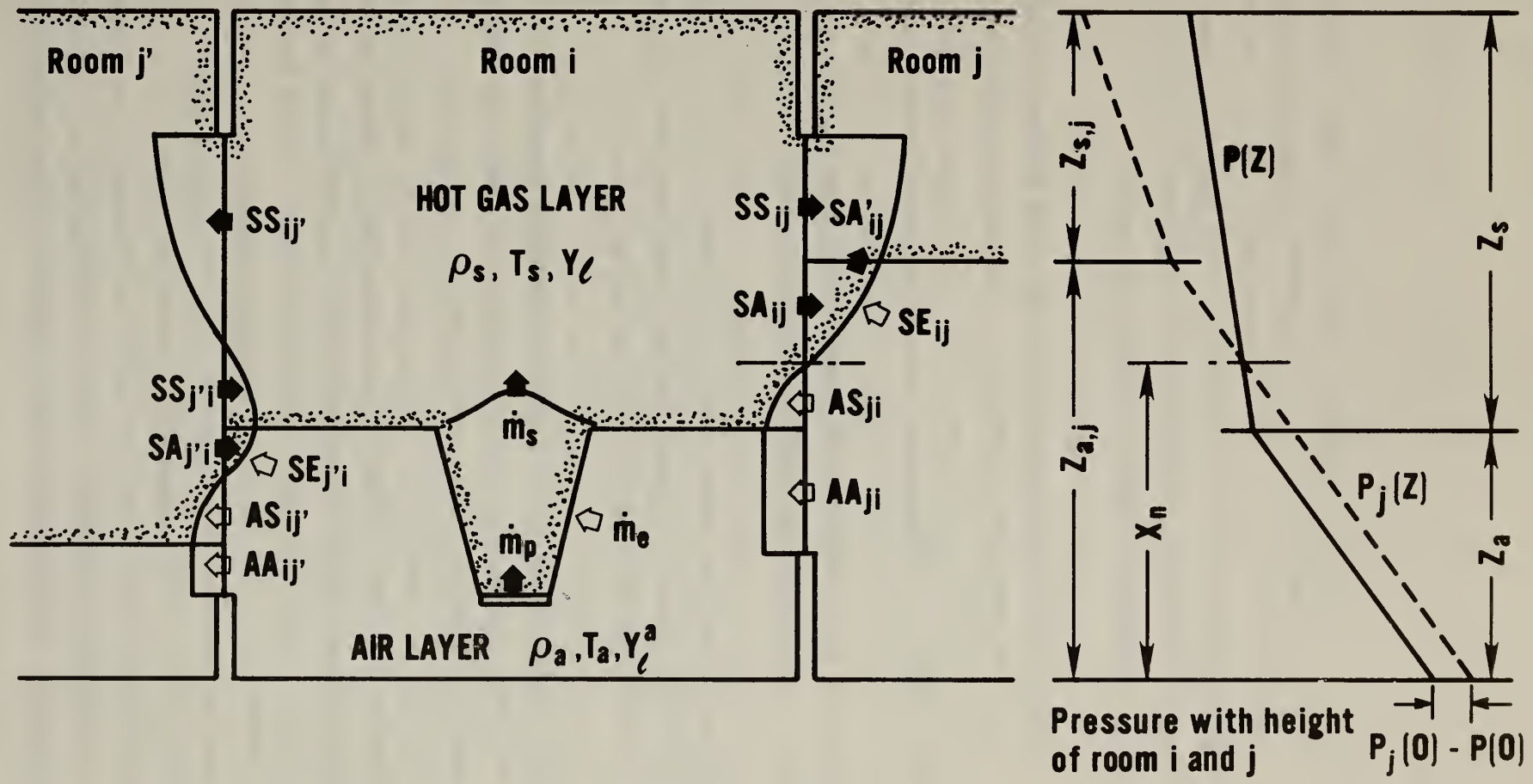

Fig. 2.1 Schematic Diagram of the Model

a model for this purpose, however, we will be obliged to significantly simplify the problem since the true phenomena involved in fire are quite complicated while our current knowledge is still limited. Among many simplifications and approximations which need to be made in zone modeling, the foliowing assumptions are considered to be the most essential and commonly used in current zone models.

(a) In any room which hot gas enters, two well defined stratified layers, i.e., a hot gas upper layer and a cool layer, are formed.

(b) Each layer is homogeneous in any physical or chemical property.

Besides these basic assumptions common in any zone model, the following are also considered to be essential in this model.

(c) The upper and the lower layer are divided by a flat discontinuity such that there is no mass and heat transport due to interface mixing unless through a fire plume or door jet.

(d) Both radiative and convective heat transfer between any lower layer and the surfaces that are in contact with the layer, namely floor and lower part of walls, are ignored.

These two assumptions (c) and (d) are introduced to keep the lower layer temperature constant so that many processes, particularly the formulation of flow rate through openings, can be simplified. These assumptions are not as essential as the first two given in (a) and (b), which are generally used in zone modeling approach. In fact, some models for single room fires have already relaxed the latter two restrictions and allowed interface mixing between the two layers and thermally non-transparent lower layer [1,2]. Some more elaborate formulation of door flow rate and advances in our understanding of layer interface mixing may make it

possible to handle the transitional lower layer even for multiroom structure cases. On the contrary, we will hardly be able to remove the former assumption without complicating the zone modeling approach. Indeed, various advantages given by zone model approach would disappear at the same time when the assumptions (a) and (b) are abandoned.

In Fig. 2.1, ρ_s, T_s and Y_ℓ, respectively, stand for the density, the absolute temperature and the mass fraction of species ℓ in the upper layer of room i, and ρ_a, T_a and Y_ℓ^a stand for those of the lower layer where subscript i is omitted from every symbol for brevity. Z_s and Z_a are the thicknesses of the upper and the lower layers respectively. Both SS_{ij} and SA_{ij} denote the rate of hot gas flow from room i to j through k-th opening between room i and j, while AS_{ij} and AA_{ij} likewise denote the rate of air flow where k is omitted again for brevity. It might be confusing that each of the hot gas and the air flow has been given two symbols, but each symbol corresponds to each of the characteristic opening pressure difference profiles as may be suggested in Fig. 1 and will be discussed later. A temporarily convenient interpretation of these symbols may be that SS_{ij} and SA_{ij} are the hot gas flow above and below the discontinuity height of room j, i.e., $Z_{a,j}$, respectively, and so forth with the air flow AS_{ij} and AA_{ij}. It will be obvious in Fig. 1 that when seen as a doorjet, SA can entrain the air from the lower layer as it travels to the upper layer while SS can only entrain the hot gas from the upper layer thereby contributing no additional mass to the layer. The sum of SA and the rate of air entrained into it is termed SA'. The mass loss rate of fuel and the air entrainment rate into the fire plume are termed $\dot{m}_p$ and $\dot{m}_e$ respectively and $\dot{m}_s (= \dot{m}_p + \dot{m}_e)$ denotes the total rate of gas that enters the upper layer through the fire plume.

2. Zone Model Equations

2.1 Zone Conservation Equations

In formulating the physical basis of the mathematical model, we have to consider first the conservation equations for mass, species and

energy of the layers. To do this, however, it is necessary to introduce some additional assumptions regarding the flows through openings, which have been termed as SS, SA, AS and AA in Fig. 2.1. The assumptions introduced here are as follows:

(a) Hot gas flows SS and SA enter into the upper layer.

(b) A part of air flow AS enters into lower layer and the rest of AS flows into the upper layer.

(c) Air flow AA enters into the lower layer.

The assumption (a) may not always be self-evident in some conceivable situations in fire: the hot gas may not be able to enter the hot upper layer when the temperature of the latter is much higher than that of the former. But it is very difficult to abandon the assumption (a) because if we introduce another layer or let the hot gas go into the lower layer to cope with this problem, we are forced to sacrifice the advantages given by the set of assumptions in section 1. The assumption (b) is introduced to take account of tall shafts filled with a thick hot gas layer. The air flow AS may no longer be able to penetrate the upper layer when it has to travel a long distance as it is heated by mixing on its way to the lower layer.

Then, under these assumptions, the layer conservation equations can be written down for any room i on any floor of a multiroom structure as follows:

Overall mass conservation of upper layer

$$\frac{d}{dt}(\rho_s A_R Z_S) = \Sigma \left\{ (SS_{ji} + SA_{ji} + \lambda AS_{ji}) - (SS_{ij} + SA_{ij}) \right\} + \dot{m}_p + \dot{m}_e \qquad (2.1)$$

Overall mass conservation of lower layer

$$\frac{d}{dt}(\rho_a A_R Z_a) = \Sigma \left\{ (1 - \lambda) AS_{ji} + AA_{ji} - (AS_{ij} + AA_{ij}) - (SA'_{ji} - SA_{ji}) \right\} - \dot{m}_e \qquad (2.2)$$

where A_R denotes the area of room i, and $\lambda (0 \leq \lambda \leq 1)$ is the fraction of air flow AS that mixes into upper layer; so $\lambda = 1$ indicates that the air flow AS wholly mixes into the layer and no portion of it reaches the lower layer, while $\lambda = 0$ indicates the opposite. The summation Σ is taken with respect to j and k, i.e., with respect to every opening between the room i and the adjacent spaces, although subscript k has been omitted from the flow terms for brevity. Needless to say, Eqs. (2.1) and (2.2) hold for any room in the structure. The fire plume flows $\dot{m}_p$ and $\dot{m}_e$, can simply be given zero values for rooms other than the room of origin.

Mass conservation of species in upper layer

$$\frac{d}{dt}(Y_\ell \rho_s A_R Z_s) = Y_\ell^P \dot{m}_p + Y_\ell^a \dot{m}_e + \gamma_\ell \dot{m}_b + \Sigma \left\{ Y_{\ell,j}(SS_{ji} + SA_{ji}) - Y_\ell (SS_{ij} + SA_{ij}) + Y_\ell^a (SA'_{ji} - SA_{ji}) + Y^a_{\ell,j} \lambda AS_{ji} \right\} \qquad (2.3)$$

where Y_ℓ^P and Y_ℓ^a stand for the mass fractions of species ℓ in the gasified fuel and air respectively, ℓ represents either fuel gas, O_2, CO_2, CO, H_2O or N_2 and $\dot{m}_b$ is the burning rate of gasified fuel, which is controlled either by fuel or oxygen supply rate, and γ_ℓ is the mass generation rate of species ℓ due to the burning of unit mass of gasified fuel, i.e.,

$$\gamma_\ell = (\nu''_\ell - \nu'_\ell) M_\ell / \nu_f M_f$$

where ν''_ℓ and ν'_ℓ are stoichiometric coefficients of species ℓ in product and reactant system respectively.

Energy conservation of upper layer

$$\frac{d}{dt}\left\{\left(\sum_{\ell} u_{\ell} Y_{\ell} \rho_s\right) A_R Z_s\right\} + P\frac{d(A_R Z_s)}{dt} = \dot{q}_{net} + \left(\sum_{\ell} h_{\ell}^{P} Y_{\ell}^{P}\right)\dot{m}_p + \left(\sum_{\ell} h_{\ell}^{a} Y_{\ell}^{a}\right)\dot{m}_e$$

$$+ \sum\left\{\left(\sum_{\ell} h_{\ell,j} Y_{\ell,j}\right)(SS_{ji} + SA_{ji}) - \left(\sum_{\ell} h_{\ell} Y_{\ell}\right)(SS_{ij} + SA_{ij})\right.$$

$$\left. + \left(\sum_{\ell} h_{\ell}^{a} Y_{\ell}^{a}\right)(SA'_{ji} - SA_{ji}) + \left(\sum_{\ell} h_{\ell,j}^{a} Y_{\ell,j}^{a}\right)\lambda AS_{ji}\right\} \qquad (2.4)$$

Energy conservation of lower layer

$$\frac{d}{dt}\left\{\left(\sum_{\ell} u_{\ell}^{a} Y_{\ell}^{a} \rho_a\right) A_R Z_a\right\} + P\frac{d(A_R Z_a)}{dt} = -\left(\sum_{\ell} h_{\ell}^{a} Y_{\ell}^{a}\right)\dot{m}_e$$

$$+ \sum\left[\left(\sum_{\ell} h_{\ell,j}^{a} Y_{\ell,j}^{a}\right)\left\{(1-\lambda)AS_{ji} + AA_{ji}\right\} - (\ell h_{\ell}^{a} Y_{\ell}^{a})(AS_{ij} + AA_{ij})\right.$$

$$\left. - (\ell h_{\ell}^{a} Y_{\ell}^{a})(SA'_{ji} - SA_{ji})\right] \qquad (2.5)$$

where u, h and p respectively stand for specific internal energy and enthalpy and absolute pressure; $\dot{q}_{net}$ is the net heat added to the hot layer by radiative and convective heat transfer. These Eqs. (2.4) and (2.5) are an expression of the first law of thermodynamics applied to this particular case.

The pressure in Eqs. (2.4) and (2.5) may vary with height due to hydrostatic effect as

$$p_z = p_o - \int_o^z \rho g dz$$

where subscripts o and z represent a reference level and height from the level. However, hydrostatic term of this equation is so small compared with p_o that in many practical conditions it can be reasonably considered as negligible. So the pressure P in the above equations can be regarded constant with height.

Finally, with the same consideration regarding the pressure, the equation of state may be written as

Equation of State

$$P = \rho_s T_s R = \rho_a T_a R \tag{2.6}$$

where gas constant R is assumed the same regardless the difference of composition among the upper and lower layers.

2.2 Practical Equations for Layer Properties

It is useful to transform the above equations so that the layer properties with which we are more familiar are given explicitly. Let's restrict the consideration here to multiroom structures such that the area of any room does not vary with height, unlike such a structure as an aircraft fuselage, then A_R can be regarded as independent with time too.

First, noting that left hand side of Eq. (2.3) can be expanded as

$$\frac{d}{dt}\left(Y_\ell \rho_s A_R Z_s\right) = \rho_s A_R Z_s \frac{dY_\ell}{dt} + Y_\ell \frac{d}{dt}\left(\rho_s A_R Z_s\right)$$

subtracting Eq. (2.1) multiplied by $Y_{\ell,i}$ from Eq. (2.3) yields:

$$\rho_s A_R Z_s \frac{dY_\ell}{dt} = \left(Y_\ell^p - Y_\ell\right) \dot{m}_p + \left(Y_\ell^a - Y_\ell\right) \dot{m}_e + \gamma_\ell \dot{m}_b$$

$$+ \Sigma \left\{ \left(Y_{\ell,j} - Y_\ell\right) \left(SS_{ji} + SA_{ji}\right) + \left(Y_\ell^a - Y_\ell\right) \left(SA'_{ji} - SA_{ji}\right) \right.$$

$$\left. + \left(Y_{\ell,j}^a - Y_\ell\right) \lambda AS_{ji} \right\} \qquad (2.7)$$

Next, noting the following relations

$$u_\ell Y_\ell \rho_s = h_\ell Y_\ell \rho_s - P_\ell \qquad (2.8)$$

where

$$P_\ell \equiv \left(\frac{\rho_s Y_\ell}{M_\ell}\right) RT_s$$

substituting Eq. (2.8) into the left side of Eq. (2.4) yields

$$\frac{d}{dt}\left\{\left(\sum_{\ell} u_{\ell} Y_{\ell} \rho_s\right) A_R Z_s\right\} + P \frac{d(A_R Z_s)}{dt}$$

$$= \frac{d}{dt}\left\{\left(\sum_{\ell} h_{\ell} Y_{\ell} \rho_s\right) A_R Z_s\right\} - \frac{d}{dt}\left\{\left(\Sigma P_{\ell}\right) A_R Z_s\right\} + P \frac{d(A_R Z_s)}{dt}$$

$$= \sum_{\ell} \left\{h_{\ell} \frac{d}{dt} (Y_{\ell} \rho_s A_R Z_s)\right\} + \sum_{\ell} \left\{(Y_{\ell} \rho_s A_R Z_s) \frac{dh_{\ell}}{dt}\right\} - \frac{d}{dt} (P A_R Z_s)$$

where use was made of $\sum_{\ell} P_{\ell} = P$. Then calculation of Eq. (2.4) - $\sum_{\ell} \left\{h_{\ell} \times \text{Eq. (2.3)}\right\}$ gives

$$\sum_{\ell} \left(Y_{\ell} \rho_s A_R Z_s \frac{dh_{\ell}}{dt}\right) - A_R Z_s \frac{dp}{dt} = \dot{q}_{net} - \left(\sum_{\ell} h_{\ell} \gamma_{\ell}\right) \dot{m}_b$$

$$+ \left\{\sum_{\ell} \left(h_{\ell}^{p} - h_{\ell}\right) Y_{\ell}^{p}\right\} \dot{m}_p + \left\{\sum_{\ell} \left(h_{\ell}^{a} - h_{\ell}\right) Y_{\ell}^{a}\right\} \dot{m}_e$$

$$+ \left[\sum \left\{\sum_{\ell} (h_{\ell,j} - h_{\ell}) Y_{\ell,j}\right\} (SS_{ji} + SA_{ji}) + \left\{\sum_{\ell} \left(h_{\ell}^{a} - h_{\ell}\right) Y_{\ell}^{a}\right\}\right.$$

$$\left. (SA'_{ji} - SA_{ji}) + \left\{\sum_{\ell} \left(h_{\ell,j}^{a} - h_{\ell}\right) Y_{\ell,j}^{a}\right\} \lambda AS_{ji}\right] \qquad (2.12')$$

The term $-\sum_{\ell} h_{\ell} \gamma_{\ell}$, which has shown up in the right hand side, is the heat of reaction of the gasified fuel ΔH, as shown below.

$$-\sum_{\ell} h_{\ell} \gamma_{\ell} = \sum_{\ell} h_{\ell} \nu'_{\ell} M_{\ell} / \nu_f M_f - \sum_{\ell} h_{\ell} \nu''_{\ell} M_{\ell} / \nu_f M_f$$

$$= h_{reactant} - h_{product}$$

$$= \Delta H \qquad (2.9)$$

When no phase change is involved, the enthalpy state equation can be written as

$$h_\ell = h_{r,\ell} + C_{p,\ell} (T - T_r) \tag{2.10}$$

where subscript r represents a reference state. Since N_2 is always considered to be the most dominant composition of both hot gas and air, it will probably be reasonable to assume the specific heat of any gas as constant regardless the change of mass fractions of species, i.e.,

$$\sum_\ell C_{p,\ell} Y_\ell = C_p \text{ (constant)} \tag{2.11}$$

Substituting Eqs. (2.9) - (2.10) into Eq. (2.12') yields

$$C_p \rho_s A_R Z_s \frac{dT_s}{dt} - A_R Z_s \frac{dP}{dt} = \dot{q}_{net} + \Delta H \cdot \dot{m}_b + C_p (T_p - T_s)\dot{m}_p$$

$$+ C_p (T_a - T_s)\dot{m}_e + C_p \Sigma \left\{ (T_{s,j} - T_s)(SS_{ji} + SA_{ji}) \right.$$

$$\left. + (T_a - T_s)(SA'_{ji} - SA_{ji}) + (T_{a,j} - T_s)\lambda AS_{ji} \right\} \tag{2.12}$$

Following the similar procedure as above, for the lower layer, we obtain:

$$C_p \rho_a A_R Z_a \frac{dT_a}{dt} - A_R Z_a \frac{dP}{dt} = C_p \Sigma (T_{a,j} - T_a) \left\{ (1 - \lambda) AS_{ji} + AA_{ji} \right\} \tag{2.13}$$

The equation for the layer thickness can be obtained as follows:

From the equation of state,

$$\frac{d\rho_s}{dt} = \frac{1}{RT_s}\frac{dP}{dt} - \frac{\rho_s}{T_s}\frac{dT_s}{dt}$$

Substituting this relation into Eq. (2.1) yields

$$\frac{d}{dt}(\rho_s A_R Z_s) = \rho_s A_R \frac{dZ_s}{dt} + A_R Z_s \frac{dp}{dt}$$

$$= \rho_s A_R \frac{dZ_s}{dt} + A_R Z_s \frac{1}{RT_s} \cdot \frac{dP}{dt} - A_R Z_s \frac{\rho_s}{T_s} \cdot \frac{dT_s}{dt}$$

Noting this and adding Eq. (2.1) multiplied by $C_p T_s$ to Eq. (2.12) gives

$$C_p \rho_s T_s A_R \frac{dZ_s}{dt} + A_R Z_s \left(\frac{C_p}{R} - 1\right)\frac{dP}{dt} = \dot{q}_{net} + \Delta H \cdot \dot{m}_b + C_p T_p \dot{m}_p$$

$$+ C_p T_a \dot{m}_e + C_p \Sigma \left\{ T_{s,j}(SS_{ji} + SA_{ji}) - T_s(SS_{ij} + SA_{ij}) \right.$$

$$\left. + T_a(SA'_{ji} - SA_{ji}) + T_{a,j}\, \lambda AS_{ji} \right\} \qquad (2.14)$$

Finally, let's obtain the equation for pressure. Multiplying Eq. (2.1) by $C_p T_s$ and adding the result to Eq. (2.12) yields

$$C_p \rho_s A_R Z_s \frac{dT_s}{dt} - A_R Z_s \frac{dP}{dt} + C_p T_s \frac{d}{dt}(\rho_s A_R Z_s) = \dot{q}_{net} + \Delta H \cdot \dot{m}_b$$

$$+ C_p T_p \dot{m}_p + C_p T_a \dot{m}_e + C_p \Sigma \left\{ T_{s,j}(SS_{ji} + SA_{ji}) \right.$$

$$\left. - T_s(SS_{ij} + SA_{ij}) + T_a(SA'_{ji} - SA_{ji}) + T_{a,j}\, \lambda AS_{ji} \right\}$$

The left hand side of the above equations turns out as

$$C_p\rho_s A_R Z_s \frac{dT_s}{dt} - A_R Z_s \frac{dP}{dt} + C_p T_s \frac{d}{dt}(\rho_s A_R Z_s)$$

$$= A_R Z_s C_p \left(\rho_s \frac{dT_s}{dt} + T_s \frac{d\rho_s}{dt}\right) + C_p \rho_s T_s \frac{d(A_R Z_s)}{dt} - A_R Z_s \frac{dP}{dt}$$

$$= A_R Z_s \frac{C_p}{R} \frac{dP}{dt} + \frac{C_p P}{R} \frac{d(A_R Z_s)}{dt} - A_R Z_s \frac{dP}{dt}$$

Therefore, it follows that

$$A_R Z_s \frac{C_p}{R} \frac{dP}{dt} + \frac{C_p P}{R} \frac{d(A_R Z_s)}{dt} - A_R Z_s \frac{dP}{dt} = \dot{q}_{net} + \Delta H \cdot \dot{m}_b + C_p T_p \dot{m}_p$$

$$+ C_p T_a \dot{m}_e + C_p \Sigma \left\{ T_{s,j}(SS_{ji} + SA_{ji}) - T_s(SS_{ij} + SA_{ij}) \right.$$

$$\left. + T_a(SA'_{ji} - SA_{ji}) + T_{a,j}\, \lambda AS_{ji} \right\} \qquad (2.15a)$$

Likewise, a similar equation can be obtained for the lower layer by adding Eq. (2.2) multiplied by $C_p T_a$ to Eq. (2.13) as follows

$$A_R Z_a \frac{C_p}{R} \frac{dP}{dt} + \frac{C_p P}{R} \frac{d(A_R Z_a)}{dt} - A_R Z_a \frac{dP}{dt} = -C_p T_a \dot{m}_e$$

$$+ C_p \Sigma \left[T_{a,j} \left\{ (1 - \lambda) AS_{ji} + AA_{ji} \right\} - T_a(AS_{ij} + AA_{ij}) \right.$$

$$\left. - T_a(SA'_{ji} - SA_{ji}) \right] \qquad (2.15b)$$

Then, noting that $Z_s + Z_a = H_R$ (i-th room height:constant) and adding Eqs. (2.15a) and (2.15b) yields

$$A_R H_R \frac{1}{r-1} \frac{dP}{dt} = \dot{q}_{net} + \Delta H \cdot \dot{m}_b + C_p T_p \dot{m}_p + C_p \Sigma \left\{ T_{s,j}(SS_{ji} + SA_{ji}) \right.$$

$$\left. - T_s(SS_{ij} + SA_{ij}) + T_{a,j}(AS_{ji} + AA_{ji}) - T_a(AS_{ij} + AA_{ij}) \right\} \tag{2.15}$$

where use was made of the relations $C_p - C_v = R$ and $r = C_p/C_v$.

Eq. (2.15) could be substituted into Eqs. (2.12) through (2.14) to eliminate the pressure term dP/dt in those equations, and a careful numerical computation with small time step might be executed for the set of ordinary differential equations (2.7) and (2.12) through (2.15) to predict the fire under any opening condition. This kind of calculation method may have an advantage when we deal with fires in buildings with very many rooms or very narrow openings. But unfortunately we have not yet established this method, therefore let us consider whether the pressure term can be neglected in practical fire conditions.

It is implied by Eq. (2.15) that the pressure in a room will rise proportionately to the net rate of the heat and fuel added if there is no opening, in other words no outflow; however, usual rooms of a building are not sealed so tightly that an extremely high pressure can be attained [3],[4]. As the pressure rises, the larger outflow will be induced through the openings to reduce the pressure elevation. It may be useful to think

of a single compartment with only one opening for simplicity. Then, Eq. (2.15) may be written approximately as follows

$$A_R H_R \left(\frac{1}{r-1}\right) \frac{dP^*}{dt} = \dot{q}_{net} + \Delta H \cdot \dot{m}_b - C_p T A_e \sqrt{2\rho P^*}$$

where fuel input is neglected. P^* represents $P^* = P_i - P_r$, i.e., pressure difference between indoor and outdoor, and A_e is the effective opening area. This equation implies that the larger heat input, the smaller room volume and the smaller opening area, the larger the rate of pressure elevation, and

$$p^* = \frac{1}{2\rho} \left(\frac{\dot{q}_{net} + \Delta H \cdot \dot{m}_b}{C_p T A_e} \right)^2$$

is the maximum pressure attainable. So the larger opening area causes a smaller maximum pressure. In addition to the leaky condition of usual rooms, there is another reason which may make the pressure unable to rise very high. In the case of usual fires, in which heat is generated by the burning of gaseous fuel emitted into rooms at a moderate rate, vitiation of oxygen and heat transfer to the walls will soon decrease the net rate of heat addition to the rooms if the openings are narrow.

The above discussion has not yet justified ignoring the pressure terms in general but at least has implied that in most of usual cases pressure elevation is not significant due to the presence of sizable openings or oxygen vitiation. So hereafter the consideration is restricted to the condition where the following assumptions hold:

(a) dP/dt term in every equation can be ignored.

(b) Pressure elevation is so small that the thermodynamic pressure in the equation of state can be replaced with a constant reference pressure.

With these assumptions, the temperature and the density of any lower layer are kept constant all the time if they are the same as those of ambience at the beginning, in other words Eq. (2.13) is no longer needed. The former assumption (a) implies that the pressures are determined such that the right hand side of Eq. (2.15), which are actually simultaneous algebraic equations for the pressures of the rooms, is balanced [5].

As a result of the neglecting of the pressure terms in the preceding equations, the final equations can be summarized as follows:

Temperature

$$\frac{dT_s}{dt} = \frac{T_s}{C_p \rho_a T_a A_R Z_s} \left\{ \dot{q}_{net} + \Delta H \cdot \dot{m}_b + C_p (T_p - T_s) \dot{m}_p + C_p (T_a - T_s) (\dot{m}_s - \dot{m}_p) \right\} + \frac{T_s}{\rho_a T_a A_R Z_s} \Sigma \left\{ (T_{s,j} - T_s)(SS_{ji} + SA_{ji}) + (T_a - T_s)(SA'_{ji} - SA_{ji} + \lambda AS_{ji}) \right\} \quad (2.16)$$

Species

$$\frac{dY_\ell}{dt} = \frac{T_s}{\rho_a T_a A_R Z_s} \left\{ \gamma_\ell \dot{m}_b + \left(Y_\ell^p - Y_\ell \right) \dot{m}_p + \left(Y_\ell^a - Y_\ell \right) (\dot{m}_s - \dot{m}_p) \right\}$$

$$+ \frac{T_s}{\rho_a T_a A_R Z_s} \Sigma \left\{ (Y_{\ell,j} - Y_\ell)(SS_{ji} + SA_{ji}) + \left(Y_\ell^a - Y_\ell \right) \right.$$

$$\left. (SA'_{ji} - SA_{ji} + \lambda AS_{ji}) \right\} \qquad (2.17)$$

Thickness

$$\frac{dZ_s}{dt} = \frac{1}{C_p \rho_a T_a A_R} \left\{ \dot{q}_{net} + \Delta H \cdot \dot{m}_b + C_p T_p \dot{m}_p + C_p T_a (\dot{m}_s - \dot{m}_p) \right\}$$

$$+ \frac{1}{\rho_a T_a A_R} \Sigma \left\{ T_{s,j}(SS_{ji} + SA_{ji}) - T_s(SS_{ij} + SA_{ij}) \right.$$

$$\left. + T_a(SA'_{ji} - SA_{ji} + \lambda AS_{ji}) \right\} \qquad (2.18)$$

Pressure

$$\frac{\dot{q}_{net} + \Delta H \cdot \dot{m}_b}{C_p T_a} + \frac{T_p}{T_a} \dot{m}_p + \frac{1}{T_a} \Sigma \left\{ T_{s,j}(SS_{ji} + SA_{ji}) - T_s(SS_{ij} + SA_{ij}) \right\}$$

$$+ \Sigma \left\{ (AS_{ji} + AA_{ji}) - (AS_{ij} + AA_{ij}) \right\} = 0 \qquad (2.19)$$

The equations for the flow terms (SS_{ji}, SA_{ji}, etc.) are taken from Ref. [10] and presented in Table 3.1.

3. Component Process Modeling

The ordinary differential equations for the layer properties, i.e., Eqs. (2.16) - (2.19), have to be complemented with the equations for the component processes involved in fire, such as heat and species generation due to the burning of fuel, radiative and convective heat transfer, fire plume and doorjet entrainment, flows through openings. This section will be devoted to the modeling of these processes.

3.1 Combustion Model

Generally, it is difficult to model the combustion of actual fire with high accuracy. One of the difficulties may arise from the fact that the fuels and the rooms involved in fire are not ideal from the viewpoint of combustion. We have to estimate the heat release of real fire based on calorimetry of the fuel, however, unlike calorimeters or well-designed combusters, fuels in real fire may contain water, leave residual char and discharge smoke and carbon monoxide. Also attention has to be paid to fuel rich combustion, where all the fuel is not burnt within the room of origin because of insufficient inflow air. In such cases, particularly in case the fuel is from a pyrolyzed solid combustible, it is not easy to estimate the heat release due to the burning of the fuel, since we do not have enough calorimetry data for such fuels.

To deal with this problem, let's introduce a simple steady state combustion model as shown in Fig. 3.1, where original fuel that contains

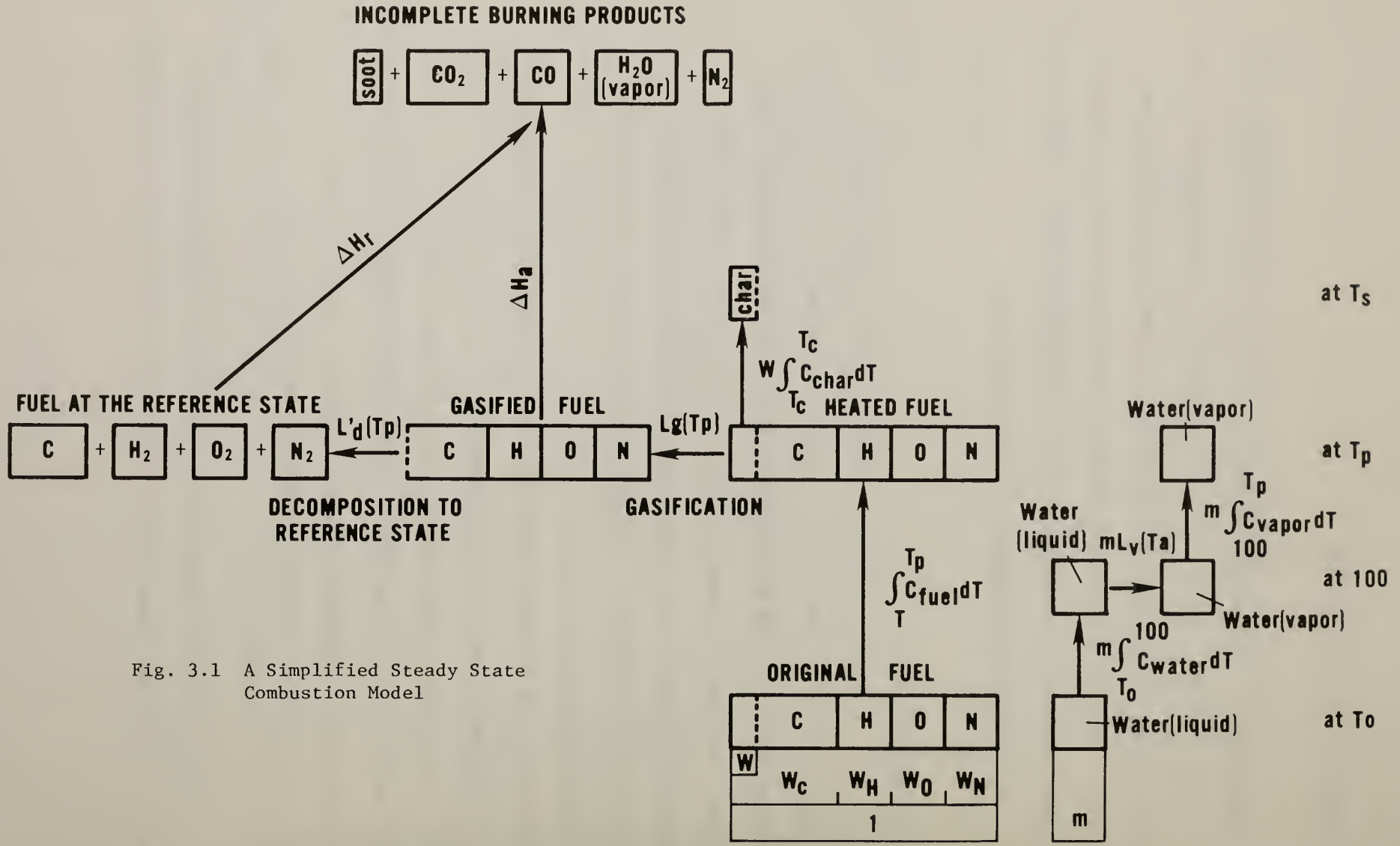

Fig. 3.1 A Simplified Steady State Combustion Model

water is being steadily heated to its decomposition temperature, gasified leaving some portion of it as residual char, and incompletely burnt producing soot and CO as well as CO_2 and H_2O. In this diagram, it is the fuel at the gasified state that may be transported outside the room of origin and burnt. The reference state of the fuel which is inserted in the diagram is not a state which real processes pass through, but the virtual state where the heat of combustion can be theoretically calculated using the heat of formation of species.

In the following, the various quantities which need be inputed into the layer equations will be derived based on the combustion model in Fig. 3.1 or the thermodynamically equivalent model in Fig. 3.2.

(i) Heat required for unit mass loss

Let's consider of the pyrolysis of the fuel composed of 1 kg of dry fuel and m kg of water, namely 1 + m kg in total. In this case, 1 - w kg of gasified portion of the fuel and m kg of water vapor are counted as the mass loss. Hence

$$\text{mass loss} = 1 - w + m \tag{3.1}$$

where w stands for charring ratio. On the other hand, the heat required to give this amount of mass loss is, as indicated by Fig. 3.2

$$\int_{T_o}^{T_p} (1 - w)C_{fuel}dt + \int_{T_o}^{T_p} mC_{vapor}dT + \int_{T_o}^{T_s} wC_{char}dT$$

$$+ L_g(T_o) + mL_v(T_o)$$

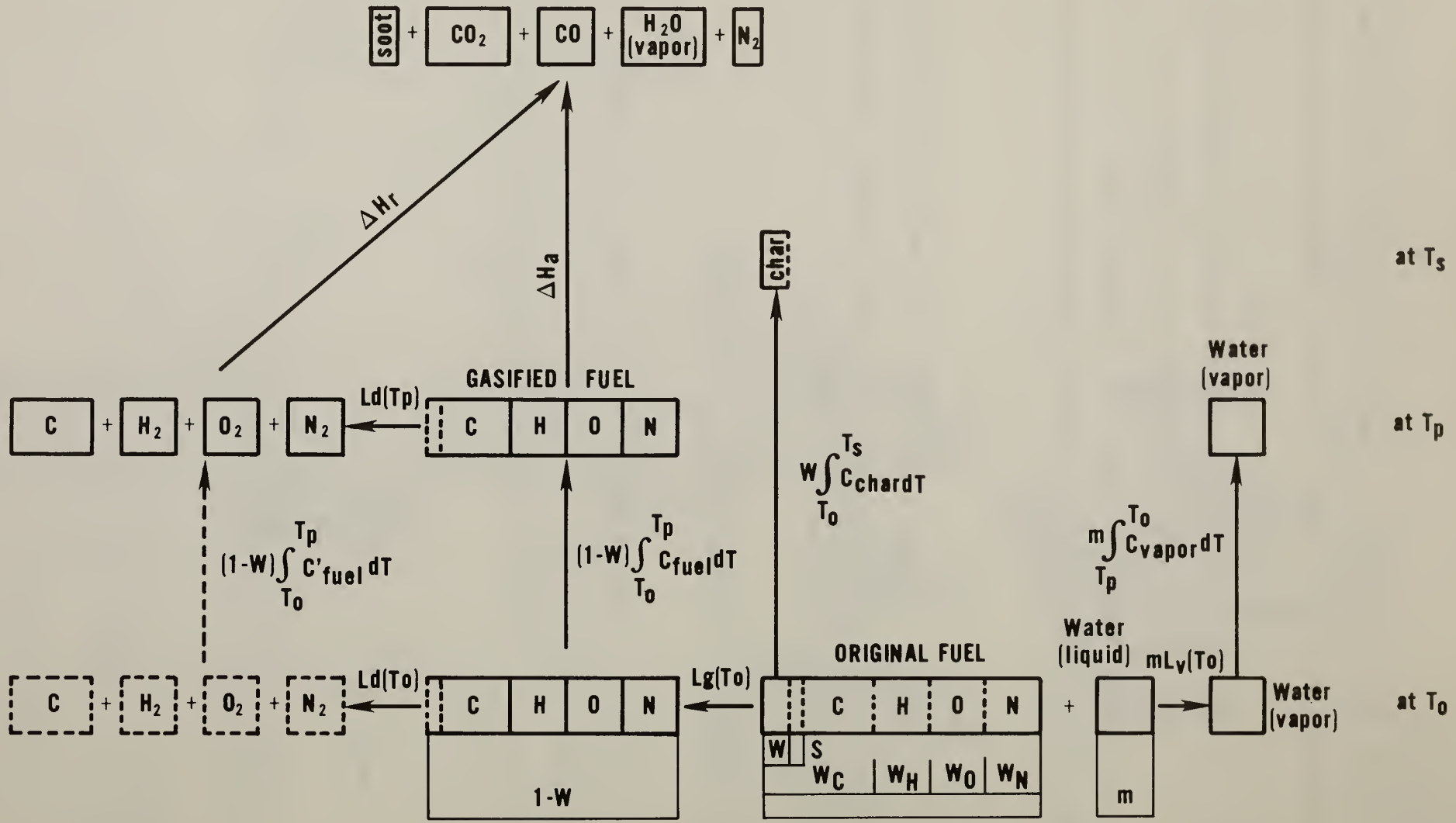

Fig. 3.2 An Alternative Diagram of the Combustion Model

where C_{fuel}, C_{vapor} and C_{char} respectively stand for the specific heat of original fuel, water vapor and residual char; T_o, T_p and T_s are respectively the temperature of a reference, pyrolysis and residual char, and $L_g(T_o)$ and $L_v(T_o)$ are the latent heat of gasification of the fuel and water at a reference temperature respectively.

The heat required per unit mass loss of the fuel Q_p is given as

$$Q_p = \frac{\int_{T_o}^{T_p} \left\{ (1 - w)C_{fuel} + mC_{vapor} \right\} dT + w \int_{T_o}^{T_s} C_{char} dT + L_g(T_o) + mL_v(T_o)}{1 - w + m} \tag{3.2}$$

Although the specific heat of the mixture of the fuel and vapor may change with the value of w and m, it will be assumed for consistency with the layer energy equations that this is constant and the same as the C_p in the layer equations, i.e.,

$$\frac{(1 - w)C_{fuel} + mC_{vapor}}{1 - w + m} = C_p \tag{3.3}$$

then, Q_p becomes

$$Q_p = C_p(T_p - T_o) + \frac{w \int_{T_o}^{T_s} C_{char} dT + L_g(T_o) + mL_v(T_o)}{1 - w + m} \tag{3.4}$$

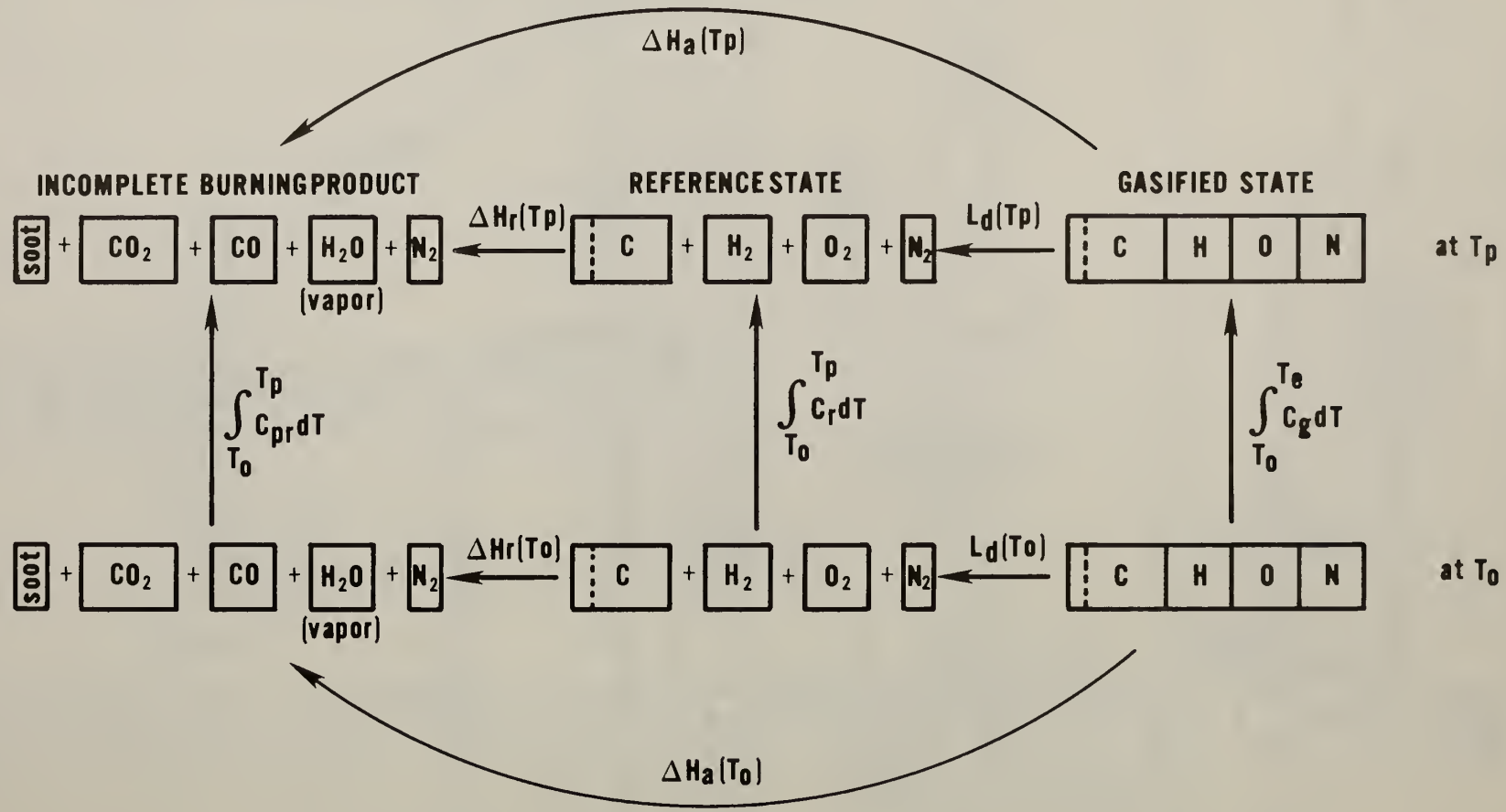

Fig. 3.3 Relation Between the Heat of Combustion of Gasified Fuel at Different Temperatures

Eq. (3.4) may be interpreted as the heat transferred to the fuel from the surroundings, e.g., the flame, the upper layer, which is obtained from the viewpoint of fuel pyrolysis.

(ii) Heat release due to incomplete burning of gasified fuel

What we need to obtain as the heat of combustion should be the enthalpy difference between the combustion products and the fuel of the gasified state at T_e as was indicated in Eq. (2.9). Let's consider here of the combustion of unit mass of the gasified fuel. Looking into the diagram in Fig. 3.3 reveals that the following thermodynamic relations hold.

$$\Delta H_a(T_p) + \int_{T_o}^{T_p} C_g dT = \Delta H_a(T_o) + \int_{T_o}^{T_p} C_{pr} dT \tag{3.5}$$

$$\Delta H_a(T_o) = \Delta H_r(T_o) + L_d(T_o) \tag{3.6}$$

where C_g and C_{pr} are specific heats of gasified fuel and product. From Eq. (3.5)

$$-\Delta H_a(T_p) = -\Delta H_a(T_o) + \int_{T_o}^{T_p} (C_g - C_{pr}) dT \tag{3.7}$$

The left side of Eq. (3.7) is the heat of combustion at temperature T_p, which we are seeking, and Eq. (3.7) implies that

$$-\Delta H_a(T_p) = -\Delta H_a(T_o) \tag{3.8}$$

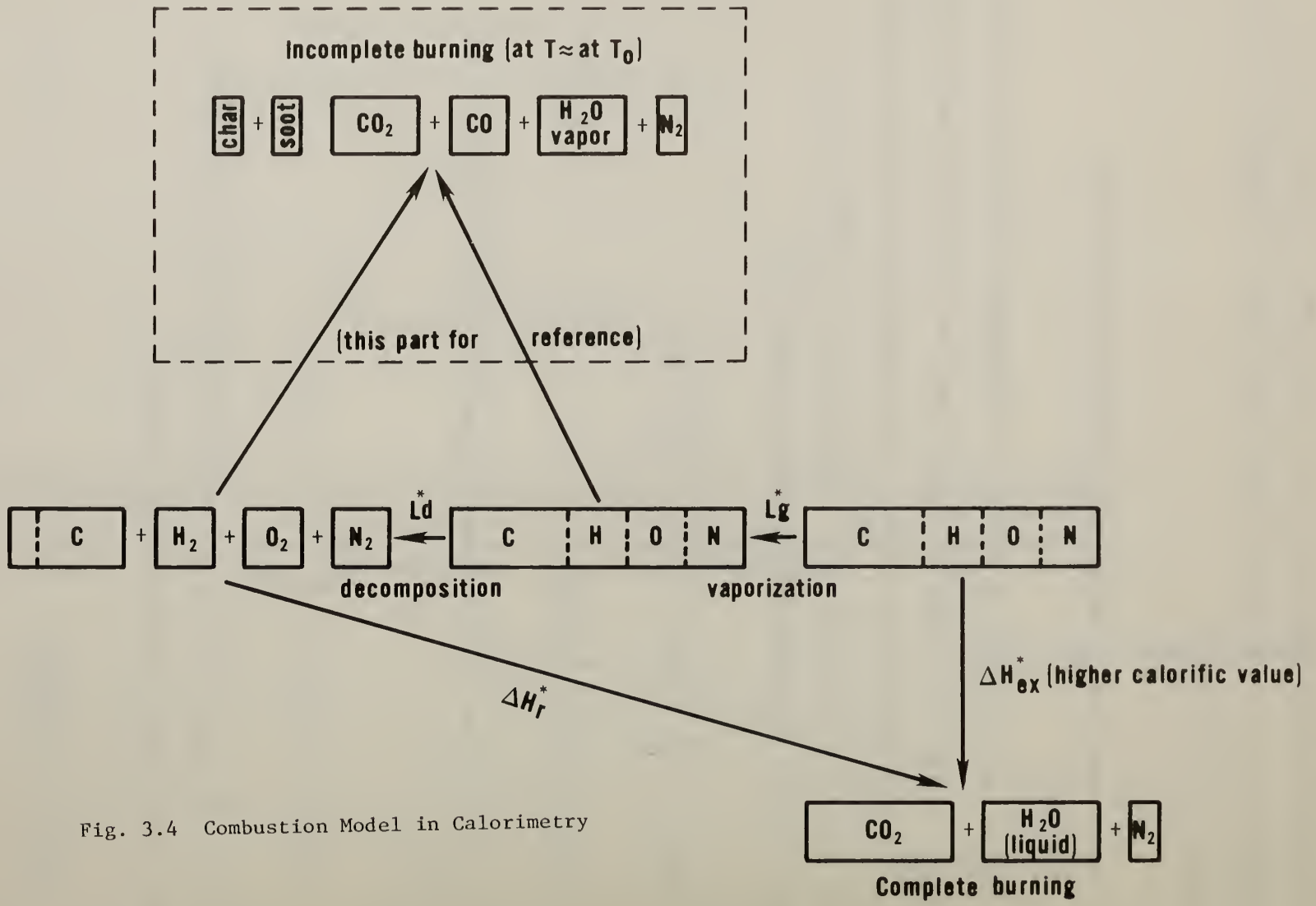

Fig. 3.4 Combustion Model in Calorimetry

if the second term in the right hand side of Eq. (3.7), which is trivial compared with the first term, is neglected.

From Eq. (3.6) and (3.8) it is obvious that

$$-\Delta H_a(T_p) = -\Delta H_r(T_o) - L_d(T_o) \tag{3.9}$$

In this equation, $-\Delta H_r(T_o)$ can be calculated using data for heat of formation of the species involved, but $L_d(T_o)$ cannot easily be obtained. So let's consider the complete burning process as in calorimetry. Looking into the diagram in Fig. 3.4, we see the following relation

$$L_d^*(T_o) = -\Delta H_r^*(T_o) - \{-\Delta H_{ex}^*(T_o)\} - L_g^*(T_o) \tag{3.10}$$

where $-\Delta H_{ex}^*(T_o)$ is the so-called heat of combustion, which has been measured for many existing materials (oxygen bomb) calorimetry, and $-\Delta H_r^*(T_o)$ is the enthalpy difference between the reference state fuel and the complete combustion products, which is again calculable as is $-\Delta H_r(T_o)$. It is not always easy to obtain the gasification energy $L_g^*(T_o)$ unless the fuel is gas or liquid. Many attempts have been made to obtain $L_g^*(T_o)$ for solid fuels, but the measured values have ranged widely, probably because of the difficulty in the measurement and the dependence of volatile composition on heating condition. Theoretically, the range of $L_g^*(T_o)$ should be

$$0 \leq L_g^*(T_o) \leq -\Delta H_r^*(T_o) - \{-\Delta H_{ex}^*(T_o)\}$$

Although the attempts to provide the data of $L_g^*(T_o)$ have not yet been so successful in case of solid materials, let's dare to assume that the data is available.

The next bold assumption is to regard that the $L_d^*(T_o)$ in Eq. (3.10) is the same as $L_d(T_o)$ in (3.9), despite the likelihood that the composition of the gasified fuel is inevitably different between the real and ideal burning because of the residual char in the real case. This assumption and the combination of Eq. (3.9) and (3.10) yields

$$-\Delta H_a(T_p) = -\Delta H_r(T_o)-\{(-\Delta H_r^*(T_o))-(-\Delta H_{ex}^*(T_o))-L_g^*(T_o)\} \tag{3.11}$$

Accordingly, it follows that the heat of reaction of the gasified fuel can be estimated, in principle, by using experimentally or theoretically available data.

In calculating $-\Delta H_r^*(T_o)$ for a specific fuel, it is necessary that the chemical composition of the fuel is known. Usually, this is given in terms of chemical formula or weight fraction of chemical species, but the latter is more widely available. So, let's start from the weight fraction. If ν_1, ν_2, ν_3 and ν_4 are the molecular number of the species C, H, O and N in unit mass of the fuel respectively, they are given from their weight fractions as follows:

$$\nu_1 = \frac{W_C}{12 \times 10^{-3}}\ ,\ \nu_2 = \frac{W_H}{1 \times 10^{-3}}\ ,\ \nu_3 = \frac{W_O}{16 \times 10^{-3}}\ ,\ \nu_4 = \frac{W_N}{14 \times 10^{-3}} \tag{3.12}$$

where W_C, W_H, W_O and W_N represents the weight fraction of C, H, O and N respectively.

The chemical equation for the complete combustion of this fuel may be written as:

$$C_{\nu_1}H_{\nu_2}O_{\nu_3}N_{\nu_4} + (\nu_1 + \frac{\nu_2}{4} - \frac{\nu_3}{2})O_2 + (L_g^* + L_d^*)$$

$$\rightarrow \nu_1 C + \frac{\nu_2}{2} H_2 + \frac{\nu_3}{2} O_2 + \frac{\nu_4}{2} N_2 + (\nu_1 + \frac{\nu_2}{4} - \frac{\nu_3}{2}) O_2$$

$$\rightarrow \nu_1 CO_2 + \frac{\nu_2}{2} H_2O + \frac{\nu_4}{2} N_2 + (-\Delta H_r^*) \qquad (3.13)$$

and $-\Delta H_r^*(T_o)$ is given as

$$-\Delta H_r^*(T_o) = 97.6\ \nu_1 + 68.3\ \frac{\nu_2}{2}$$

$$= 97.6\ \frac{W_C}{12} \times 10^3 + 68.3\ \frac{W_H}{2} \times 10^3 \qquad \text{(kcal/kg)} \qquad (3.14)$$

Next, let's calculate $-\Delta H_r(T_o)$. Various species may be discharged in case of incomplete burning, however, it is assumed here that only soot, CO_2, CO, H_2O and N_2 are involved in the product. The gasified fuel no longer has the same chemical composition as the original fuel since a part of carbon has been left as solid char through the gasification process. The new weight fractions of C, H, O and N should be $(W_C - w)/(1-w)$, $W_H/(1-w)$, $W_O/(1-w)$ and $W_N/(1-w)$ respectively. Let $s/(1-w)$ be the fraction of the carbon that turns into soot and η be the fraction among the rest of the carbon, i.e., $(W_C - w-s)/(1-w)$, that turns into CO. Then, the chemical equation for the incomplete burning can be expressed as

$$C_{\nu'_1} H_{\nu'_2} O_{\nu'_3} N_{\nu'_4} + \left(\nu'''_1 - \frac{\nu''''_1}{2} + \frac{\nu'_2}{4} - \frac{\nu'_3}{2}\right) O_2 + (L_g + L_d)$$

$$\rightarrow \nu''_1 [\text{soot}] + \nu'''_1 C + \frac{\nu'_2}{2} H_2 + \frac{\nu'_3}{2} O_2 + \frac{\nu'_4}{2} N_2 + \left(\nu'''_1 - \frac{\nu''''_1}{2} + \frac{\nu'_2}{4} - \frac{\nu'_3}{2}\right) O_2$$

$$\rightarrow \nu''_1 [\text{soot}] + (\nu'''_1 - \nu''''_1) CO_2 + \nu''''_1 CO + \frac{\nu'_2}{2} H_2O + \frac{\nu'_4}{2} N_2 + (-\Delta H_r) \qquad (3.15)$$

where the stoichiometric coefficients are:

$$\nu'_1 = \frac{W_C - w}{1 - w} \cdot \frac{1}{12 \times 10^{-3}}, \quad \nu''_1 = \frac{s}{1 - w} \cdot \frac{1}{12 \times 10^{-3}}$$

$$\nu'''_1 = \frac{W_C - w - s}{1 - w} \cdot \frac{1}{12 \times 10^{-3}}, \quad \nu''''_1 = \eta \nu'''_1 \qquad (3.16)$$

$$\nu'_2 = \frac{W_H}{1-w} \cdot \frac{1}{1 \times 10^{-3}}, \quad \nu'_3 = \frac{W_O}{1-w} \cdot \frac{1}{16 \times 10^{-3}}, \quad \nu'_4 = \frac{W_N}{1-w} \cdot \frac{1}{14 \times 10^{-3}}$$

Then, $-\Delta H_r$ can be given as follows:

$$-\Delta H_r = 97.6 \left(\nu'''_1 - \nu''''_1\right) + 27.6\, \nu''''_1 + 57.6 \frac{\nu'_2}{2}$$

$$= \{97.6(1-\eta) + 27.6\eta\} \frac{W_C - w - s}{1-w} \cdot \frac{1}{12 \times 10^{-3}} + 57.6 \quad \frac{1}{2} \cdot \frac{W_H}{1-w} \cdot \frac{1}{1 \times 10^{-3}} \qquad (3.17)$$

Substituting thus obtained Eqs. (3.14) and (3.17) together with experimentally obtained $-\Delta H^*_{ex}(T_o)$ and $L^*_g(T_o)$ into Eq. (3.11) yields the value of $-\Delta H_a(T_p)$.

(iii) Mass generation rate of species

The mass generation rate of each species due to the burning described in the chemical Eq. (3.15) is given by applying the following general formula:

$$\gamma_\ell = (\nu_\ell'' - \nu_\ell')M_\ell/\nu_f M_f \tag{3.18}$$

where ν_ℓ'' and ν_ℓ' are stoichiometric coefficient of species ℓ in product and reactant system, and $\nu_f M_f = 1$ because in this case γ_ℓ is considered for unit mass loss. So each γ_ℓ turns out as follows

$$\gamma_{fuel} = (0-1)M_f/1xM_f = -1$$

$$\gamma_{soot} = (\nu_1'' - 0) \times 12 \times 10^{-3} = \frac{s}{1-w}$$

$$\gamma_{O_2} = \{0 - (\nu_1''' - \frac{\nu_1''''}{2} + \frac{\nu_2'}{4} - \frac{\nu_3'}{2})\} \times 32 \times 10^{-3}$$

$$= -\{(1 - \frac{\eta}{2}) \frac{1}{12} \cdot \frac{W_C-w-s}{1-w} + \frac{1}{4} \cdot \frac{W_H}{1-w} - \frac{1}{2} \cdot \frac{1}{16} \cdot \frac{W_O}{1-w}\} \times 32$$

$$\gamma_{CO_2} = \{(\nu_1'''-\nu_1'''')-0\} \times 44 \times 10^{-3} = (1-\eta) \frac{W_C-w-s}{1-w} \cdot \frac{44}{12} \tag{3.19}$$

$$\gamma_{CO} = (\nu_1''''-0) \times 28 \times 10^{-3} = \eta \frac{W_C-w-s}{1-w} \cdot \frac{28}{12}$$

$$\gamma_{H_2O} = (\frac{\nu_2'}{2} - 0) \times 18 \times 10^{-3} = \frac{1}{2} \cdot \frac{W_H}{1-w} \cdot \frac{18}{1}$$

$$\gamma_{N_2} = (\frac{\nu_4'}{2} - 0) \times 28 \times 10^{-3} = \frac{1}{2} \cdot \frac{W_N}{1-w} \cdot \frac{28}{14} = \frac{W_N}{1-w}$$

(iv) Burning rate of gasified fuel

Generally, burning rate is a function of the local concentration of fuel and oxygen and temperature, however, since the flame temperature is usually so high, it is practically quite reasonable to assume that fuel and oxygen cannot

coexist at the same spatial point and the burning rate is governed by the supply rate of fuel or oxygen into the flame region. In the case of combustion in the upper layer the supply rates will be controlled by local turbulent mixing of the fire plume, ceiling jet, door jet and so forth, however, it is now difficult to reasonably model every mixing process involved. So, let's assume that the mixing rate in an upper layer is so large that fuel and oxygen cannot coexist in the layer and by this reason the supply rates of either fuel and oxygen into the layer becomes the controlling mechanism of the burning process.

With this assumption, the burning rate of the gasified fuel can be given as follows:

$$\dot{m}_b = \begin{cases} \sum\{Y_{f,j}(SS_{ji} + SA_{ji}) - Y_f(SS_{ij}+SA_{ij}) + Y_f^a(SA'_{ji}-SA_{ji}+\lambda AS_{ji})\} \\ \quad + Y_f^p \dot{m}_p + Y_f^a(\dot{m}_s-\dot{m}_p) & (Y_{O_2} > 0 \quad \text{:fuel control}) \\ \dfrac{1}{\gamma_{O_2}}\left[\sum\{Y_{O_2,j}(SS_{ji}+SA_{ji}) - Y_{O_2}(SS_{ij}+SA_{ij}) + Y_{O_2}^a(SA'_{ji}-SA_{ji}+\lambda AS_{ji})\}\right. \\ \quad \left. + Y_{O_2}^p \dot{m}_p + Y_{O_2}^a(\dot{m}_s - \dot{m}_p)\right] & (Y_{O_2} = 0 \quad \text{:oxygen control}) \end{cases} \tag{3.20}$$

Note that since the mixing rate in the layer is so large that fuel and oxygen cannot coexist in the layer, the criterion to determine mass burning rate must be the oxygen concentration Y_{O_2}.

3.2 Entrainment

Entrainment by fire plumes and door jets play an important role in hot gas transport in a structure. The nature of fire plume, which rises up vertically from a horizontal fire source, has been comparatively so well investigated, both theoretically and experimentally, that a fairly reliable model is available here. Regarding door jet entrainment, however, no reliable data are available, so a somewhat crude model will be presented by just stretching the result on fire plume entrainment.

(i) Fire plume

The following equations proposed by McCaffrey are used to calculate the rate of flow that enters the hot upper layer of the room of origin $\dot{m}_s$ [6].

(a) Continuous flame region ($0<Z/\dot{Q}^{2/5}<0.08$)

$$\frac{\dot{m}}{\dot{Q}} = 0.011 \left(\frac{Z}{\dot{Q}^{2/5}}\right)^{0.566}$$

(b) Intermittent region ($0.08 \leq Z/Q^{2/5} < 0.20$)

$$\frac{\dot{m}}{\dot{Q}} = 0.026 \left(\frac{Z}{\dot{Q}^{2/5}}\right)^{0.909} \qquad (3.21)$$

(c) Plume region ($0.20 \leq Z/Q^{2/5}$)

$$\frac{\dot{m}}{\dot{Q}} = 0.124 \left(\frac{Z}{\dot{Q}^{2/5}}\right)^{1.895}$$

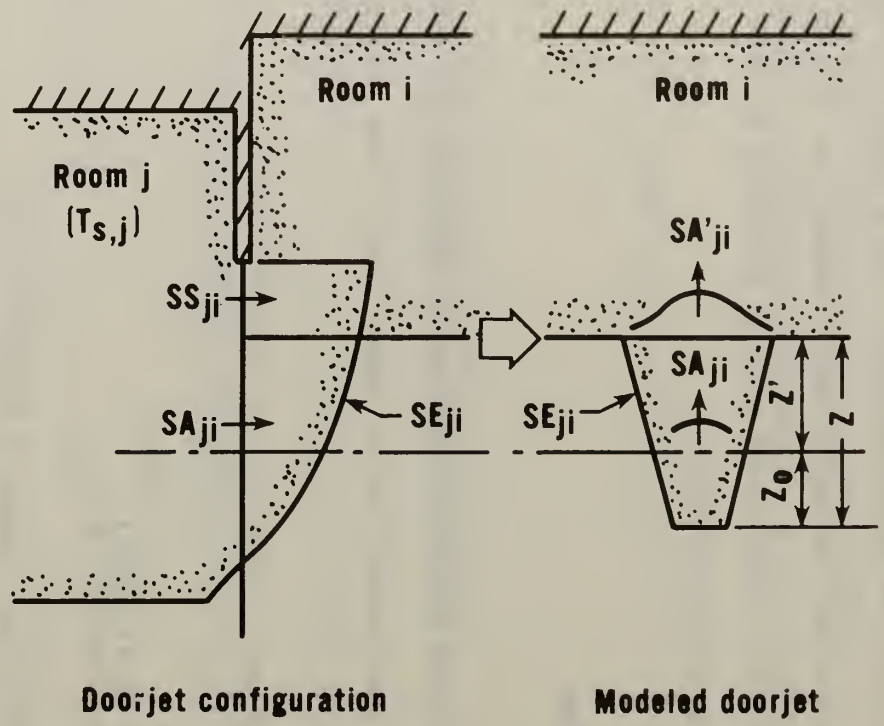

Fig. 3.5 Doorjet Model

where m, Z and $\dot{Q}$ respectively stand for mass flow rate (kg/s), height above heat source (m) and nominal heat release rate (kW). Since the flow rate m should not be smaller than the mass loss rate $\dot{m}_p$ an adjustment is made as follows

$$\dot{m}_s = \max \{\dot{m}_p, \dot{m} \text{ by Eq. (3.21)}\} \tag{3.21}$$

(ii) Door jet

Since little is known about door jet entrainment at least for the purpose of quantitative estimation, it is assumed that the door jet behaves as if it were vertical thermal plume rising up from a source horizontally placed on a plane so that the fire plume equation given by Eq. (3.21) can be utilized. A fictitious source is assumed at the distance Z_o below door jet center level so that the flow rate given by Eq. (3.21) becomes equal to the door jet flow rate at the level. The distance Z_o can be obtained by substituting $\dot{m} = SA_{ji}$ and $Q = C_p SA_{ji}(T_{s,j} - T_a)$ into Eq. (3.21), and the following relations are substituted again into Eq. (3.21) to yield the rate of door jet flow that enters the upper layer of i-th room (Fig. 3.5).

$$\dot{m}_p = SA_{ji}$$

$$\dot{Q} = C_p \, SA_{ji} \, (T_{s,j} - T_a) \tag{3.22}$$

$$Z' = H_R - Z_S - \{\min.(H_h, H_R - Z_S) + \max(X_{nas}, H_\ell, H_{R,j} - Z_{s,j})\}/2 + Z_o$$

where SA_{ji} and $T_{s,j}$ are respectively stand for the flow rate and the temperature of door jet; H_R and Z_s are room height and upper layer thickness; H_h is the soffit height of the opening; X_{nas} is the neutral zone height; and subscripts i and j denote room numbers (Fig. 3.6).

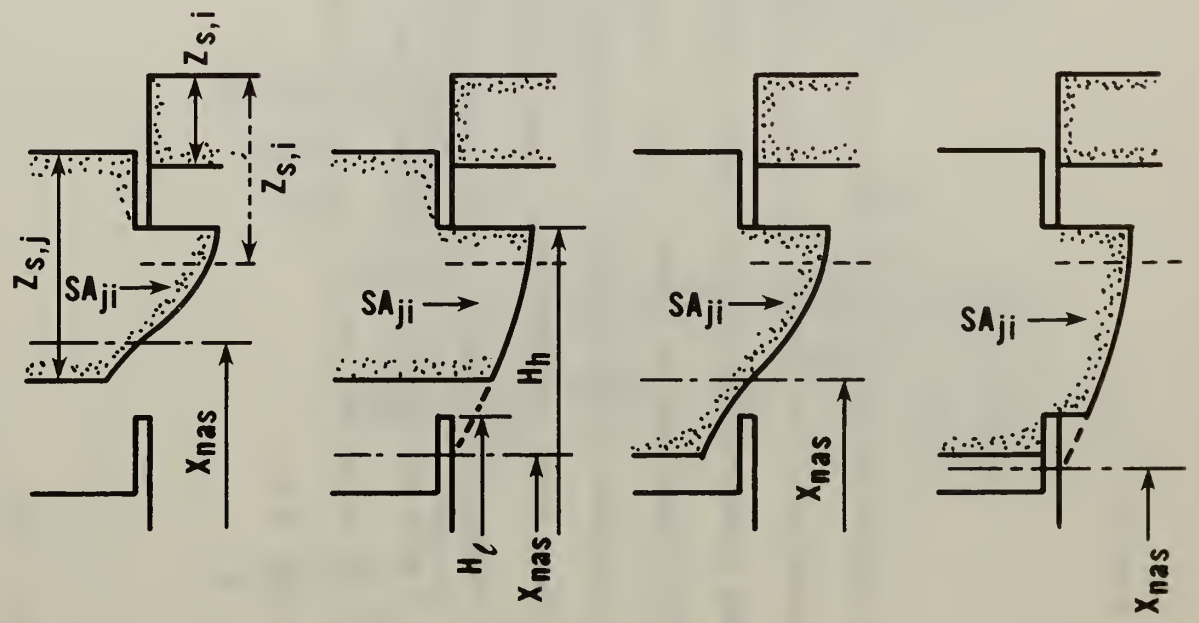

Fig. 3.6 Conceivable Doorjet Configurations

3.3 Heat Transfer

Heat transfer is the precursor of fire spread since every ordinary material has to be heated before it ignites. Also heat transfer may have an effect on the gas flows in structures because the flows are driven by buoyancy. Every mode of heat transfer is involved in fire. This section will be devoted to the practical modeling of these heat transfer process.

(i) Radiative heat transfer

The procedure to calculate the radiative heat transfer may be classified into two, i.e., how to calculate the heat transfer under given configuration, temperature and emissivity, and how to estimate the emissivity of the hot layer which contain soot, H_2O and CO_2. The former question is solved by using net-radiation method, which was first introduced by Hottel and developed by many others, and the latter is conveniently obtained by using ABSORB [7].

a) Radiative heat transfer in two layer configuration

It may be said that a room which contains a hot gas layer under its ceiling is one of the most characteristic heat transfer configurations in building fire (see Figure 3.7). With the highly advanced outcome in radiation heat transfer science, it may be possible to consider furthermore complicated situations, but it still may be useful to simplify the problem as follows to fit the current purpose.

So, let's assume that the interior wall of a room can be divided by discontinuity surface into two parts, i.e., one that is in contact with the upper layer and the other that is in contact with the lower layer, and each

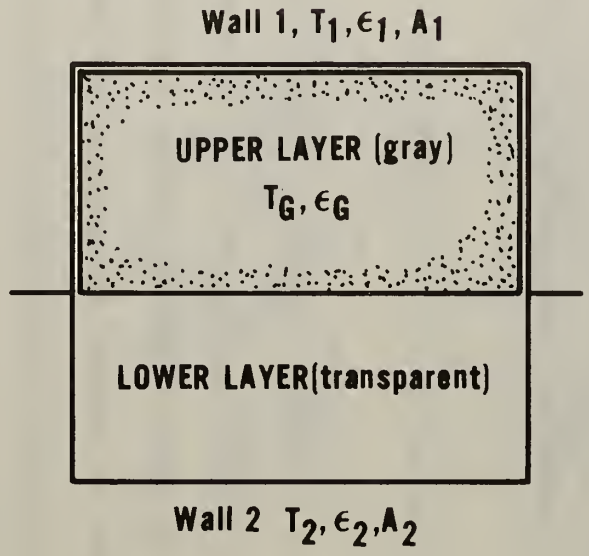

Fig. 3.7 Radiative Heat Transfer Model

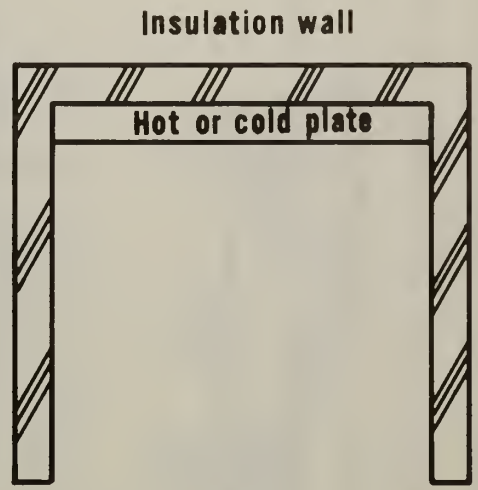

Fig. 3.8 Convective Heat Transfer Model

part is uniform in temperature respectively. It is also assumed that the surfaces of the walls and the gas are gray. For this heat transfer system, net-radiation method gives the following relation

$$\dot{Q}_1 = A_1 \frac{\varepsilon_1}{1-\varepsilon_1} (\sigma T_1^4 - \dot{q}''_{0,1})$$

$$\dot{Q}_1 = A_1 \{\dot{q}''_{0,1} - (1-\varepsilon_G) F_{11}\dot{q}''_{0,1} - (1-\varepsilon_G)F_{12}\dot{q}''_{0,2}\} - A_1\dot{q}''_{0,G}$$

$$\dot{Q}_2 = A_2 \frac{\varepsilon_2}{1-\varepsilon_2} (\sigma T_2^4 - \dot{q}''_{0,2}) \qquad (3.23)$$

$$\dot{Q}_2 = A_2 \{\dot{q}''_{0,2} - (1-\varepsilon_G)F_{21}\dot{q}''_{0,1} - F_{22}\dot{q}''_{0,2}\} - A_d\dot{q}''_{0,G}$$

$$\dot{q}''_{0,G} = \varepsilon_G \sigma T_G^4$$

$$\dot{Q}_G = -(\dot{Q}_1 + \dot{Q}_2)$$

where subscripts 1, 2, G and d respectively stand for ceiling, floor, upper gas and discontinuity; $\dot{q}''_{0,k}$ is respectively radiative heat flux leaving from surface k; Q_k is the net radiative heat loss of surface k; σ, ε and T are respectively Stefan-Boltzmann constant, emissivity and temperature, and F_{kj} is the view factor between surfaces k and j, which is given as follows in this specific case.

$$F_{11} = 1 - \frac{A_d}{A_1}, \quad F_{12} = F_{1d} = \frac{A_d}{A_1}, \quad F_{21} = F_{2d} = \frac{A_d}{A_2}, \quad F_{22} = 1 - \frac{A_d}{A_2} \qquad (3.24)$$

where A denotes surface area.

The solution of Eq. (3.23) gives $\dot{Q}_1$, $\dot{Q}_2$ and $\dot{Q}_G$ as follows

$$\dot{Q}_1 = A_1\varepsilon_1 \frac{P_1}{D}\ ,\ \dot{Q}_2 = A_2\varepsilon_2 \frac{P_2}{D}\ ,\ \dot{Q}_G = -(Q_1 + Q_2) \tag{3.25}$$

where

$$D = \{1-(1-\varepsilon_1)(1-\varepsilon_G)F_{11}\}\{1-(1-\varepsilon_2)F_{22}\}-(1-\varepsilon_1)(1-\varepsilon_2)(1-\varepsilon_G)^2F_{12}F_{21}$$

$$P_1 = [\{1-(1-\varepsilon_G)F_{11}\}\{1-(1-\varepsilon_2)F_{22}\}-(1-\varepsilon_2)(1-\varepsilon_G)^2F_{12}F_{21}]\sigma T_1^4$$

$$- (1-\varepsilon_G)F_{12}\varepsilon_2\sigma T_2^4 - [1 + (1 - \varepsilon_2)\{(1-\varepsilon_G)F_{12}F_{2d} - F_{22}\}]\varepsilon_G\sigma T_G^4 \tag{3.26}$$

$$P_2 = [\{1 - (1-\varepsilon_1)(1-\varepsilon_G)F_{11}\}(1-F_{22})-(1-\varepsilon_1)(1-\varepsilon_G)^2F_{12}F_{21}]\sigma T_2^4$$

$$- (1-\varepsilon_G)F_{21}\varepsilon_1\sigma T_1^4-[\{1-(1-\varepsilon_1)(1-\varepsilon_G)F_{11}\}F_{2d} + (1-\varepsilon_1)(1-\varepsilon_G)F_{21}]\varepsilon_G\sigma T_2^4$$

In spite of the significant simplification on the configuration, the solution given by Eqs. (3.25)-(3.26) may seem still lengthy, but it is one of the simplest solutions in the sense that every view factor can be obtained only from surface areas.

If the upper gas is black, i.e., $\varepsilon_G = 1$, it follows from Eqs. (3.25)-(3.26) that:

$$\dot{Q}_1 = \varepsilon_1 A_1 \sigma (T_1^4 - T_G^4)$$

$$\dot{Q}_2 = \frac{\varepsilon_2 A_d \sigma (T_2^4 - T_G^4)}{1-(1-\varepsilon_2)(1-A_d/A_2)} \tag{3.27}$$

b) Emissivity of upper layer

The calculation code ABSORB [7], gives the absorptivity of isothermal and homogeneous mixture of soot, CO_2 and H_2O whose total pressure is 1 atm. Modak's calculation may functionally be expressed as

$$\alpha = \text{ABSORB}\ (T_s,\ T,\ k_s,\ P_{CO_2},\ P_{H_2O},\ L_m) \tag{3.28}$$

where T_s and T represent the temperature of blackbody source and mixture; k_s is the absorption coefficient of soot at a wavelength of 0.94 μm; P_{CO_2} and P_{H_2O} are the partial pressure of CO_2 and H_2O; and L_m is the mean path length of the layer.

The emissivity of the layer may differ from its absorptivity when the temperature of radiation source is not the same as that of the layer but the difference is not significant so practically the layer temperature can be substituted into T_s of Eq. (3.28) to obtain the emissivity.

The absorption coefficient of soot at a wavelength of 0.94 μm is given as

$$k_s = \frac{7}{0.94 \times 10^{-6}} f_v \tag{3.29}$$

where f_v is the soot volume fraction and given as

$$f_v = Y_{soot}\rho_s/\rho_{soot} \tag{3.30}$$

where Y_{soot}, ρ_s and ρ_{soot} are the soot mass fraction of the layer, the layer gas density and the density of soot.

The partial pressure P_{CO_2} and P_{H_2O} are given in terms of the mass fraction of gas species of the layer as

$$P_{H_2O} = \left(\frac{\rho_s Y_{H_2O}}{M_{H_2O}}\right) \Big/ S, \quad P_{CO_2} = \left(\frac{\rho_s Y_{CO_2}}{M_{CO_2}}\right) \Big/ S \tag{3.31}$$

and

$$S = \left(\frac{Y_{H_2O}}{M_{H_2O}} + \frac{Y_{CO_2}}{M_{CO_2}} + \frac{Y_{CO}}{M_{CO}} + \frac{Y_{N_2}}{M_{N_2}} + \frac{Y_f}{M_f}\right) \rho_s \tag{3.22}$$

where Y and M are mass fraction of species in the layer and the molecular weight of the species respectively.

The path length L_m is given as

$$L_m = 0.9\,\frac{4V}{A} \tag{3.33}$$

where V and A are the volume and total surface are of the upper layer.

(ii) Convective heat transfer

In the room of origin, whose temperature is considerably high, the role of convective heat transfer may be relatively small as compared with radiation, but in the rooms other than the room of origin it may still be relatively significant.

A conventional method is used to estimate the convective heat transfer to ceilings although it may not be adequate for the room of origin, in which special patters of flow due to fire plume, ceiling jet and so forth, are involved.

For a horizontal surface surrounded by thermally insulated wall, the mean Nusselt number is given as (see Figure 3.8).

$$Nu = \begin{cases} 0.054\ (Gr \cdot P_r)^{0.38} & (T_G > T_W) \\ 0.003\ (Gr \cdot P_r)^{0.38} & (T_G < T_W) \end{cases} \tag{3.34}$$

where T_G and T_W are the temperature of the upper layer and the surface of the wall that is in contact with the layer. Grashof number Gr and Prandtl number Pr are given as

$$Gr = \frac{g\ell^3(T_G - T_W)}{\nu^2 T_G} \tag{3.35}$$

$$Pr = \frac{\nu}{a}$$

where g denotes gravitational acceleration, ν and a are respectively kinematic viscosity and thermal diffusivity of the gas, and ℓ is the reference heat transfer length.

Using Nu given in Eq. (3.34), we can obtain the convective heat flux $\dot{q}''_c$ as

$$\dot{q}''_c = \frac{k}{\ell} \text{Nu} \ (T_G - T_W) \tag{3.36}$$

where k is the thermal conductivity of the gas. The physical properties of the gas may be substituted by those of air and approximated as follows:

$$\text{Pr} = 0.72$$

$$\nu = 7.18 \times 10^{-10} \left(\frac{T_G + T_W}{2} \right)^{7/4} \tag{3.37}$$

$$k = 6.50 \times 10^{-8} \left(\frac{T_G + T_W}{2} \right)^{4/5}$$

(iii) Thermal conduction

The importance of the wall thermal conduction lies in the fact that both the radiative and the convective heat transfer to the walls are related to the wall surface temperatures. The calculation of the thermal conduction will turn out to be very complicated if the effects of water content, thermal property variation with temperature, decomposition and so forth, which are commonplace in real fire, are taken into account. However, since little has been considered in dealing with those problems, a one dimensional thermal conduction equation for uniform thermal properties as follows is solved in this model to obtain the wall temperature.

Thermal conduction equation

$$\frac{\partial T}{\partial t} = \left(\frac{k}{c\rho}\right) \frac{\partial^2 T}{\partial x^2} \tag{3.38}$$

Boundary condition

$$- k \left.\frac{\partial T}{\partial x}\right|_{x=0} = \dot{q}''_{in}$$

$$- k \left.\frac{\partial T}{\partial x}\right|_{x=\ell} = \dot{q}''_{out} \tag{3.39}$$

where k, c, ρ and ℓ are respectively the thermal conductivity, the specific heat, the density and the thickness of the wall; $\dot{q}''_{in}$ and $\dot{q}''_{out}$ are the net incident heat flux to the wall surface and the net heat loss flux from the back of the wall.

3.4 Flow Through Opening

The primary tasks that have to be considered in the calculation of the flows through openings of a structure are to describe the rate of the flows as a function of the pressures, and to solve the pressures so that Eq. (2.19) can be satisfied.

(i) Rate of flow through opening

The rates of the flows of hot gas and air are affected by the temperature and the thickness of the upper layer and the pressure of each side of the opening. Let's consider the case where each side of the opening has a hot layer of arbitrary temperature and thickness as the most general case, which is shown in Figure 3.9.

The hydrostatic pressure drop with height of each room is also shown in Figure 3.9 and it is obvious that there are three regions where the increase rate of pressure difference between the rooms with height differ from one to another; i.e., below $Z_{a,i}$ the pressure difference is kept constant, while it varies proportionally to $\rho_a - \rho_{s,i}$ between $Z_{a,i}$ and $Z_{a,j}$ and to $\rho_{s,j} - \rho_{s,i}$ above $Z_{a,j}$. The pressures of the rooms at the height Z are described as follows:

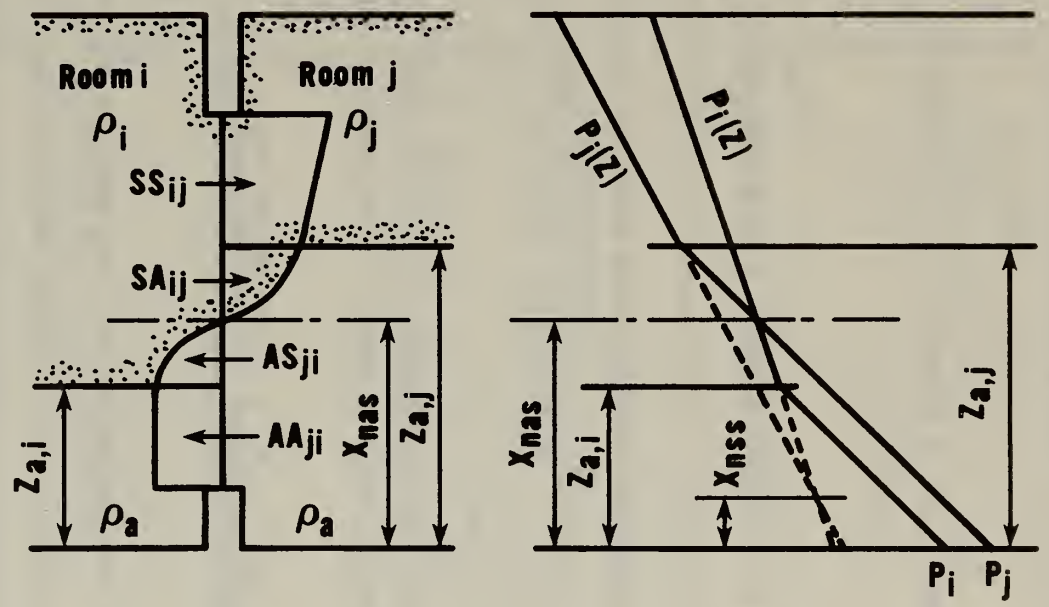

Fig. 3.9 Pressure Difference Profile
Across an Opening

$$P_i(Z) = \begin{cases} P_i - \rho_a g Z & (Z \leq Z_{a,i}) \\ P_i - \rho_a g Z_{a,i} - \rho_{s,i} g(Z - Z_{a,i}) & (Z > Z_{a,i}) \end{cases}$$

$$P_j(Z) = \begin{cases} P_j - \rho_a g Z & (Z \leq Z_{a,j}) \\ P_j - \rho_a g Z_{a,i} - \rho_{s,j} g(Z - Z_{a,j}) & (Z > Z_{a,j}) \end{cases} \tag{3.40}$$

Before formulating the rate of the flows, it is useful to obtain the neutral zone heights associated with the above pressure profiles. The first one is obtained by equating the second and the third equation in Eq. (3.40) as follows

$$X_{nas} = \frac{P_j - P_i}{(\rho_a - \rho_{s,i})g} + Z_{a,i} \tag{3.41}$$

Likewise equating the second and the forth of the equation yields

$$X_{nss} = \frac{P_j - P_i}{(\rho_{s,j} - \rho_{s,i})g} + \frac{\rho_a - \rho_{s,i}}{\rho_{s,j} - \rho_{s,i}} Z_{a,i} + \frac{\rho_{s,j} - \rho_a}{\rho_{s,j} - \rho_{s,i}} Z_{a,j} \tag{3.42}$$

It should be noted that the densities and the pressures varies as the fire goes on, so the pressure difference at an opening may take various profiles. All the possible pressure difference profiles are covered in Figure 3.10 and the rates of flow of hot gas and air for each case are shown in Table 3.1. It may be clear that the symbols for the hot gas flow rates SS and SA and for the air flow rates AS and AA are assigned to each different pressure difference profile, and are convenient to formulate the rate of the flows. Also, it should be noted that although the formulas in Table 3.1 are described using the neutral zone heights, they are still functions of the pressures because the neutral zone

Table 3.1(a) Flow Rate of Hot Gas and Air
($P_{s,i} < P_{s,j}$)

$X_{nas} \le Z_{a,i}$ 	$SS_{ij} = \begin{cases} \frac{2}{3}\alpha B_w \sqrt{2g\rho_{s,i}\lvert\rho_{s,i}-\rho_{s,j}\rvert}\left\{(H_h - X_{nss})^{3/2} - (\max(H_l, Z_{a,j}) - X_{nss})^{3/2}\right\} & (H_h > Z_{a,j}) \\ 0. & (H_h \le Z_{a,j}) \end{cases}$ $SS_{ji} = 0.$ $SA_{ij} = \begin{cases} \frac{2}{3}\alpha B_w \sqrt{2g\rho_{s,i}\lvert\rho_{s,i}-\rho_a\rvert}\left\{(\min(H_h, Z_{a,j}) - X_{nas})^{3/2} - (\max(H_l, Z_{a,i}) - X_{nas})^{3/2}\right\} & (H_l > Z_{a,i} \,\&\, H_l < Z_{a,j}) \\ 0. & (H_l \le Z_{a,i} \text{ or } H_l \ge Z_{a,j}) \end{cases}$ $SA_{ji} = 0.$ $AS_{ij} = AS_{ji} = 0.$ $AA_{ij} = \begin{cases} \alpha' B_w \{\min(H_h, Z_{a,i}) - H_l\}\sqrt{2\rho_a\lvert\rho_i - \rho_j\rvert} & (H_l < Z_{a,i}) \\ 0. & (H_l \ge Z_{a,i}) \end{cases}$ $AA_{ji} = 0.$
$Z_{a,i} < X_{nas} \le Z_{a,j}$ 	$SS_{ij} = \begin{cases} \frac{2}{3}\alpha B_w \sqrt{2g\rho_{s,i}\lvert\rho_{s,i}-\rho_{s,j}\rvert}\left\{(H_h - X_{nss})^{3/2} - (\max(H_l, Z_{a,j}) - X_{nss})^{3/2}\right\} & (H_h > Z_{a,j}) \\ 0. & (H_h \le Z_{a,j}) \end{cases}$ $SS_{ji} = 0.$ $SA_{ij} = \begin{cases} \frac{2}{3}\alpha B_w \sqrt{2g\rho_{s,j}\lvert\rho_{s,i}-\rho_a\rvert}\left\{(\min(H_h, Z_{a,j}) - X_{nas})^{3/2} - (\max(H_l, X_{nas}) - X_{nas})^{3/2}\right\} & (H_l > X_{nas} \,\&\, H_l < Z_{a,j}) \\ 0. & (H_l \le X_{nas} \text{ or } H_l \ge Z_{a,j}) \end{cases}$ $SA_{ji} = 0.$ $AS_{ij} = 0.$ $AS_{ji} = \begin{cases} \frac{2}{3}\alpha B_w \sqrt{2g\rho_a\lvert\rho_a - \rho_{s,i}\rvert}\left\{(X_{nas} - \max(Z_{a,i}, H_l))^{3/2} - (X_{nas} - \min(H_h, X_{nas}))^{3/2}\right\} & (H_l > Z_{a,i} \,\&\, H_l < X_{nas}) \\ 0. & (H_l \le Z_{a,i} \text{ or } H_l \ge X_{nas}) \end{cases}$ $AA_{ij} = 0.$ $AA_{ji} = \begin{cases} \alpha' B_w \{\min(H_h, Z_{a,i}) - H_l\}\sqrt{2\rho_a\lvert\rho_j - \rho_i\rvert} & (H_l < Z_{a,i}) \\ 0 & (H_l \ge Z_{a,i}) \end{cases}$
$Z_{a,j} < X_{nas}$ 	$SS_{ij} = \begin{cases} \frac{2}{3}\alpha B_w \sqrt{2g\rho_{s,j}\lvert\rho_{s,i}-\rho_{s,j}\rvert}\left\{(H_h - X_{nss})^{3/2} - (\max(H_l, X_{nss}) - X_{nss})^{3/2}\right\} & (H_h > X_{nss}) \\ 0. & (H_h \le X_{nss}) \end{cases}$ $SS_{ji} = \begin{cases} \frac{2}{3}\alpha B_w \sqrt{2g\rho_{s,j}\lvert\rho_{s,i}-\rho_{s,i}\rvert}\left\{(X_{nss} - \max(H_l, Z_{a,j}))^{3/2} - (X_{nss} - \min(H_h, X_{nss}))^{3/2}\right\} & (H_l > Z_{a,j} \,\&\, H_l < X_{nss}) \\ 0. & (H_l \le Z_{a,j} \text{ or } H_l \ge X_{nss}) \end{cases}$ $SA_{ij} = SA_{ji} = 0.$ $AS_{ij} = 0.$ $AS_{ji} = \begin{cases} \frac{2}{3}\alpha B_w \sqrt{2g\rho_a\lvert\rho_a - \rho_{s,i}\rvert}\left\{(X_{nas} - \max(H_l, Z_{a,i}))^{3/2} - (X_{nas} - \min(H_h, Z_{a,j}))^{3/2}\right\} & (H_l > Z_{a,i} \,\&\, H_l < Z_{a,j}) \\ 0. & (H_l \le Z_{a,i} \text{ or } H_l \ge Z_{a,j}) \end{cases}$ $AA_{ij} = 0.$ $AA_{ji} = \begin{cases} \alpha' B_w (\min(H_h, Z_{a,i}) - H_l)\sqrt{2\rho_a\lvert\rho_j - \rho_i\rvert} & (H_l < Z_{a,i}) \\ 0. & (H_l \ge Z_{a,i}) \end{cases}$

Table 3.1(b) Flow Rate of Hot Gas and Air
($P_{s,i} > P_{s,j}$)

$X_{nas} \le Z_{a,i}$

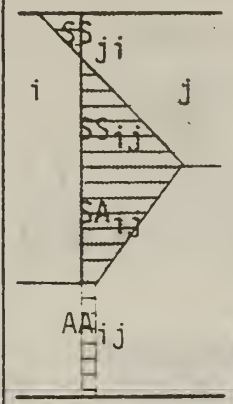

$$SS_{ji} = \begin{cases} \frac{2}{3}\alpha B_w \sqrt{2g\rho_{s,j}|\rho_{s,j}-\rho_{s,i}|}\left\{(H_e-X_{nss})^{3/2}-(\max(H_e,X_{nss})-X_{nss})^{3/2}\right\} & (H_e>X_{nss}) \\ 0. & (H_e\le X_{nss}) \end{cases}$$

$$SS_{ij} = \begin{cases} \frac{2}{3}\alpha B_w \sqrt{2g\rho_{s,i}|\rho_{s,i}-\rho_{s,j}|}\left\{(X_{nss}-\max(H_e,Z_{a,j}))^{3/2}-(X_{nss}-\min(H_h,X_{nss}))^{3/2}\right\} & (H_e>Z_{a,j} \ \&\ H_e<X_{nss}) \\ 0. & (H_e\le Z_{a,j} \text{ or } H_h\ge X_{nss}) \end{cases}$$

$$SA_{ij} = \begin{cases} \frac{2}{3}\alpha B_w \sqrt{2g\rho_{s,i}|\rho_{s,i}-\rho_a|}\left\{(\min(H_h,Z_{a,j})-X_{nas})^{3/2}-(\max(H_e,Z_{a,i})-X_{nas})^{3/2}\right\} & (H_e>Z_{a,i} \ \&\ H_e<Z_{a,j}) \\ 0. & (H_e\le Z_{a,i} \text{ or } H_e\ge Z_{a,j}) \end{cases}$$

$SA_{ji} = 0.$

$AS_{ij} = AS_{ji} = 0.$

$$AA_{ij} = \begin{cases} \alpha' B_w\{\min(H_h,Z_{a,i})-H_e\}\sqrt{2\rho_a|P_i-P_j|} & (H_e<Z_{a,i}) \\ 0. & (H_e\ge Z_{a,i}) \end{cases}$$

$AA_{ji} = 0.$

$Z_{a,i} < X_{nas} < Z_{a,j}$

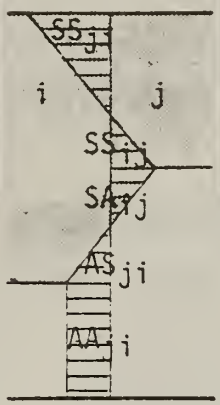

$$SS_{ji} = \begin{cases} \frac{2}{3}\alpha B_w \sqrt{2g\rho_{s,j}|\rho_{s,j}-\rho_{s,i}|}\left\{(H_e-X_{nss})^{3/2}-(\max(H_e,X_{nss})-X_{nss})^{3/2}\right\} & (H_e>X_{nss}) \\ 0. & (H_e\le X_{nss}) \end{cases}$$

$$SS_{ij} = \begin{cases} \frac{2}{3}\alpha B_w \sqrt{2g\rho_{s,i}|\rho_{s,i}-\rho_{s,j}|}\left\{(X_{nss}-\max(H_e,Z_{a,j}))^{3/2}-(X_{nss}-\min(H_h,X_{nss}))^{3/2}\right\} & (H_e>Z_{a,j} \ \&\ H_e<X_{nss}) \\ 0. & (H_e\le Z_{a,i} \text{ or } H_h\ge X_{nss}) \end{cases}$$

$$SA_{ij} = \begin{cases} \frac{2}{3}\alpha B_w \sqrt{2g\rho_{s,i}|\rho_{s,i}-\rho_a|}\left\{(\min(H_h,Z_{a,j})-X_{nas})^{3/2}-(\max(H_e,X_{nas})-X_{nas})^{3/2}\right\} & (H_e>X_{nas} \ \&\ H_e<Z_{a,j}) \\ 0 & (H_e\le X_{nas} \text{ or } H_e\ge Z_{a,i}) \end{cases}$$

$SA_{ji} = 0.$

$AS_{ij} = 0.$

$$AS_{ji} = \begin{cases} \frac{2}{3}\alpha B_w \sqrt{2g\rho_a|\rho_a-\rho_{s,i}|}\left\{(X_{nas}-\max(H_e,Z_{a,j}))^{3/2}-(X_{nas}-\min(H_h,X_{nas}))^{3/2}\right\} & (H_e>Z_{a,i} \ \&\ H_e<X_{nas}) \\ 0. & (H_e\le Z_{a,i} \text{ or } H_e\ge X_{nas}) \end{cases}$$

$AA_{ij} = 0.$

$$AA_{ji} = \begin{cases} \alpha' B_w\{\min(H_h,Z_{a,i})-H_e\}\sqrt{2\rho_a|P_j-P_i|} & (H_e<Z_{a,j}) \\ 0. & (H_e\ge Z_{a,i}) \end{cases}$$

$Z_{a,j} < X_{nss}$

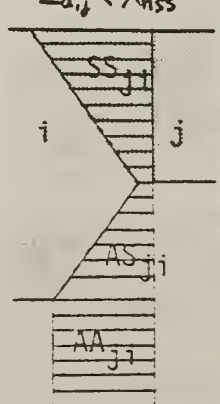

$SS_{ij} = 0.$

$$SS_{ji} = \begin{cases} \frac{2}{3}\alpha B_w \sqrt{2g\rho_{s,j}|\rho_{s,j}-\rho_{s,i}|}\left\{(H_e-X_{nss})^{3/2}-(\max(H_e,Z_{a,j})-X_{nss})^{3/2}\right\} & (H_e>Z_{a,i}) \\ 0. & (H_e\le Z_{a,i}) \end{cases}$$

$SA_{ij} = SA_{ji} = 0.$

$AS_{ij} = 0.$

$$AS_{ji} = \begin{cases} \frac{2}{3}\alpha B_w \sqrt{2g\rho_a|\rho_a-\rho_{s,i}|}\left\{(X_{nas}-\max(H_e,Z_{a,i}))^{3/2}-(X_{nas}-\min(H_e,Z_{a,i}))^{3/2}\right\} & (H_e>Z_{a,i} \ \&\ H_e<Z_{a,i}) \\ 0 & (H_e\le Z_{a,i} \text{ or } H_e\ge Z_{a,i}) \end{cases}$$

$AA_{ij} = 0.$

$$AA_{ji} = \begin{cases} \alpha' B_w\{\min(H_e,Z_{a,i})-H_e\}\sqrt{2\rho_a|P_j-P_i|} & (H_e<Z_{a,i}) \\ 0. & (H_e\ge Z_{a,i}) \end{cases}$$

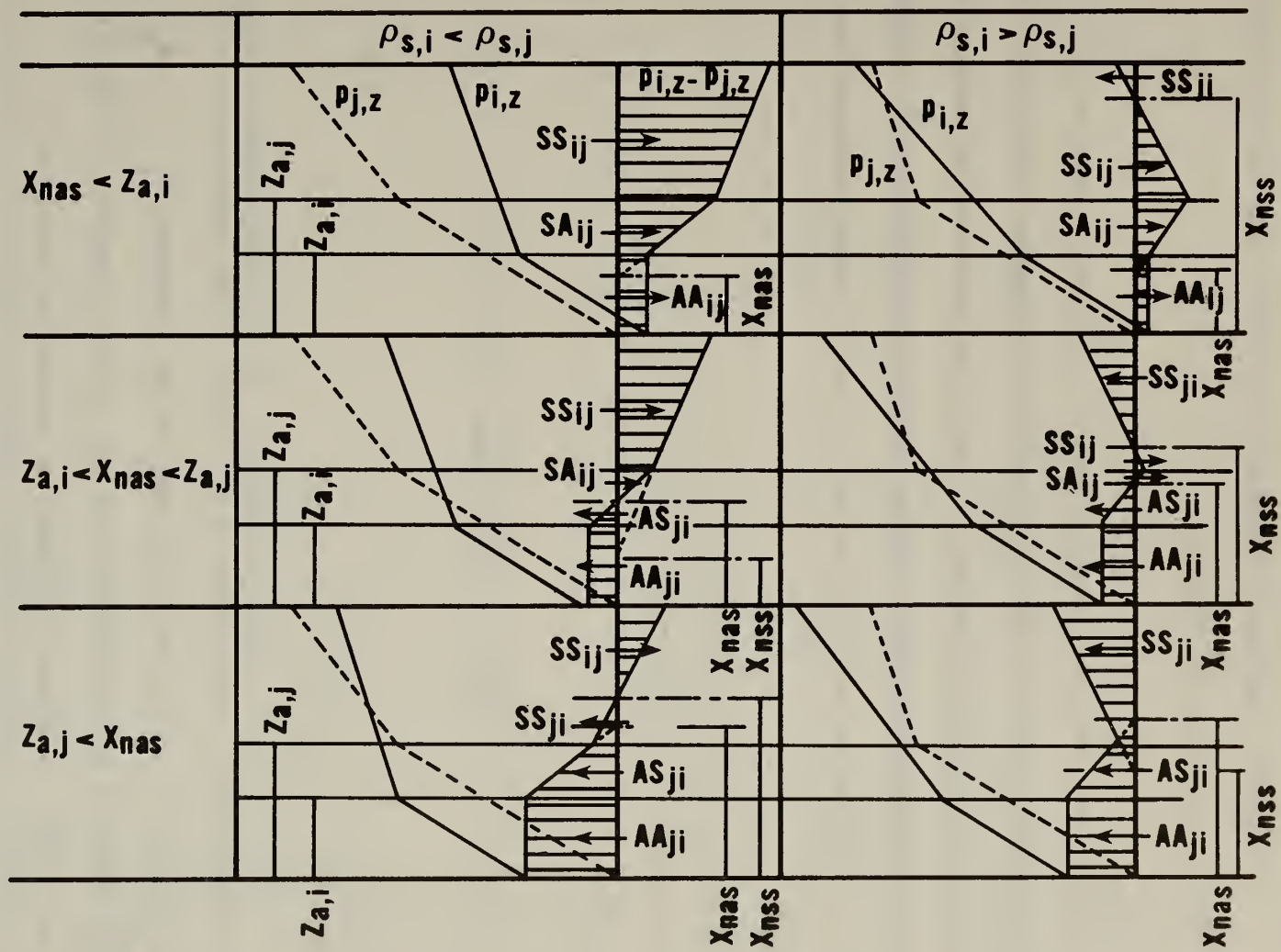

Fig. 3.10 Conceivable Pressure Difference Profiles Across an Opening

heights are functions of the pressures as known from Eqs. (3.41) and (3.42).

(ii) Solution of pressure equation

The equation that the pressures in the flow rate formula in Table 3.1 must satisfy is given by Eq. (2.19). Eq. (2.19) is actually simultaneous algebraic equations each of which holds for a room in the structure and may involve any of the room pressures. Since the real form of Eq. (2.19) is too complex and lengthy to discuss the solution procedure, let's rewrite the equation functionally as follows

$$
\begin{aligned}
& f_1 (P_1, P_2, \ldots, P_n) = 0 \\
& \vdots \\
& f_k (P_1, P_2, \ldots, P_k, \ldots, P_n) = 0 \\
& \vdots \\
& f_n (P_1, P_2, \ldots, P_n) = 0
\end{aligned}
\tag{3.43}
$$

where n denotes the total number of the rooms in the structure. In the real configuration of a structure, only some of the pressures $P_1, \ldots, P_n$ are actually involved in each equation of Eq. (3.43), however, the equation for k-th room $f_k(\hat{P}) = 0$ always includes the pressure of k-th room P_k.

A primitive method to solve Eq. (3.43) is explained as follows. Let's consider first the case where n=1, then Eq. (3.43) is reduced to

$$f_1 (P_1) = 0 \tag{3.44}$$

Although still nonlinear, there is no substantial difficulty in solving this equation numerically. In a numerical procedure, P_1 may be changed iteratively until Δ_1, which is defined as follows, reaches a convergence criterion.

$$\Delta_1 = f_1 (P_1) \tag{3.45}$$

The feature that Δ_1 is a monotonous decreasing function of P_1 may be utilized in devising some efficient numerical method. Noting that numerical solution of the pressure equation for single variable pressure is never difficult, let's go on to the case where n=2, i.e.,

$$f_1 (P_1, P_2) = 0 \tag{3.46a}$$

$$f_2 (P_1, P_2) = 0 \tag{3.46b}$$

Let's assume that P_1 is solved by any means from Eq. (3.46a) as

$$P_1 = f_1^* (P_2) \tag{3.47}$$

then, this can be substituted into Eq. (3.46 b) to yield

$$f_2(f_1^*(P_2), P_2) = 0 \tag{3.48}$$

This equation has only one variable pressure and can be solved as stated above. Eq. (3.47) can not be obtained analytically. A numerical method can be applied to Eq. (3.46a) to obtain P_1 only when P_2 is fixed, however, it can be applied whatever fixed value P_2 takes, which is practically equivalent to the existence of analytical solution as given by Eq. (3.48). What is only needed is that P_1

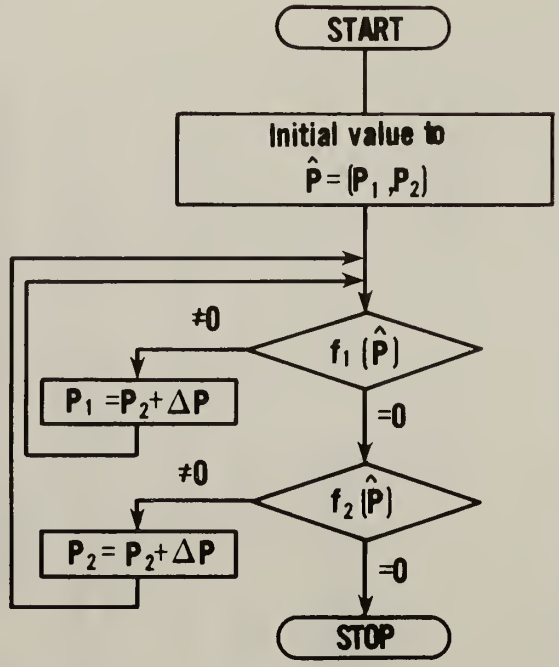

Fig. 3.11 Pressure Calculation Chart for Two Rooms

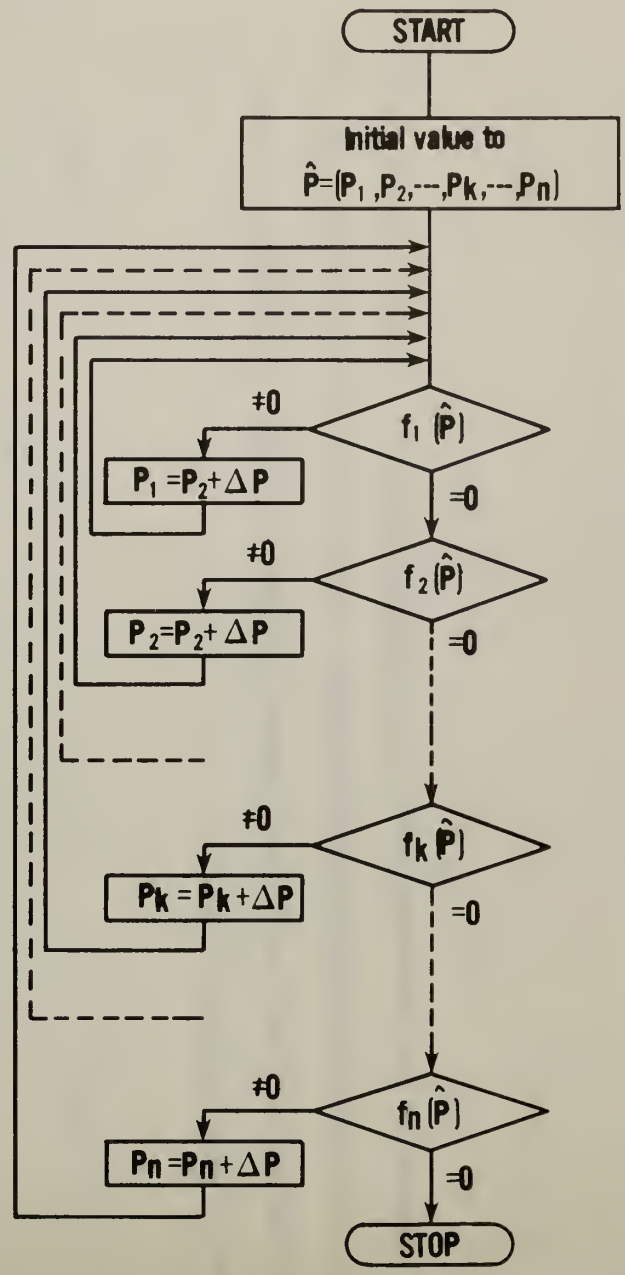

Fig. 3.12 Pressure Calculation Chart for a General Case

should be renewed by solving Eq. (3.46a) whenever P_2 is changed on the process of numerical solution of Eq. (3.48). This procedure may be made clearer by the chart in Figure 3.11. Likewise, in case of n rooms, the solution procedure is given by the chart in Figure 3.12. In a real structure, however, it is quite rare that one room is connected with every other room in the structure. Looking into the way the rooms are connected in a specific structure will provide more efficient charts of the procedure. For instance, in case of the building shown in Figure 3.13, Eq. (3.43) is reduced to

$$\begin{aligned} f_1 (P_1, P_4) &= 0 \\ f_2 (P_2, P_4) &= 0 \\ f_3 (P_3, P_4) &= 0 \\ f_4 (P_1, P_2, P_3, P_4) &= 0 \end{aligned} \tag{3.49}$$

Eq. (3.49) implies that any of P_1, P_2, and P_3 is the function of P_4 alone, i.e.,

$$P_1 = f_1^* (P_4), \; P_2 = f_2^* (P_4), \; P_3 = f_3^* (P_4) \tag{3.50}$$

so these pressure need to be renewed only when P_4 is changed. The chart for this procedure is also given in Figure 3.13. This kind of simplification can be made for almost every real building and will help save the computation time.

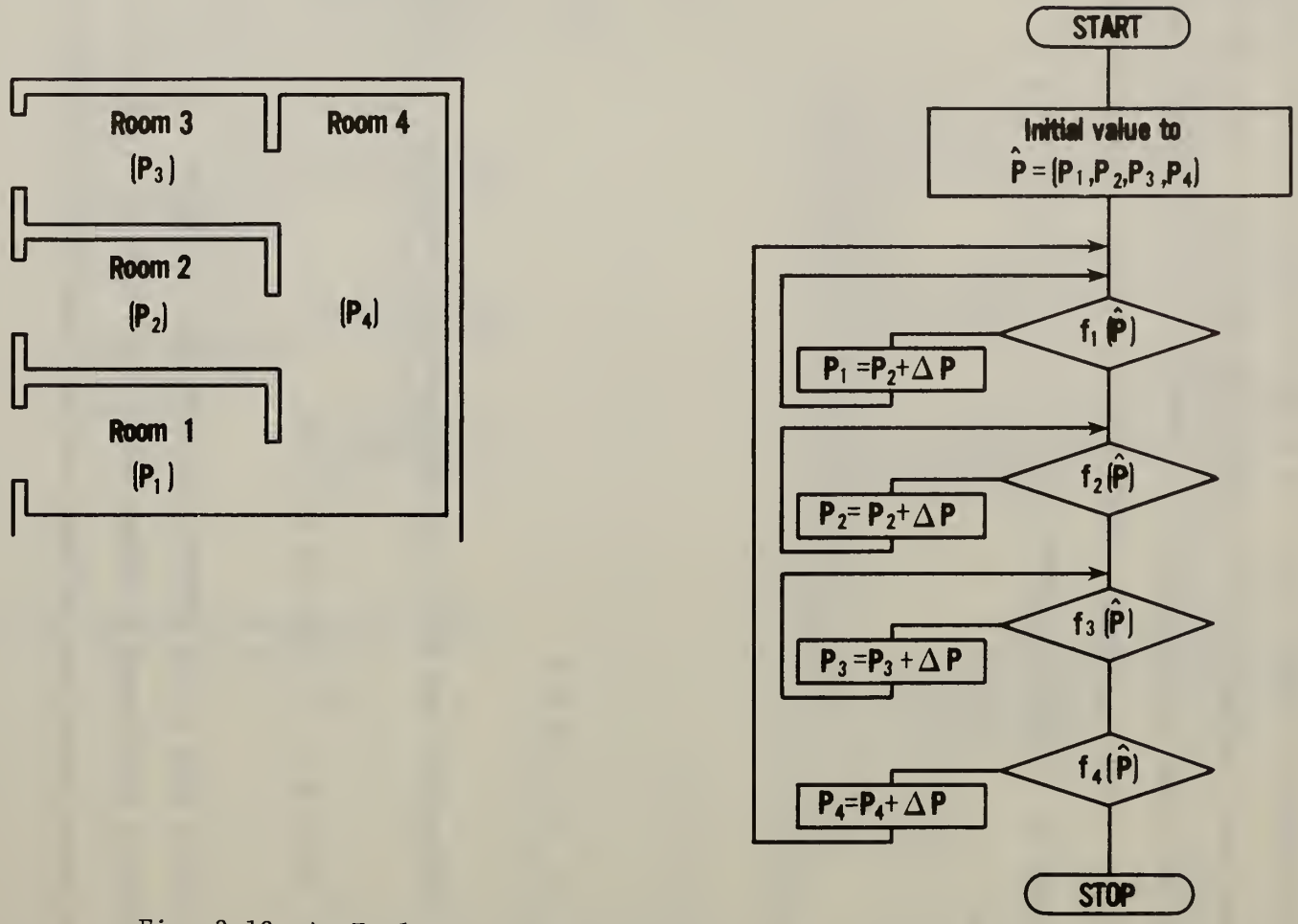

Fig. 3.13 An Explanatory Building Model and Its Pressure Calculation Chart

III. PROGRAM

The theories of the model to predict the state and motion of the fire induced hot gas were outlined in the previous sections. In this section, the skeleton of the program to compute numerically the model is briefly described and also the features of the subroutines included in the program are summarized. A full listing of the program has not been included due to its length, but may be acquired from the author at the Building Research Institute, Japan.

4. Program Structure

The structure of the program is, as can be seen in Figure 4.1, comparatively simple. Four of the five subroutines called from the main program, namely PARAM, TROP, DFIRE and WPRS, primarily deal with input and pre-treatment of the data to prepare the necessary information for subsequent computation.

The essence in computation of this model is to solve the ordinary differential equations given by Eqs. (2.16) - (2.18) and the algebraic equations (2.19). RKG is a numeric subroutine to solve the differential equations by Runge-Kutta Gill method together with DFNC, which yields the value of the differential coefficients of the equations. Most subroutines referenced from DFNC are related to physics and devoted to yield the value of the terms in the

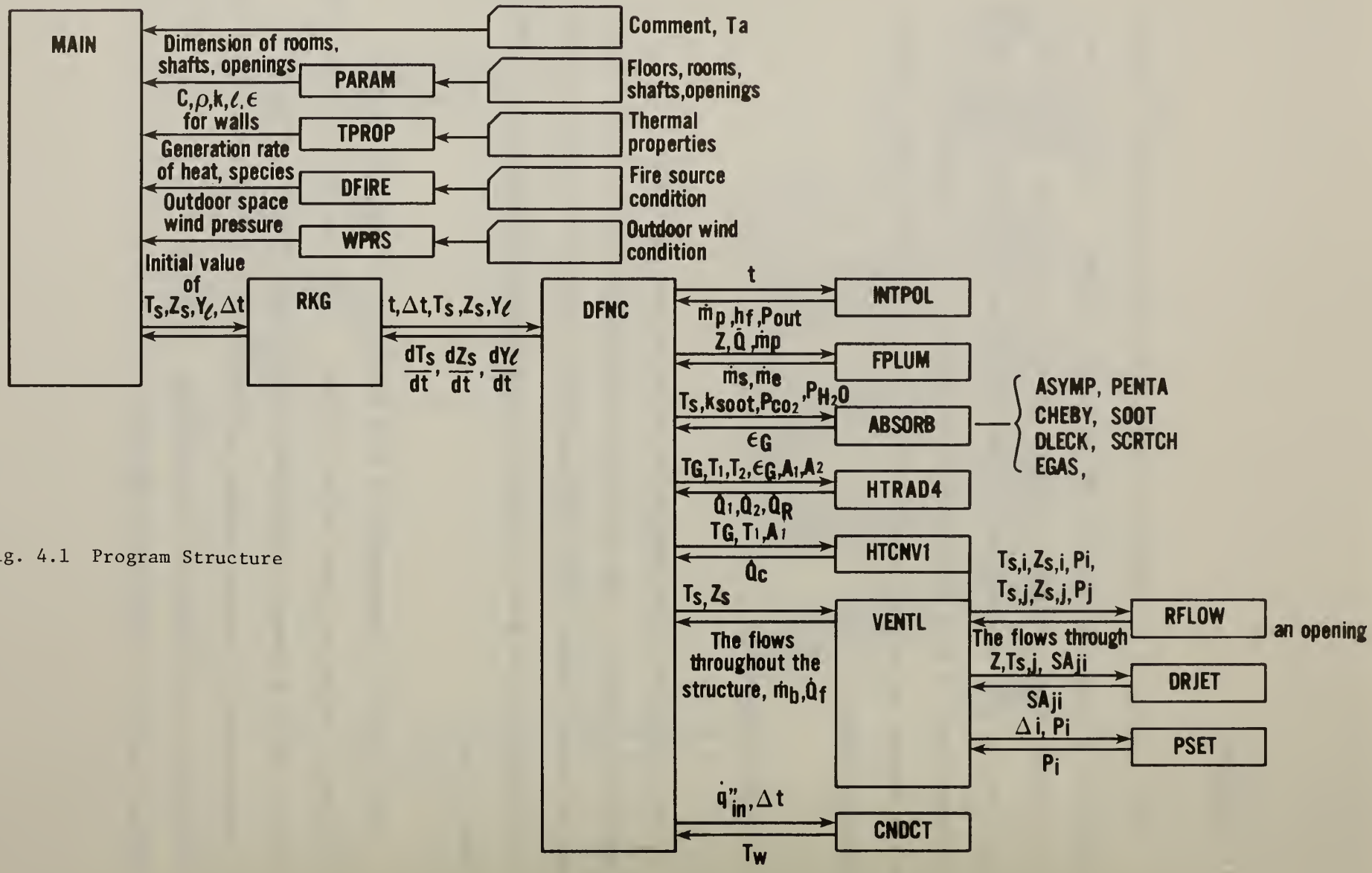

Fig. 4.1 Program Structure

right hand side of Eq. (2.16) - (2.18). Subroutine VENTL, together with RFLOW, PSET and DRJET, solves the algebraic equations (2.19) and yields the flow rates through openings.

5. Description of the Subprograms

In the following, brief descriptions on each subroutine of the present code are given. These descriptions are organized into several components. The task of the subroutines is stated, followed by some remarks which elaborate on the nature of the subroutine. The symbols corresponding to the computer coding and mathematical variables addressed in the subroutine are described. The input and output variables are listed along with their relationship to other subroutines. Lastly, the calculations made in the subroutine are listed. In the input/output list in the descriptions, the following symbols respectively are defined:

Data: Data Source

/AAAA/: Blocked common of which the name is AAAA

BBBB: Subroutine of which the name is BBBB respectively, when they are listed under the heading From of To.

The readers may feel that the description about the calculation in each subroutine is not sufficiently given, but this is so partly because the model itself is truely so simple that redundant explanation would make its point rather confusing.

Further details of the routine ABSORB can be found in ref. [7].

5.1 MAIN PROGRAM

(i) Task

To prepare the data and the initial condition for the model computation.

(ii) Remarks

The Main program primarily deals with the data input and initiation of the computation. Universal constants and common data are directly given here while the specific data for a calculation are given through subroutines PARAM, TPROP DFIRE and WPRS, which are called from the Main program.

(iii) Symbols

Code	Paper	Description
TITLE		Comments about the specific calculation
G	g	Gravitational acceleration (= 9.8 m/s^2)
SIGM	σ	Stefan-Boltzmann constant (= 1.356 x 10^{-11} $kcal/m^2sk^4$)
CP	C_p	Specific heat of gas (= 0.25 kcal/kgK)
TA	T_a	Temperature (K) of ambience and lower layer
RA	ρ_a	Density (kg/m^3) of ambience and lower layer
RSOOT	ρ_{soot}	Soot density (= 2,000 kg/m^3)
ALP	α	Flow coefficient
ALD	α	Flow coefficient
CR	λ	Fraction of air flow AS that mixes into upper layer of a room
CF	λ	Fraction of air flow AS that mixes into upper layer of a shaft

YP(L)	Y_{ℓ}^{p}	Mass fraction of species ℓ in volatile where ℓ is assigned as in 5.6 RKG
YAM(L)	Y_{ℓ}^{a}	Mass fraction of species ℓ in air
QF(N,I)	$\Delta H \cdot m_b$	Heat release rate of gasified fuel of i-th room on n-th floor (kcal/s)
QR(N,I)	$\dot{Q}_R$, $\dot{Q}_G$	Radiative } heat gain of the upper layer of i-th room on n-th floor (kcal/s)
QC(N,I)	$\dot{Q}_C$	Convective }
EPG(N,I)	ε_G	Layer emissivity of i-th room on n-th floor
YO(L,N,I)		Initial property of upper layer of i-th room on n-th floor where ℓ is assigned as in 5.6 RKG
PP(L,N,I)		Initial partial pressure of species ℓ of i-th room on n-th floor where ℓ is assigned as 5.6 RKG
P(N,NRMX2+I)		Relative pressure of i-th outdoor space due to wind (Pa)
H	Δt	Time interval for the computation(s)
NX		Number of time steps of the computation
XO		Initial time
W	w	Charring ratio of fuel
PM	m	Water content per unit fuel
NFLR, NFLR1 NRMX, NRMX2, NRMX4		See 5.2 PARAM
DDT, NTMAX		See 5.4 DFIRE
PWIND1, PWIND2, PWIND3, PWIND4		See 5.5 WPRS
SS(N,I,J,K), SA(N,I,J,K) AS(N,I,J,K), AA(N,I,J,K) SAD(N,I,J,K)		See 5.7 DFNC
EMP(N,I),EMS(N,I),EME(N,I)		See 5.7 DFNC

(iv) Input

Input	From	Input	From
TA	Data	W	/FUEL/
DDT	/FIRE/	PM	/FUEL/
NTMAX	/FIRE/	PWIND1(1)	/WIND/
NRMX	/BULG/	PWIND2(1)	/WIND/
NRMX2	/BULG/	PWIND3(1)	/WIND/
NRMX4	/BULG/	PWIND4(1)	/WIND/
NFLR	/BULG/		
NFLR1	/BULG/		

(v) Output

Output	To	Output	To
G	/UNIV/	YO(L,N,I)	RKG
SIGM	/UNIV/	H	RKG
CP	/UNIV/	NX	RKG
TA	/UNIV/	XO	RKG
RA	/UNIV/	NFLR	RKG
RSOOT	/UNIV/	NFLR1	RKG
ALP	/UNIV/	NRMX	RKG
ALD	/UNIV/	NRMX2	RKG
YP(L)	/CONS/	NRMX4	RKG
YAM(L)	/CONS/	P(N,NRMX2+I)	/PRES/
PP(L,N,I)	/CONS/		

(vi) Calculation

(a) Ambient density

$$\rho_a = \frac{353}{T_a}$$

(b) Mass fraction of fuel and H_2O

$$Y_f^P = \frac{1-w}{1-w+m}$$

$$Y_{H_2O}^P = \frac{m}{1-w+m}$$

5.2 PARAM

(i) Task

To input and pre-treat the data needed to set up the image of the objective structure.

(ii) Remarks

Generally, four conditions may be mentioned as the major physical factors that control fire behavior, namely, configuration and thermal condition of the structure, outdoor weather, and nature of fire source. This subroutine deals with the first matter, i.e., how to provide configuration data needed for the computation.

(iii) Symbols

Code	Paper	Description
N	n	Floor number in the structure
I	i	Room number on each floor *1)
J	j	Room number on each floor
K	k	Opening number between each two rooms
NFLR		Total number of floors in the structure
NEFLR		Number of specially designed floors
NSHFT		Number of shafts in the structure
NROM		Number of rooms on a commonly designed floor
HFLR		Height of a commonly designed floor (m)

NEF(L)		Floor number where ℓ-th specially designed floor is located
NEROM(L)		Number of rooms on ℓ-th specially designed floor
HEFLR(L)		Height of ℓ-th specially designed floor (m)
BRN(I)	$B_{R,i}$	Width of i-th room on a commonly designed floor (m)
DRN(I)	$D_{R,i}$	Depth of i-th room on a commonly designed floor (m)
HRN(I)	$H_{R,i}$	Height of i-th room on a commonly designed floor (m)
BRE(L,I)	$B_{R,i}$	Width of i-th room on ℓ-th specially designed floor (m)
DRE(L,I)	$D_{R,i}$	Depth of i-th room on ℓ-th specially designed floor (m)
HRE(L,I)	$H_{R,i}$	Height of i-th room on ℓ-th specially designed floor (m)
BRS(I)	$B_{R,i}$	Width of i-th shaft (m)
DRS(I)	$D_{R,i}$	Depth of i-th shaft (m)
HRST(I)		Top height of i-th shaft from a reference (ground) level (m)
HRSB(I)		Bottom height of i-th shaft from a reference (ground) level (m)
BWO		Width of opening (m)
HHO		Soffit height of opening from floor level (m)
HLO		Sill height of opening from floor level (m)
IPR(I)		The room number to which pressure calculation proceeds after Eq. (2.19) is cleared for i-th room (common floor)
IRE(I)		The room number to which pressure calculation returns when Eq. (2.19) is not cleared for i-th room (common floor)
IPRE(I)		Equivalent to IPR(I) (but for specially designed floor)
IREE(I)		Equivalent to IRE(I) (but for specially designed floor)
NRMX		The maximum number of the rooms on any floor
NRMX1		≡ NRMX + 1
NRMX2		≡ NRMX + NSHFT (number of the shafts)
NEX		Floor number of a specially designed floor

NRMX3		≡ NRMX2 + 1
NRMX4		≡ NRMX2 + 4
NFLR1		≡ NFLR + 1
BR(N,I)	$B_{R,i}$	Width (m) } of i-th room on n-th floor *2)
DR(N,I)	$D_{R,i}$	Depth (m) } of i-th room on n-th floor *2)
HR(N,I)	$H_{R,i}$	Height (m) } of i-th room on n-th floor *2)
AR(N,I)	$A_{R,i}$	Floor area (m^2) } of i-th room on n-th floor *2)
HRP(N,I)		Ceiling height (m) } of i-th room on n-th floor from a reference level
HRL(N,I)		Floor height (m) } of i-th room on n-th floor from a reference level
BW(N,I,J,K)	B_W	Width (m) of k-th opening between room i and j on n-th floor
HH(N,I,J,K)	H_h	Soffit height (m) } of k-th opening between room i and j from n-th floor level
HL(N,I,J,K)	H_ℓ	Sill height (m) } of k-th opening between room i and j from n-th floor level
HHP(N,I,J,K)	H_h	Soffit height (m) } of k-th opening between room i and j from a reference (ground) level
HLP(N,I,J,K)	H_ℓ	Sill height (m) } of k-th opening between room i and j from a reference (ground) level
NW(N,I,J)		Number of openings between room i and j on n-th floor
IPRG(N,I)		The room number to which pressure calculation proceeds after Eq. (2.19) is cleared for i-th room on n-th floor
IRET(N,I)		The room number to which pressure calculation returns when Eq. (2.19) is not cleared for i-th room on n-th floor
NRM(N)		Number of the rooms on n-th floor
NDMX(N)		Maximum number of the openings between every combination of two rooms on n-th floor

---

*1) A shaft space must be numbered from NRMX+1; i.e., the smallest number that is assigned to a shaft must be one larger than the maximum number of rooms on any floor.

*2) As a concept, a shaft space is considered to be NFLR+1 times lapped over, in other words, AR(N,I), HRP(N,I), HRL(N,I) etc. are given the same value for any N (N=1, NFLR+1).

(iv) Input

Input	From	Input	From
NFLR	Data	BRS(I)	Data
NEILR	Data	HRST(I)	Data
NSHFT	Data	HRSB(I)	Data
NROM	Data	BWO	Data
HFLR	Data	HHO	Data
NEF(L)	Data	HLO	Data
NEROM(L)	Data	IPR(I)	Data
HEFLR(L)	Data	IRE(I)	Data
BRN(I)	Data	IPRE(I)	Data
DRN(I)	Data	IREE(I)	Data
HRN(I)	Data		
BRE(L,I)	Data		
DRE(L,I)	Data		
HRE(L,I)	Data		

(v) Output

Output	To	Output	To
NFLR	/BULG/	HR(N,I)	/ROOM/
NEFLR	/BULG/	HRP(N,I)	/ROOM/
NSHFT	/BULG/	HLP(N,I)	/ROOM/
NROM	/BULG/	AR(N,I)	/ROOM/
HFLR	/BULG/	BW(N,I,J,K)	/OPEN/
NFLR1	/BULG/	HH(N,I,J,K)	/OPEN/
NRMX	/BULG/	HL(N,I,J,K)	/OPEN/
NRMX1	/BULG/	HHP(N,I,J,K)	/OPEN/
NRMX2	/BULG/	HLP(N,I,J,K)	/OPEN/
NRMX3	/BULG/	NW(N,I,J)	/OPEN/
NRMX4	/BULG/	NRM(N)	/BULG/
NEF(L)	/BULG/	NDMX(N)	/BULG/
NEROM(L)	/BULG/	IPRG(N,I)	/PRES/
HEFLR(L)	/BULG/	IRET(N,I)	/PRES/
BR(N,I)	/ROOM/		
DR(N,I)	/ROOM/		

(vi) Calculation

(a) Floor area of i-th room on n-th floor

$$AR(N,I) = BR(N,I) * DR(N,I)$$

(b) Ceiling height of i-th room on n-th floor from the ground level

$$HRP(N,I) = \begin{cases} HR(N,I) + \sum_{n=1}^{n-1} (\text{n-th floor height}) & \text{(room)} \\ HRST(I) & \text{(shaft)} \\ 999. & \text{(outdoor)} \end{cases}$$

(c) Floor height of i-th room on n-th floor from the ground level

$$HRL(N,I) = \begin{cases} 0 + \sum_{n=1}^{n-1} (\text{n-th floor height}) & \text{(room)} \\ HRSB(I) & \text{(shaft)} \\ 0. & \text{(outdoor)} \end{cases}$$

(d) Height of openings from the ground level

$$HHP(N,I,J,K) = HH(N,I,J,K) + \sum_{n=1}^{n-1} (\text{n-th floor height}) \qquad \text{(soffit)}$$

$$HLP(N,I,J,K) = HL(N,I,J,K) + \sum_{n=1}^{n-1} (\text{n-th floor height}) \qquad \text{(sill)}$$

5.3 TPROP

(i) Task

To input the information on thermal conditions of the rooms in the objective structure.

(ii) Remarks

Generally, the thermal properties of ceiling, floor and walls of a room in a structure may be different from one to another, moreover, each of the walls may consist of various materials. However, here the thermal properties only for homogeneous ceiling and floor are input because the current radiation model has assumed the system composed of only two surfaces, and thermal conduction model has assumed homogeneous slabs.

(iii) Symbols

Code	Paper	Description	
NDIV	N	Number of wall element slices fictitiously assumed for numerical temperature computation	
NDIV1		≡ NDIV + 1: number of points where internal wall temperatures are calculated	
FKWO(I,IW)	k	Thermal conductivity (kcal/msK)	
CWO(I,IW)	c	Specific heat (kcal/kgK)	of the wall of i-th room on commonly designed floor (IW=1; ceiling, IW=2; floor) *1)
RWO(I,IW)	ρ	Density (kg/m^3)	
FLWO(I,IW)	ℓ	Thickness (m) *2)	
EPWO(I,IW)	ε	Emissivity	

FKW(N,I,IW)	k	Thermal conductivity (kcal/msk)	
CW(N,I,IW)	c	Specific heat (kcal/kgK)	of the wall of i-th room on n-th floor (IW=1; ceiling, IW=2; floor)
RW(N,I,IW)	ρ	Density (kg/m^3)	
FLW(N,I,IW)	ℓ	Thickness (m) *2)	
EPW(N,I,IW)	ε	Emissivity	
NFLR, NFLR1, NRMX1, NRMX2 NROM, NEROM(L), NEF(L)		See 5.2 PARAM	

(iv) Input

Input	From	Input	From
FKWO(I,IW)	Data	NDIV	Data
CWO(I,IW)	Data	NFLR	/BULG/
RWO(I,IW)	Data	NFLR1	/BULG/
FLWO(I,IW)	Data	NRMX	/BULG/
EPWO(I,IW)	Data	NRMX1	/BULG/
FKW(NEF(L),I,IW)	Data	NRMX2	/BULG/
CW(NEF(L),I,IW)	Data	NEF(L)	/BULG/
RW(NEF(L),I,IW)	Data	NEROM(L)	/BULG/
FLW(NEF(L),I,IW)	Data		
EPW(NEF(L),I,IW)	Data		

(v) Output

Output	To	Output	To
FKW(N,I,IW)	/WALL/	NDIV	/WALL/
CW(N,I,IW)	/WALL/	FLW(N,I,IW)	/WALL/
RW(N,I,IW)	/WALL/	EPW(N,I,IW)	/WALL/

---

*1) In this model, internal surface of a room, which consists of the ceiling, the floor and the vertical walls, is divided into two parts, i.e., one that is in contact with the upper layer and the other that is in contact with the lower layer for the purpose of simplification of both radiative and convective heat transfer calculation, and it is assumed that each surface is all the time homogeneous, and represented by either the ceiling or the floor. Consequently, when the thermal properties of the walls are significantly different, there is a doubt whether the heat transfer model provides accurate enough predictions.

*2) So far as a fire of relatively short duration is considered, the wall thickness here does not have to be actual thickness. Since it is somewhat tedious to take account of heat flux to the back surface of the wall, this model has assumed the wall thermally insulated on the back whose thickness is a half of that of the actual wall.

5.4 DFIRE

(i) Task

To input the data on fire source and derive the necessary information on heat and species generation due to the combustion of the fuel.

(ii) Remarks

In this subroutine, various information on fire source, e.g., location of fire, chemical composition of fuel, fuel mass loss rate and some other parameters are input. And using these input data, heat of combustion of gasified fuel and rates of species generation are derived based on the combustion model described previously in section 3.1.

(iii) Symbols

Code	Paper	Description
NFF		Floor number where fire is located
IFR		Room number of fire is located
LFP		Parameter regarding fire location in the room of origin (LFP = 1, 2, and 4 represent center, wall and corner respectively
DDT	Δt	Time interval of data input on mass loss rate, area and height of fuel (s)
NTMAX		Number of input data on mass loss rate, area and height of fuel
WC	W_C	Mass fraction of C
WH	W_H	Mass fraction of H
WO	W_O	Mass fraction of O
WN	W_N	Mass fraction of N

(WC, WH, WO, WN: in the dry fuel)

QEXP	$-\Delta H^*_{exp}$	Higher calorific value (enthalpy) of the fuel due to complete combustion (kcal/kg)
TE	T_p	Mean temperature of pyrolysis (K)
QGFY	L^*_g	Heat of gasification (kcal/kg)
WMFL	M_f	Molecular weight of fuel (g/mol) (defaulted value: $M_f = 50$)
W	w	Fraction of dry fuel that turns into char
S	s	Fraction of dry fuel that turns into soot
PM	m	Water content to unit dry fuel
ETA	η	Fraction of the carbon in gasified fuel that results into CO
DHCO	$-\Delta H^*_r$	Enthalpy difference between a reference state fuel and products of complete combustion (kcal/kg)
DHCl	$-\Delta H_r$	Enthalpy difference between a reference state and products of actual burning (kcal/kg)
DHA	$-\Delta H_a$, ΔH	Heat of combustion (enthalpy) of gasified fuel (kcal/kg)
QP	Q_p	Heat needed for unit mass loss (kcal/kg)
GAMA(3)	γ_f	Fuel
GAMA(4)	γ_s	Soot
GAMA(5)	γ_{O_2}	O_2 } generation rate due to the combustion of unit mass of gasified fuel (kg/kg)
GAMA(6)	γ_{CO_2}	CO_2
GAMA(7)	γ_{CO}	CO
GAMA(8)	γ_{H_2O}	H_2O
GAMA(9)	γ_{N_2}	N_2
BFIRED(I)	$\dot{m}_p$	Mass loss rate (kg/s) } of fuel where i is a data number numbered from time = 0
AFIRED(I)		Area (m^2) (not referenced)
HFIRED(I)		Height (m)
CP	C_p	Specific heat of gas (kcal/kgK)
TA	T_a	Ambient temperature (k)

(iv) Input

Input	From	Input	From
NFF	Data	QEXP	Data
IFR	Data	TE	Data
LFP	Data	QGFY	Data
DDT	Data	WMFL	Data
NTMAX	Data	W	Data
WC	Data	S	Data
WH	Data	↑	↑
WO	Data	PM	Data
WN	Data	ETA	Data
		CP	/UNIV/
		TA	/UNIV/

(v) Output

Output	To	Output	To
NFF	/FIRE/	WMFL	/FUEL/
IFR	/FIRE/	W	/FUEL/
LFP	/FIRE/	S	/FUEL/
DDT	/FIRE/	PM	/FUEL/
NTMAX	/FIRE/	ETA	/FUEL/
WC	/FUEL/	DHA	/FUEL/
WH	/FUEL/	QP	/FUEL/
WO	/FUEL/	GAMA(L)	/UNIV/
WN	/FUEL/	BFIRED(I)	/FIRE/
QEXP	/FUEL/	AFIRED(I)	/FIRE/
TE	/FUEL/	HFIRED(I)	/FIRE/

(vi) Calculation

(a) Enthalpy difference between the fuel at a reference state and the products due to complete combustion

$$-\Delta H_r^* = \left(97.6 \frac{W_C}{12} + 68.3 \frac{W_H}{2}\right) \times 10^3$$

(b) Enthalpy difference between the fuel at a reference state and the products due to incomplete combustion

$$-\Delta H_r = \left[\{97.6(1-\eta) + 27.6\eta\} \frac{W_C - w - S}{12(1-w)} + 57.6 \frac{W_H}{2(1-w)}\right] \times 10^3$$

(c) Actual heat of combustion of gasified fuel

$$-\Delta H_a = -\Delta H_r - \{-\Delta H_r^* - (-\Delta H_{exp}^*) - L_g^*\}$$

(d) The heat needed for unit mass loss

$$Q_p = C_p(T_p - T_a) + \frac{0.32W(773-T_a) + L_g^* + 580m}{1 - w + m}$$

(e) Mass generation rate of species

$$\gamma_f = -1$$

$$\gamma_s = \frac{s}{1-w}$$

$$\gamma_{O_2} = -\{(1 - \frac{\eta}{2}) \frac{W_C - w - s}{12} + \frac{W_H}{4} - \frac{1}{2}\frac{W_O}{16}\} \frac{32}{1-w}$$

$$\gamma_{CO_2} = (1-\eta)\ \frac{W_C - w - s}{12}\ \frac{44}{1-w}$$

$$\gamma_{CO} = \eta\ \frac{W_C - w - s}{12}\ \frac{28}{1-w}$$

$$\gamma_{H_2O} = \frac{1}{2}\ W_H\ \frac{18}{1-w}$$

$$\gamma_{N_2} = \frac{W_N}{1-w}$$

5.5 WPRS

(i) Task

To yield the data on outdoor pressure due to wind.

(ii) Remarks

This subroutine inputs outdoor wind velocity and wind pressure coefficient for each of the four external walls of a structure and calculates the pressures of outdoor spaces.

(iii) Symbols

Code	Paper	Description
NWMAX		Number of input data
DWT	Δt	Data input interval (s)
WV(J)	v	j-th input value of wind velocity (m/s)
COEW(I)	C	Wind pressure coefficient for i-th outdoor space
PWIND1(J)	P_1	1-st outdoor space pressure due to wind (P_a) *)
PWIND2(J)	P_2	2-nd outdoor space pressure due to wind (P_a) *)
PWIND3(J)	P_3	3-rd outdoor space pressure due to wind (P_a) *)
PWIND4(J)	P_4	4-th outdoor space pressure due to wind (P_a) *)
RA	ρ_a	Ambient density (kg/m^3)

(iv) Input

Input	From	Input	From
NWMAX	Data	WV(J)	Data
DWT	Data	COEW(I)	Data
RA	/UNIV/		

(v) Output

Output	To	Output	To
PWIND1(J)	/WIND/	NWMAX	/WIND/
PWIND2(J)	/WIND/	DWT	/WIND/
PWIND3(J)	/WIND/		
PWIND4(J)	/WIND/		

(vi) Calculation

$$P_i = C_i \frac{1}{2} \rho_a v^2 \quad (i=1,4)$$

---

*) Elsewhere the four outdoor spaces are numbered following maximum number of indoor spaces on any floor, including shaft spaces, in other words, their number begins with NRMX2+1. But in this subroutine, renumber them from one to four in numerical order of the spaces.

5.6 RKG

(i) Task

To solve the ordinary differential equation for temperature, thickness and species concentration of every upper layer given by Eqs. (2.16) - (2.18) with Runge-Kutta-Gill method.

(ii) Remarks

One of the two main strategies of numerical calculation of this model is in short to integrate the ordinary differential equations for the temperature, the thickness and the species concentrations of the upper layers. In this program, Runge-Kutta-Gill method is picked up among many available methods.

(iii) Symbols

Code	Paper	Description
XO		Initial time
YO(L)		Initial value of upper layer properties
H		Time interval (s)
NX		Number of the time steps
IX		Time step number
X		Time (s)

YW(L,N,I)
Y1(L,N,I)
Y2(L,N,I)
Y3(L,N,I)
} T_s, Z_s, Y_ℓ

Upper layer properties of i-th room on n-th floor.

FRKG(L,N,I) { dT_s/dt, dZ_s/dt, dY_ℓ/dt

The value of differential coefficient

L ℓ

Number assigned to each upper layer property as follows

- 1: Temperature of upper layer
- 2: Thickness of upper layer
- 3: Fuel
- ℓ = { 4: Soot, 5: O_2, 6: CO_2 } mass fraction of upper layer
- 7: CO
- 8: H_2O
- 9: N_2

NFLR, NFLR1
NRMX, NRMX2, NRMX4

See 5.2 PARAM

W(L,N,I)
R1(L,N,I), R2(L,N,I), R3(L,N,I), R4(L,N,I)
Q1((L,N,I), Q2(L,N,I), Q3(L,N,I), Q4(L,N,I)

Work variables

(iv) Input

Input	From	Input	From
XO	MAIN	NX	MAIN
YO	MAIN	IX	MAIN
H	MAIN	FRKG(L,N,I)	DFNC
NX	MAIN		

(v) Output

Output	To	Output	To
YW(L,N,I)	DFNC	H	DFNC
Y1(L,N,I)	DFNC	X	DFNC
Y2(L,N,I)	DFNC		
Y3(L,N,I)	DFNC		

(v) Calculation

Since the scheme used here, Runge-Kutta Gill method, is one of the most popular ones for solving ordinary differential equations, the description is omitted. The readers who are interested in this scheme are advised to reference some appropriate documents, or coded subroutine RKG itself.

5.7 DFNC

(i) Task

To calculate the value of the differential coefficients given by the right hand side of Eqs. (2.16) - (2.18).

(ii) Remarks

The value of the differential coefficients at a given time can be calculated by substituting into each term in the right side of Eqs. (2.16) - (2.18) its value at the time. But the way each term relates to the layer properties is so complex that some subroutines are needed to yield its value. Consequently, physics subroutines are called before the value of the differential coefficients are calculated.

(iii) Symbols

Code	Paper	Description
Y(L,N,I)	T_s, Z_s, T_ℓ	Upper layer property of i-th room on n-th floor that is assigned as follows according to L

$$Y(L,N,I) = \begin{cases} L = 1: & \text{Temperature (K)} \\ L = 2: & \text{Thickness (m)} \\ L = 3: & \text{Fuel} \\ L = 4: & \text{Soot} \\ L = 5: & O_2 \\ L = 6: & CO_2 \\ L = 7: & CO \\ L = 8: & H_2O \\ L = 9: & N_2 \end{cases} \quad \text{mass fraction}$$

TIME	t	Elapsed time from the start of fire (sec)
DT		Time interval (s)
EMP(NFF,IFR)	$\dot{m}_p$	Mass loss rate of fire source in the room of origin (kg/s)
EMS(NFF,IFR)	$\dot{m}_s$	Rate of gas flow that enters the upper layer through fire plume (kg/s)
EME(NFF,IFR)	$\dot{m}_e$	Air entrainment rate into the fire plume ($\dot{m}_e = \dot{m}_s - \dot{m}_p$) (kg/s)
HFEL	h_f	Fire source height from the floor level (m)
HPLM	Z	Distance between fire source and discontinuity (m)
QPLM	$\dot{Q}$	Heat release rate of fire source (kg/s)
P(N,I)	P_i	Relative pressure of i-th room on n-th floor at reference level (P_a)
AW(1)	A_1	Total area (m^2) of
TW(1)	T_1	Surface temperature (K) of — the wall that contact with upper layer
EP(1)	ε_1	Surface emissivity of — the wall that contact with upper layer
QRAD(1)	$\dot{Q}_1$	Total radiative heat (kcal/s) to — the wall that contact with upper layer
QSRAD(1)	$\dot{Q}_1/A_1$	Radiative heat flux ($kcal/m^2s$) to
AW(2)	A_2	Total area (m^2) of
TW(2)	T_2	Surface temperature (K) of — the wall that contact with lower layer
EP(2)	ε_2	Surface emissivity of — the wall that contact with lower layer
QRAD(2)	$\dot{Q}_2$	Total radiative heat (kcal/s) to — the wall that contact with lower layer
QSRAD(2)	$\dot{Q}_2/A_2$	Radiative heat flux ($kcal/m^2s$)
QCV	$\dot{q}_c$	Total convective heat transfer to wall (kcal/s)
QSCV	$\dot{q}_c''$	Convective heat flux to wall ($kcal/m^2s$)
QR(N,I)	$-\dot{Q}_G$	Radiative heat gain — of upper layer (kcal/s) of i-th room on n-th floor
QC(N,I)	$\dot{Q}_C$	Convective heat gain — of upper layer (kcal/s) of i-th room on n-th floor
TWJ(N,I,IW,K)	T	Temperature of the wall (IW = 1: ceiling, IW = 2: floor) of i-th room on n-th floor at k-th interior point

QRADW(N,I,IW)		Total radiative heat (kcal/s)
QSRADW(N,I,IW)		Radiative heat flux ($kcal/m^2s$
QCNV(N,I,IW)		Total convective heat (kcal/s)
QSCNV(N,I,IW)		Convective heat flux ($kcal/m^2s$)

} to the wall of i-th room on n-th floor where IW=1, 2 respectively denote ceiling and surface

VGAS	V	Upper layer volume (m^3)
AGAS	A	Entire boundary area of upper layer (m^2)
PATH	L_m	Upper layer mean path length (m)
TEGAS		Temperature defined as

$$TEGAS = \begin{cases} 300. & (Y(1,N,I) \leq 300.) \\ Y(1,N,I) & (300 < Y(1,N,I) < 2000.) \\ 2000. & (2000. \leq Y(1,N,I)) \end{cases}$$

RSOOT	ρ_{soot}	Soot density (kg/m^3)
FV	f_v	Volume fraction of soot
SOOTK	k_{soot}	Absorption coefficient of soot at a wavelength of 0.94 μm (m^{-1})
EPG(N,I)	ε_G	Emissivity of upper layer of i-th room on n-th floor
PP(4,N,I)		≡ SOOTK of the upper layer of i-th room on n-th floor
PP(L,N,I)		Partial pressure of the gases in the upper layer of i-th room on n-th floor where L is assigned as in Y(L,N,I)
SS(N,I,J,K)	SS_{ij}	Hot gas flow rate above
SA(N,I,J,K)	SA_{ij}	Hot gas flow rate below
AS(N,I,J,K)	AS_{ij}	Air flow rate above
AA(N,I,J,K)	AA_{ij}	Air flow rate below

} the discontinuity of j-th room through k-th opening between i-th and j-th room on n-th floor (kg/s)

SAD(N,I,J,K)	SA'_{ij}	Flow rate of air that enters the upper layer of j-th room through a door jet SA_{ij} (kg/s)
YAM(L)	Y^a_ℓ	Mass fraction of species ℓ in the ambient air
YP(L)	Y^p_ℓ	Mass fraction of species ℓ in the fuel volatile

BURF(N,I)	$\dot{m}_b$	Burning rate	of gasified fuel in the upper layer of i-th room on n-th floor (kg/s)
QF(N,I)	$\Delta H \cdot \dot{m}_b$	Heat release rate	
CP,TA,RA,CR,CF		See 5.1 MAIN	
NFLR,NFLR1,NRM(N),NW(N,I,J) NRMX,NRMX1,NRMX2,NRMX3,NRMX4 HR(N,I),HRP(N,I),HRL(N,I) BR(N,I),DR(N,I),AR(N,I)		See 5.2 PARAM	
BFIRED,DDT,NTMAX DHA,QP,TE,GAMA(L),WMFEL		See 5.4 DFIRE	
PWIND1,PWIND2,PWIND3,PWIND4 DWT,NWMAX		See 5.5 WPRS	
FRKG(L,N,I)		See 5.6 RKG	

(iv) Input

Input	From	Input	From
Y(L,N,I)	RKG	NFLR	/BULG/
TIME	RKG	NFLR1	/BULG/
DT	RKG	NRMX	/BULG/
BFIRED	/FIRE/	NRMX1	/BULG/
HFIRED	/FIRE/	NRMX2	/BULG/
DDT	/FIRE/	NRMX4	/BULG/
NTMAX	/FIRE/	NRM(N)	/BULG/
NFF	/FIRE/	HR(N,I)	/BULG/
IFR	/FIRE/	HRP(N,I)	/BULG/
LFP	/FIRE/	HRL(N,I)	/BULG/
PWIND1	/WIND/	BR(N,I)	/BULG/
PWIND2	/WIND/		

PWIND3	/WIND/	DR(N,I)	/BULG/
PWIND4	/WIND/	AR(N,I)	/BULG/
DWT	/WIND/	NW(N,I,J)	/OPEN/
NWMAX	/WIND/	CP	/UNIV/
SS(N,I,J,K)	/FLOW/	TA	/UNIV/
SA(N,I,J,K)	/FLOW/	RA	/UNIV/
AS(N,I,J,K)	/FLOW/	RSOOT	/UNIV/
AA(N,I,J,K)	/FLOW/	DHA	/FIRE/
SAD(N,I,J,K)	/FLOW/	QP	/FIRE/
YAM(L)	/CONS/	TE	/FIRE/
YP(L)	/CONS/	GAMA(L)	/FIRE/
EMP(NFF,IFR)	INTPOL	WMFL	/FIRE/
EMS(NFF,IFR)	FPLUM	TWJ(N,I,IW,K)	/WALL/
EME(NFF,IFR)	FPLUM	EPW(N,I,IW)	/WALL/
EPG(N,I)	ABSORB	BURF(N,I)	/QGAS/
QR(N,I)	HTRAD4	QF(N,I)	/QGAS/
QC(N,I)	HTCNV1	P(1,NRMX2+I)	INTPOL
CR	/UNIV/	QRAD(IW)	HTRAD4
CF	/UNIV/	QSAD(IW)	HTRAD4
		QCV(IW)	HTCNV1
		QSCV(IW)	HTCNV2

(v) Output

Output	To	Output	To
FRKG(L,N,I)	RKG	EMP(NFI,IFR)	FPLUM
TIME	INTPOL	QPLM	FPLUM
BFIRED	INTPOL	HPLM	FPLUM
HFIRED	INTPOL	TEGAS	ABSORB
DDT	INTPOL	PATH	ABSORB
NTMAX	INTPOL	SOOTK	ABSORB
PWIND1	INTPOL	Y(6,N,I)	ABSORB
PWIND2	INTPOL	Y(8,N,I)	ABSORB
PWIND3	INTPOL	PP(L,N,I)	/CONS/
PWIND4	INTPOL	TW(IW)	HTRAD4, HTCHV1
DWT	INTPOL	AW(IW)	HTRAD4, HTCNV1
NWMAX	INTPOL	EP(IW)	HTRAD4
QSRADW(N,I,IW)	CNDCT	Y(1,N,I)	HTRAD4, HTCNV1
QSCNV(N,I,IW)	CNDCT	QR(N,I)	/QGAS/
DT	CNDCT	QC(N,I)	/QGAS/
EMP(N,I)	FPLUM, /PLUM/	Y(L,N,I)	VENTL
EMS(N,I)	/PLUM/		
EME(N,I)	/PLUM/		

(vi) Calculation

(a) Mass loss rate

$$\dot{m}_p = \text{INTPOL}(t)$$

(b) Outdoor space pressure

$$P_{NRMX2+i} = \text{INTPOL}(t)$$

(c) Fire plume entrainment

$$\dot{Q} = \{\Delta H_a - Q_p + C_p(T_p - T_a)\}\,\dot{m}_p \qquad \text{Heat release rate}$$

$$Z = H_R - h_f - Z_s \qquad \text{Distance between discontinuity and source}$$

$$\left.\begin{matrix}\dot{m}_s \\ \dot{m}_e\end{matrix}\right\} = \text{FPLUM}(\dot{Q}, Z, \dot{m}_p) \qquad \text{Rate of plume flow and air entrainment}$$

(d) Emissivity of upper layer

$$A_1 = A_R + 2(B_R + D_R)\,Z_s \qquad \text{Total wall area that contact with upper layer}$$

$$A = A_R + A_1 \qquad \text{Entire boundary area of upper layer}$$

$$V = A_R Z_s \qquad \text{Upper layer volume}$$

$$L_m = 3.6\,\frac{V}{A} \qquad \text{Mean path length}$$

$$f_v = \frac{\rho_s}{\rho_{soot}} Y_{soot} = \frac{\rho_a T_a}{T_s} \cdot \frac{Y_{soot}}{\rho_{soot}}$$ Volume fraction of soot

$$k_{soot} = \frac{7 f_v}{0.94 \times 10^{-6}}$$ Soot absorption coefficient

$$S = \frac{Y_{O_2}}{32} + \frac{Y_{CO_2}}{44} + \frac{Y_{CO}}{28} + \frac{Y_{H_2O}}{18} + \frac{Y_{N_2}}{28} + \frac{Y_f}{M_f}$$

$$P_{CO_2} = \left(\frac{Y_{CO_2}}{44} \right) / S$$ CO_2 partial pressure

$$P_{H_2O} = \left(\frac{Y_{H_2O}}{18} \right) / S$$ H_2O partial pressure

ε_G = ABSORB (T_S, L_m, k_{soot}, P_{CO_2}, P_{H_2O}) Hot gas layer emissivity

(e) Radiation heat transfer

$$A_1 = A_R + 2(B_R + D_R) Z_S$$

$$A_2 = A_R + 2(B_R + D_R)(HRP - HRL - Z_S)$$ Total wall area that contact with lower layer

$$\left.\begin{matrix} \dot{Q}_1 \\ \dot{Q}_2 \\ \dot{Q}_1/A_1 \\ \dot{Q}_2/A_2 \\ \dot{Q}_G \end{matrix}\right\} = \text{HTRAD4}(T_1, T_2, T_s, A_1, A_2, A_R, \varepsilon_1, \varepsilon_2, \varepsilon_G)$$

(f) Convective heat transfer

$$\left.\begin{matrix}\dot{q}_c \\ \\ \dot{q}''_c\end{matrix}\right\} = \text{HTCNV1}\ (T_s,\ T_l,\ A_l)$$

(g) Thermal conduction

TWJ = CNDCT ($\dot{q}''_{in}$, $\dot{q}''_{out}$) Wall temperature

(h) Rate of opening flow

$$\left.\begin{matrix}SS_{ij} \\ SA_{ij} \\ AS_{ij} \\ AA_{ij} \\ SA_{ij}\end{matrix}\right\} = \text{RFLOW(Y)}$$

$\dot{m}_b$

$\dot{Q}_F$

(i) Differential coefficient

$$\frac{dT_s}{dt} = \frac{T_s}{C_p \rho_a T_a A_R Z} \left(\dot{Q}_F + \dot{Q}_R + \dot{Q}_C - Q_p \dot{m}_p\right)$$

$$+ \frac{T_s}{\rho_a T_a A_R Z_s} \left[\sum \{(T_{s,j} - T_s)(SS_{ji} + SA_{ji}) + (T_a - T_s)(SA'_{ji} - SA_{ji} + \lambda AS_{ji})\}\right.$$

$$\left. + (T_p - T_s)\dot{m}_p + (T_a - T_s)(\dot{m}_s - \dot{m}_p)\right]$$

$$\frac{dZ_s}{dt} = \frac{1}{C_p \rho_a T_a A_R} \left(\dot{Q}_F + \dot{Q}_R + \dot{Q}_C - Q_p \dot{m}_p\right)$$

$$+ \frac{1}{\rho_a T_a A_R} \left[\sum \{T_{s,j}(SS_{ji} + SA_{ji}) - T_S(SS_{ij} + SA_{ij}) + T_a(SA'_{ji} - SA_{ji} + \lambda AS_{ji})\}\right.$$

$$\left. + T_p \dot{m}_p + T_a (\dot{m}_s - \dot{m}_p)\right]$$

$$\frac{dY_\ell}{dt} = \frac{T_S}{P_a T_a A_R Z_S} \left[\sum \{(Y_{\ell,j} - Y_\ell)(SS_{ji} + SA_{ji}) + (Y^a_\ell - Y_\ell)(SA'_{ji} - SA_{ji} + \lambda AS_{ji})\}\right.$$

$$\left. + \gamma_\ell \dot{m}_b + (Y^P_\ell - Y_\ell)\dot{m}_p + (Y^a_\ell - Y_\ell)(\dot{m}_s - \dot{m}_p)\right]$$

in which

summation $\sum$ is taken with respect to $\begin{cases} j \text{ and } k \text{ (when i represents a room)} \\ n, j \text{ and } k \text{ (when i represents a shaft)} \end{cases}$

5.8 INTPOL

(i) Task

To interpolate the input data for a given time.

(ii) Remarks

This subroutine is used to obtain mass loss rate, fire source height and outdoor pressure for a given time by interpolating their data which have been input at every constant time interval.

(iii) Symbols

Code	Paper	Description
TIME	t	Elapsed time after the start of fire (s)
DLTT	Δt	Time interval (constant) of data input (s)
DSRCE(I)	d_i	Value of i-th input datum (i=1 corresponds to t=0)
TI1	t_{i+1}	Time at which (i+1)-th datum is located (= Δt x i)
TI	t_i	Time at which i-th datum is located (= Δt x (i-1))
NMAX	n_{max}	Number of input data
TMAX	t_{max}	Time at which the last input datum is located
DATT	d_t	Interpolated value of data at a given time t

(iv) Input

Input	From	Input	From
TIME	DFNC	NMAX	DFNC
DLTT	DFNC	DSRCE	DFNC

(v) Output

Output	To
DATT	DFNC

(vi) Calculation

(a) When $t < t_{max}$

$$d_t = \frac{(t_{i+1} - t)\, d_i - (t_i - t)\, d_{i+1}}{\Delta t}$$

(b) When $t_{max} < t$

$$d_t = d_{n_{max}}$$

5.9 FPLUM

(i) Task

To calculate the mass flow rate of plume gas that enters the hot upper layer of the room of origin.

(ii) Remarks

This subroutine calculates the mass flow rate of plume gas that enters the upper layer. The equations here were presented by McCaffrey (NBS) based on his experimental analysis of burner fire.

(iii) Symbols

Code	Paper	Description
Z	Z	Distance between discontinuity and fire source (see 5.7 DFNC)
QFPLUM	$\bar{Q}$	Heat release rate (kcal/s)
R	$\dot{m}_p$	Mass loss rate (kg/s)
FMZ	$\dot{m}_s$	Flow rate of plume gas that enters upper layer (kg/s)
EMZ	$\dot{m}_e$	Air entrainment into the plume (kg/s)
LFP		Fire location parameter

(iv) Input

Input	From	Input	From
QFPLM	DFNC	Z	DFNC
LFP	DFNC	R	DFNC

(v) Output

Output	To	Output	To
FMZ	DFNC	EMZ	DFNC

(vi) Calculation

$$\dot{Q} = 4.187\ \bar{Q} \cdot LFP$$

$$\frac{\dot{m}_s}{\dot{Q}} = \begin{cases} 0.011\ \left(\frac{Z}{\dot{Q}^{2/5}}\right)^{0.566} /LFP & \left(0 < \frac{Z}{\dot{Q}^{2/5}} < 0.08\right) \\ 0.026\ \left(\frac{Z}{\dot{Q}^{2/5}}\right)^{0.909} /LFP & \left(0.08 < \frac{Z}{\dot{Q}^{2/5}} < 0.2\right) \\ 0.124\ \left(\frac{Z}{\dot{Q}^{2/5}}\right)^{1.895} /LFP & \left(0.2 < \frac{Z}{\dot{Q}^{2/5}}\right) \end{cases}$$

$$\dot{m}_e = \dot{m}_s - \dot{m}_p$$

5.10 DRJET

(i) Task

To calculate mass flow rate of doorjet gas that enters the hot upper layer.

(ii) Remarks

The nature of buoyant doorjet entrainment has not yet been fully clarified, nevertheless we need some means to estimate the entrainment rate. So this model is devised based on the crude assumption that doorjet behaves as if it were a vertical thermal plume rising up from the doorjet level, which means the same equations as for fire plume entrainment are used only by replacing the heat release rate of fire source with the enthalpy of the doorjet. It may be more desirable to take account of heat release of combustion when the doorjet flow contains fuel, but this is ignored for its complexity.

(iii) Symbols

Code	Paper	Description
Z	Z	Distance between discontinuity and doorjet
TJ	$T_{s,j}$	Doorjet temperature, which is the same as upper layer temperature of j-th room (K)
SA	SA_{ji}	Opening flow rate of hot gas below the discontinuity of i-th room
FMZ	SA'_{ji}	Flow rate of doorjet gas that enters the upper layer of i-th room (kg/s)
CP	C_p	Specific heat of gas at constant pressure (kcal/kgK)
TA	T_a	Ambient temperature (K)
QJ	Q	Door jet enthalpy (kW)

(iv) Input

Input	From	Input	From
TJ	VENTL	Z	VENTL
SA	VENTL	CP	/UNIV/
		TA	/UNIV/

(v) Output

Output	To
FMZ	VENTL

(vi) Calculation

$$\dot{Q} = 4.187\ C_p SA_{ji}(T_{s,j} - T_a)$$

$$\frac{Z_o}{\dot{Q}^{2/5}} = \begin{cases} \left(\frac{SA_{ji}}{\dot{Q}} \cdot \frac{1}{0.0011}\right)^{1/0.566} & \left(0 < \frac{Z_o}{\dot{Q}^{2/5}} < 0.08\right) \\ \left(\frac{SA_{ji}}{\dot{Q}} \cdot \frac{1}{0.026}\right)^{1/0.909} & \left(0.08 < \frac{Z_o}{\dot{Q}^{2/5}} < 0.20\right) \\ \left(\frac{SA_{ji}}{\dot{Q}} \cdot \frac{1}{0.124}\right)^{1/1.895} & \left(0.20 < \frac{Z_o}{\dot{Q}^{2/5}}\right) \end{cases}$$

$$0.011 \left(\frac{Z+Z_o}{\dot{Q}^{2/5}} \right)^{0.566} \qquad \left(0 < \frac{Z+Z_o}{\dot{Q}^{2/5}} < 0.08\right)$$

$$\frac{SA'_{ji}}{\dot{Q}} = \begin{cases} 0.026 \left(\frac{Z+Z_o}{\dot{Q}^{2/5}} \right)^{0.909} & \left(0.08 < \frac{Z+Z_o}{\dot{Q}^{2/5}} < 0.2\right) \\ 0.124 \left(\frac{Z+Z_o}{\dot{Q}^{2/5}} \right)^{1.895} & \left(0.2 < \frac{Z+Z_o}{\dot{Q}^{2/5}}\right) \end{cases}$$

5.11 ABSORB (Code by Ashok T. Modak)

(i) Task

To compute the emissivity of hot upper layer.

(ii) Remarks

This subroutine, which is a Modak's creation, together with subroutines ASYMP, CHEBY, DLECK, EGAS, PENTA, SOOT and SCRTCH, computes the absorptivity of isothermal and homogeneous mixture of soot, CO_2 and H_2O at a total pressure of 1 atm and a temperature 300 $\sim$ 2,000 K [7].

The gas emissivity generally differs from its absorptivity when temperature of radiation source is not the same as that of gas, however, the difference between the two is not so significant in many practical fire situations. Accordingly, the gas temperature is simply input in place of external radiation source temperature to obtain the gas emissivity.

(iii) Symbols (arguments only)

Code	Paper	Description
TS		Blackbody source temperature (K)
T	T_S	Mixture temperature (K)
PATH	L_m	Mixture path length (m)
SOOTK	k_{soot}	Absorption coefficient of soot at a wave length of 0.94 μm (m^{-1})
PCO2	P_{CO_2}	CO_2 } partial pressure whose
PH2O	P_{H_2O}	H_2O } total pressure is 1 atm
ALPHA	ε_G	Absorptivity (emissivity) of the mixture

(iv) Input

Input	From	Input	From
T	DFNC	PCO2	DFNC
PATH	DFNC	PH2O	DFNC
SOOTK	DFNC		

(v) Output

Output	To
ALPHA	ε_G

(vi) Calculation

See ref. [7], [8].

5.12 HTRAD4

(i) Task

To calculate radiation heat transfer to the walls in a room that contains a hot upper layer.

(ii) Remarks

This subroutine computes the radiation heat transfer to the internal room surface assuming that the surface is divided into two uniform surfaces, i.e., one that is in contact with upper layer and the other that is in contact with lower layer. The two internal surfaces and hot gas layers are assumed gray.

(iii) Symbols

Code	Paper	Description
I	i	Wall surface number (i=1,2 respectively represents the wall that is in contact with upper and lower layer)
T(I)	T_i	Surface temperature (K) of wall i
AW(I)	A_i	Surface area (m^2) of wall i
EP(I)	ϵ_i	Emissivity of wall i
AD	A_d	Area of discontinuity (the same as the floor area) (m^2)
EG	ϵ_G	Upper layer emissivity
TG	T_G, T_S	Upper layer temperature (K)
QRAD(I)	$-\dot{Q}_i$	Total radiative heat transfer to wall i (kcal/s)

QSRAD(I)	$-\dot{Q}_i/A_i$	Radiative heat flux to wall i (kcal/s)
QRADG	$-\dot{Q}_G$, $\dot{Q}_R$	Radiative heat gain of upper layer (kcal/s)
F11	F_{11}	
F12	F_{12}	
F21	F_{21}	View factor between the surfaces
F22	F_{22}	
F2G	F_{2G}	
SIGM	σ	Stefan-Boltzmann constant

(iv) Input

Input	From	Input	From
T(I)	DFNC	EG	DFNC
AW(I)	DFNC	TG	DFNC
EP(I)	DFNC	SIGM	/UNIV/
AD	DFNC		

(v) Output

Output	To	Output	To
QRAD(I)	DFNC	QRADG	DFNC
ASRAD(I)	DFNC		

(vi) Calculation

(a) View factors

$$F_{11} = 1-A_d/A_1$$

$$F_{12} = A_d/A_1$$

$$F_{21} = A_d/A_2$$

$$F_{22} = 1-A_d/A_2$$

$$F_{2G} = A_d/A_2$$

(b) Radiative heat transfer

$$\dot{Q}_1/A_1 = - \varepsilon_1 P_1/D$$

$$\dot{Q}_2/A_2 = - \varepsilon_2 P_2/D$$

$$\dot{Q}_G = -(\dot{Q}_1 + \dot{Q}_2)$$

where

$$D = \{1-(1-\varepsilon_1)(1-\varepsilon_G)F_{11}\}\{1-(1-\varepsilon_2)F_{22}\}-(1-\varepsilon_1)(1-\varepsilon_2)(1-\varepsilon_G)^2F_{12}F_{21}$$

$$P_1 = [\{1-(1-\varepsilon_G)F_{11}\}\{1-(1-\varepsilon_2)F_{22}\}-(1-\varepsilon_2)(1-\varepsilon_2)(1-\varepsilon_G)^2F_{12}F_{21}]\sigma T_1^4$$
$$-(1-\varepsilon_G)F_{12}\varepsilon_2\sigma T_2^4-[1+(1-\varepsilon_2)\{(1-\varepsilon_G)F_{12}F_{2G}-F_{22}\}]\varepsilon_G\sigma T_G^4$$

$$P_2 = [\{1-(1-\varepsilon_1)(1-\varepsilon_G)F_{11}\}(1-F_{22})-(1-\varepsilon_1)(1-\varepsilon_G)^2F_{12}F_{21}]\sigma T_2^4$$
$$-(1-\varepsilon_G)F_{21}\varepsilon_1\sigma T_1^4-[\{1-(1-\varepsilon_1)(1-\varepsilon_G)F_{11}\}F_{2G}+(1-\varepsilon_1)(1-\varepsilon_G)F_{21}]\varepsilon_G\sigma T_G^4$$

5.13 HTCNV1

(i) Task

To calculate convective heat transfer to the walls that are in contact with upper layer.

(ii) Remarks

This subroutine includes the formulas for convective heat transfer for vertical wall, ceiling and floor. However, only the heat transfer to the wall that is in contact with hot upper layer is computed using the formula for ceiling because the heat transfer to lower layer has been ignored in the current model.

The gas properties associated with the heat transfer are substituted by those of air. The formulas for Nusselt number were quoted from the results for natural convection, which may not be fairly adequate in the presence of turbulence caused by fire plume and/or doorjet.

(iii) Symbols

Code	Paper	Description
TG	T_G, T_S	Gas temperature (K)
TW	T_w	Surface temperature (K) of the wall that is in contact with upper layer
AW	A_W, A_1	Surface area (m^2) of the wall that is in contact with upper layer
L	ℓ	Reference length of heat transfer (m)

V	ν	Kinematic viscosity (m^2/s)	of the gas
A	a	Thermal diffusivity (m^2/s)	
LMD	k	Thermal conductivity (kcal/msK)	
G	g	Gravitational acceleration (m/s^2)	
PR	Pr	Prandtl number ($\equiv \nu/a$)	
GR	Gr	Gashof number ($\equiv g\ell^3(T_G-T_W)/\nu^2 T_G$)	
NU	Nu	Mean nusselt number ($\equiv h\ell/k$)	
ACC	h	Mean heat transfer coefficient ($kcal/m^2sK$)	
QSCNV	$\dot{q}''_c$	Convective heat flux to the wall ($kcal/m^2s$)	
QCNV	$\dot{q}_c$	Rate of convective heat transfer to the wall (kcal/s)	

(iv) Input

Input	From	Input	From
TG	DFNC	G	/UNIV/
TW	DFNC		
AW	DFNC		

(v) Output

Output	To	Output	To
QSCNV	DFNC	QCNV	DFNC

(vi) Calculation

(a) Reference length of heat transfer

$$\ell = \sqrt{A_w}$$

(b) Gas properties

$$\nu = 7.18 \times 10^{-10} \left(\frac{T_G + T_W}{2} \right)^{7/4}$$

$$k = 6.50 \times 10^{-8} \left(\frac{T_G + T_W}{2} \right)^{4/5}$$

$$P_r = 0.72$$

$$G_r = \frac{g\ell^3 (T_G - T_W)}{\nu^2 T_G}$$

(c) Nusselt number for a ceiling and heat transfer

$$Nu = \begin{cases} 0.054 \ (G_r \cdot P_r)^{0.38} & (T_G > T_W) \\ 0.0029 \ (G_r \cdot P_r)^{0.38} & (T_G < T_W) \end{cases}$$

$$h = \frac{k}{\ell} N_u$$

$$\dot{q}''_c = h(T_G - T_W)$$

$$\dot{q}_c = \dot{q}''_c A_w$$

5.14 CNDCT

(i) Task

To obtain surface temperature of a wall by solving thermal conduction equation for the wall.

(ii) Remarks

This subroutine solves one dimensional (inward direction) thermal conduction equation by Gauss-Seidel iteration scheme. Temperature dependence of thermal properties and moisture content of a wall are neglected for simplicity, and only a wall of uniform material is considered.

(iii) Symbols

Code	Paper	Description
NL, NDIV	N	Number of wall element slice fictitiously assumed for numerical temperature computation
NL1		Number of points where internal wall temperature are calculated (=N+1)
FKW(N,I,L)	k	Thermal conductivity (kcal/msK)
FLW(N,I,L)	ℓ	Thickness (m)
CW(N,I,L)	c	Specific heat (kcal/kgK)
RW(N,I,L)	ρ	Density (kg/m^3)
TWJ(N,I,L,K)	T	Temperature of ℓ-th wall of i-th room on n-th floor at k-th internal point

(FLW, CW, RW: of the wall of i-th room on n-th floor (L=1: ceiling, L=2: floor))

TJ(K)	$T_{k,j}$	Temperature of k-th internal point at preceding time step (K)
TJ1(K)	$T_{k,j+1}$	Temperature of k-th internal point at current time step (K)
QDIN	$\dot{q}''_{in}$	Heat flux to the front surface of the wall ($kcal/m^2s$)
QDOUT	$\dot{q}''_{out}$	Heat loss flux from the back surface of the wall ($kcal/m^2s$) *1)
ACR		Conversion criteria
DT	Δt	Time interval (s)
DX	Δx	Distance between internal points where temperature is calculated (m)
	n	Iteration step number
K	k	Internal point number where temperature is calculated
	j	Number to distinguish the current time step from the preceding step

(iv) Input

Input	From	Input	From
FKW(N,I,L)	/WALL/	NDIV	/WALL/
FLW(N,I,L)	/WALL/	QDIN	DFNC
CW(N,I,L)	/WALL/	QDOUT	DFNC
RW(N,I,L)	/WALL/	DT	DFNC
TWJ(N,I,L,K)	/WALL/		

(v) Output

Output	To
TWJ(N,I,L,K)	/WALL/

(vi) Calculation

(a) Constants

$$\Delta x = \frac{\ell}{N}$$

$$r = \frac{\Delta t}{(\Delta x)^2} \quad (\frac{k}{c\rho})$$

(b) Temperature of internal points

$$T^{n+1}_{o,j+1} = \frac{r}{1+r}\left(T^{n}_{1,j+1} + \frac{\Delta x}{k}\dot{q}''_{in}\right) + \frac{b_{o,j}}{1+r} \qquad \text{(front surface k=1)}$$

$$T^{n+1}_{k,j+1} = \frac{r}{2(1+r)}\left(T^{n}_{k+1,j+1} + T^{n+1}_{k-1,j+1}\right) + \frac{b_{k,j}}{1+r} \qquad \text{(internal point)}$$

$$T^{n+1}_{N,j+1} = \frac{r}{1+r}\left(T^{n+1}_{N-1,j+1} - \frac{\Delta x}{k}\dot{q}''_{out}\right) + \frac{b_{N,j}}{1+r} \qquad \text{(back surface k=N+1)}$$

where superscript n denote iteration step number and

$$b_{o,j} = T_{o,j} + r\left(T_{1,j} - T_{o,j} + \frac{\Delta x}{k}\dot{q}''_{in}\right)$$

$$b_{k,j} = T_{k,j} + \frac{r}{2}\left(T_{k+1,j} - 2T_{k,j} + T_{k-1,j}\right)$$

$$b_{N,j} = T_{N,j} + r\left(T_{N-1,j} - T_{N,j} - \frac{\Delta x}{k}\dot{q}''_{out}\right)$$

---

*1) In this program, $\dot{q}''_{out}$ has been taken as 0 assuming that a fire duration is so short that it does not raise the temperature of the back surface of the wall.

5.15 VENTL

(i) Task

To solve the pressure equation given by Eq. (2.19) to yield the flows through openings.

(ii) Remarks

This subroutine primarily deals with the solution of the algebraic equation given by (2.19) together with subroutines RFLOW, PSET, and DRJET. The calculation is executed iteratively changing the pressures until a convergence criterion is cleared for every room in the objective structure. And once Eq. (2.19) is solved for every pressure, the solution of the opening flows throughout the structure and the burning rate of gasified fuel are automatically obtained.

(iii)

Code	Paper	Description
ACR		Convergence criterion
ACR2		Convergence criterion *1)
KA(N,I)		Work variable
M(N,I)		Work variable to count the iteration step
ZD	Z	Distance between discontinuity and door jet (m)
XNAS	X_{nas}	Neutral zone height at the opening

*1) A convergence criterion to ease the criterion that is given by ACR when convergence for a shaft has not been obtained within certain number of iteration steps

LCNTL		The number of species that control burning rate LCNTL = {3: fuel 5: oxygen
YLCNT(N,I)		Mass fraction of burning control species of the upper layer of i-th room on n-th floor *2)
BURF(N,I)	$\dot{m}_b$	Burning rate of gasified fuel in the upper layer of i-th room on n-th floor (kg/s)
P(N,I)	P_i	Relative pressure of i-th room on n-th floor at a reference level (Pa)
SGQ(N,I)	Δ_i	The value of pressure equation for guess pressures
Y(L,N,I),YAM(L),YP(L)		
SS(N,I,J,K),SA(N,I,J,K)		See 5.7 DFNC
AS(N,I,J,K),AA(N,I,J,K),SAD(N,I,J,K)		See 5.7 DFNC
QF(N,I),QR(N,I),QC(N,I)EMP(N,I),EMS(N,I)		See 5.7 DFNC
NFLR,NFLR1,NSHFT,NW(N,I,J),NRM(N)		See 5.2 PARAM
NRMX2,NRMX4		See 5.2 PARAM
HHP(N,I,J,K), HLP(N,I,J,K),HRP(N,I)		See 5.2 PARAM
IPRG(N,I),IRET(N,I)		
CP, TA, RA		See 5.1 MAIN
DHA, GAMA(L), TE		See 5.4 DFIRE

*2) This variable equals Y(LCNTL,N,I) for Y(LCNTL,N,I) $\geq$ 0 and equals 0 for Y(LCNTL,N,I) < 0. This is introduced to avoid the concentration of species that controls burning rate from taking negative value for numerical reason.

(iv) Input

Input	From	Input	From
Y(L,N,I)	DFNC	HHP(N,I,J,K)	/OPEN/
YAM(L)	/CONS/	HRP(N,I)	/ROOM/
YP(L)	/CONS/	HRL(N,I)	/ROOM/
SS(N,I,J,K)	/FLOW/	NRM(N)	/BLDG/
SA(N,I,J,K)	/FLOW/	NW(N,I,J)	/OPEN/
AS(N,I,J,K)	/FLOW/	IPRG(N,I)	/PRES/
AA(N,I,J,K)	/FLOW/	IRET(N,I)	/PRES/
SAD(N,I,J,K)	DRJET	NFLR	/BULG/
QR(N,I)	/QGAS/	NFLR1	/BULG/
QC(N,I)	/QGAS/	NSHFT	/BULG/
EMP(N,I)	/PLUM/	NRMX2	/BULG/
EMS(N,I)	/PLUM/	NRMX4	/BULG/
CP	/UNIV/	TE	/FUEL/
TA	/UNIV/	QP	/FUEL/
XNAS	RFLOW	GAMA(L)	/FUEL/
		DHA	/FUEL/

(v) Output

Output	To	Output	To
KA(N,I)	PSET	ZD	DRJET
M(N,I)	PSET	SA(N,I,J,K)	DRJET, /FLOW/
SGQ(N,I)	PSET	SAD(N,I,J,K)	/FLOW/
P(N,I)	PSET, RFLOW	BURF(N,I)	/QGAS/
Y(L,N,I)	RFLOW	QF(N,I)	/QGAS/
Y(1,N,J)	DRJET		

(vi) Calculation

(a) Rates of opening flow

$$\left.\begin{matrix} SS_{ij} \\ SA_{ij} \\ AS_{ij} \\ AA_{ij} \end{matrix}\right\} = \text{RFLOW}\ (P_i,\ P_j,\ T_s,\ T_{s,j},\ Z_s,\ Z_{s,j})$$

(b) Doorjet entrainment

$$Z = H_R - Z_S - \{\min(H_h,\ H_R - Z_s) + \max(X_{nas},\ H_\ell,\ H_{R,j} - Z_{s,j})\}/2$$

$$SA'_{ji} = \text{DRJET}\ (T_{s,j},\ SA_{ji},\ Z)$$

(c) Burning rate

$$\dot{m}_p = \begin{cases} \Sigma\{Y_{f,j}(SS_{ji}+SA_{ji}) - Y_f(SS_{ij}+SA_{ij}) + Y_f^a(SA'_{ji}-SA_{ji}+\lambda AS_{ji})\} \\ \quad + Y_f^p\,\dot{m}_p + Y_f^a\,(\dot{m}_s - \dot{m}_p) \qquad (Y_{O_2} > 0) \\ \dfrac{1}{Y_{O_2}}\,[\Sigma\{Y_{O_2,j}(SS_{ji}+SA_{ji}) - Y_{O_2}(SS_{ij}+SA_{ij}) + Y_{O_2}^a(SA'_{ji}-SA_{ji}+\lambda AS_{ji})\} \\ \quad + Y_{O_2}^p\,\dot{m}_p + Y_{O_2}^a\,(\dot{m}_s - \dot{m}_p)] \qquad (Y_{O_2} = 0) \end{cases}$$

in which summation is taken with respect to j and k in case of a room and n, j and k in case of a shaft.

(d) Heat release rate of gasified fuel

$$\dot{Q}_F = \Delta H_a \dot{m}_b$$

(e) Pressure equation

$$\Delta_i = \frac{\dot{Q}_F + \dot{Q}_R + \dot{Q}_C - \dot{Q}_p \dot{m}_p}{C_p T_a} + \frac{1}{T_a} \Sigma\{T_{s,j}(SS_{ji}+SA_{ji})-T_S(SS_{ij}+SA_{ij})\}$$

$$+ \Sigma\{(AS_{ji} + AA_{ji}) - (AS_{ij} + AA_{ij})\} + \frac{T_p}{T_a} \dot{m}_p$$

in which Σ is taken as in (c) Burning rate

(f) New pressure guess

$$i \leftarrow \begin{cases} IPRG(i) & (|\Delta_i| \leq ACR) \\ IRET(i) & (|\Delta_i| > ACR) \end{cases}$$

and

$$P_i = PSET\ (\Delta_i)$$

5.16 RFLOW

(i) Task

To calculate the rate of flows through an opening when the conditions of each side of the opening are given.

(ii) Remarks

This subroutine computes the rates of hot gas and air flows through a given opening when the relative pressure at a reference level, and the temperature and the thickness of the upper layer of each side of the opening are known.

(iii) Symbols

Code	Paper	Description
ZA(N,I)	$Z_{a,i}$	Distance between the discontinuity in i-th room on n-th floor and a reference (ground) level (m)
RS(N,I)	$\rho_{s,i}$	Density of the upper layer of i-th room on n-th floor (kg/m^3)
XNAS	X_{nas}	Neutral zone height between the upper layer and the lower layer in the adjacent room (m)
XNSS	X_{nss}	Neutral zone height between the two adjacent upper layers (m)
Y(1,N,I)	$T_{s,i}$	Temperature (K) of the upper layer in i-th room on n-th floor
Y(2,N,I)	$Z_{s,i}$	Thickness (m) of the upper layer in i-th room on n-th floor
P(N,I)	P_i	Relative pressure of i-th room on n-th floor at a reference (ground) level (Pa)

SS(N,I,J,K), SA(N,I,J,K) AS(N,I,J,K), AA(N,I,J,K)	See 5.7 DFNC
HHP(N,I,J,K), HLP(N,I,J,K), HRP(N,I)	See 5.2 PARAM
BWI(N,I,J,K) = BW(N,I,J,K)	See 5.2 PARAM
RA, TA, ALP, ALD, G	See 5.1 MAIN

(iv) Input

Input	From	Input	From
Y(1,N,I)	VENTL	RA	/UNIV/
Y(2,N,I)	VENTL	TA	/UNIV/
P(N,I)	VENTL	ALP	/UNIV/
HHP(N,I,J,K)	/OPEN/	ALD	/UNIV/
HLP(N,I,J,K)	/OPEN/	G	/UNIV/
BWO(N,I,J,K)	/OPEN/		
HRP(N,I)	/ROOM/		

(v) Output

Output	To	Output	To
SS(N,I,J,K)	/FLOW/	AS(N,I,J,K)	/FLOW/
SA(N,I,J,K)	/FLOW/	AA(N,I,J,K)	/FLOW/

(vi) Calculation

(a) Height of discontinuity from a reference level

$$Z_{a,i} = H_{RP,i} - Z_{s,i}$$

$$Z_{a,i} = H_{RP,j} - Z_{s,j}$$

This subroutine provides the formulas of opening flow rates only when $Z_{a,i}$ is smaller that $Z_{a,j}$; so subscripts i and j are exchanged when $Z_{a,i}$ is larger than $Z_{a,j}$.

(b) Hot layer density

$$P_S = \rho_a T_a / T_s$$

however, the following manipulation is made to avoid zero divide in the calculation of neutral zone height when the concerning layer temperatures are the same.

$$\rho_s = \rho_a - 1.0 \times 10^{-4} \qquad (\rho_a - \rho_s \leq 1.0 \times 10^{-4})$$

and

$$\rho_{s,i} = \rho_{s,j} - 1.0 \times 10^{-4} \qquad (0 < \rho_{s,j} - \rho_{s,i} \leq 1.0 \times 10^{-4})$$

$$\rho_{s,j} = \rho_{s,i} - 1.0 \times 10^{-4} \qquad (0 \leq \rho_{s,i} - \rho_{s,j} \leq 1.0 \times 10^{-4})$$

(c) Neutral zone height

$$X_{nas} = \frac{P_j - P_i}{(\rho_a - \rho_{s,i})g} + Z_{a,i}$$

$$X_{nss} = \frac{P_j - P_i}{(\rho_{s,j} - \rho_{s,i})g} + \frac{\rho_a - \rho_{s,i}}{\rho_{s,j} - \rho_{s,i}} Z_{a,i} + \frac{\rho_{s,j} - \rho_a}{\rho_{s,j} - \rho_{s,i}} Z_{a,j}$$

(d) Rate of opening flows

See Table 3.1

5.17 PSET

(i) Task

To give the pressure of a room new guess value.

(ii) Remarks

This subroutine to guess the pressure solution, which is basically a Regula-Falsi method, is devised considering the fact that the pressure function Δ_i is a monotonously decreasing function with respect to P_i.

(iii) Symbols

Code	Paper	Description
DP	ΔP	Pressure increment
P(N,I)	P	The latest
P1(N,I)	P_1	A preceding
P2(N,I)	P_2	A preceding
		pressure guess of i-th room on n-th floor
SQ(N,I)	Δ	The latest
SQ1(N,I)	Δ_1	A preceding
SQ2(N,I)	Δ_2	A preceding
		value of pressure function of i-th room on n-th floor
KA(N,I), M(N,I)		See 5.8 VENTL

(iv) Input

Input	From	Input	From
P(N,I)	VENTL	SQ(N,I)	VENTL

(v) Output

Output	To
P(N,I)	VENTL

(vi) Calculation

(a) Before marching first changes the sign of Δ_i

$$P_1 \leftarrow P,\ \Delta_1 \leftarrow \Delta$$

and

$$P = \begin{cases} P_1 + \Delta P & (\Delta > 0) \\ P_1 - \Delta P & (\Delta < 0) \end{cases}$$

(b) After marching first changed the sign of Δ_i

$$P_1 \leftarrow P \ (\Delta^x \Delta_1 > 0)$$

$$P_2 \leftarrow P \ (\Delta^x \Delta_1 < 0)$$

and

$$P = \frac{P_2\Delta_1 - P_1\Delta_2}{\Delta_1 - \Delta_2}$$

6. Data Structure

Symbols	Format	Input at
TITLE	20A4	MAIN
TA	F5.1	MAIN
NFLR[*1)], NEFLR, NSHFT[*2)]	3I5	PARAM
NROM[*2)], HFLR	I5, F5.1	PARAM
NEF(L), NEROM(L)[*2)], HEFLR(L)	2I5, F5.1	PARAM
BRN(I), DRN(I), HRN(I) — I = 1, NROM	5X, 15F5.1	PARAM
BRE(L,I), DRE(L,I), HRE(L,I) — I = 1, NEROM(L)	5X, 15F5.1	PARAM
BRS(I), DRS(I), HRST(I), HRSB(I) — I = 1, NSHFT	5X, 7F10.1	PARAM
I, J, K, BWO, HHO, HLO	5X, 3I5, 3F5.1	PARAM
999	5X, 3I5, 3F5.1	PARAM
NEX, I, J, K, BWO, HHO, HLO	4I5, 3F5.1	PARAM
999	4I5, 3F5.1	PARAM
IPR(I), IRE(I) — I = 1, NRMX2	5X, 15I5	PARAM
IPRE(I), IREE(I) — I = 1, NRMX2	5X, 15I5	PARAM

N

FKWO(I,1)

CWO(I,1)
RWO(I,1)
FLWO(I,1) } I = 1, NROM } 8E10.3 } TPROP

EPWO(I,1)

FKWO(I,2)

CWO(I,2)
RWO(I,2)
FLWO(I,2) } I = 1, NROM } 8E10.3 } TPROP

EPWO(I,2)

FKW(NEF(L), I,1)

CW(NEF(L), I,1)
RW(NEF(L), I,1)
FLW(NEF(L), I,1) } I = 1, NEROM(L) } 8E10.3 } TPROP

EPW(NEF(L), I,1)

FKW(NEF(L), I,2)

CW(NEF(L), I,2)
RW(NEF(L), I,2)
FLW(NEF(L), I,2) } I = 1, NEROM(L) } 8E10.3 } TPROP

EPW(NEF(L), I,2)

FKW(1,I,1)

CW(1,I,1)
RW(1,I,1)
FLW(1,I,1) } I = NRMX1, NRMX2 } 8E10.3 } TPROP

EPW(1,I,1)

FKW(1,I,2) CW(1,I,2) RW(1,I,2) FLW(1,I,2) EPW(1,I,2)	I = NRMX2, NRMX2	8E10.3	TPROP
NFF, IFR, LFP, DDT, NTMAX		3I5, F5.0, I5	DFIRE
WC, WH, WO, WN		4F10.3	DFIRE
WEXP, TE, QGFT, WMFL		4F10.2	DFIRE
W, S, PM, ETA		4F10.3	DFIRE
BFIRED(I), I=1, NTMAX		5E10.3	DFIRE
AFIRED(I), I=1, NTMAX		5F10.3	DFIRE
HFIRED(I), I=1, NTMAX		5F10.3	DFIRE
NWMAX, DWT		I5, F5.0	WPRS
WV(J), J=1, NWMAX		10F5.1	WPRS
COEW(I), I=1,4		4F5.2	WPRS

Note

*1) Total number of floor NFLR should be less than five unless corresponding arrays are enlarged.

*2) Max (NROM, NEROM(L)) + NSHFT should be less than seven unless corresponding arrays are enlarged.

*3) Regarding the symbols, reference the descriptions of the program in which the data are input.

IV. SAMPLE CALCULATIONS

Some results of several sample calculations are depicted in this section. Since the conditions given for each sample are somewhat artificial especially in that the fuel input rates are given independently of the thermal conditions in the room of origin, one cannot be too eager to draw from these sample results conclusive insight about how a real fire behaves. One should keep in mind that what is shown here is nothing more than how the current model, particularly when the model of excess fuel transport is introduced, behaves under various conditions. As can be seen in the following, some examples have yielded predictions that may be somewhat surprising to us. In this regard, the newly introduced excess fuel transport model has to be subjected to experimental validation.

Another purpose of the sample calculations is, though somewhat incidentally and unsystematically, to show the kind of features that have been provided in the current program. This program can give additional information, other than those variables shown in the following examples, such as mean radiative and convective heat flux to the room surfaces, temperature of the walls, room pressures, and the concentration of smoke and CO.

Some of the typical conditions for each sample calculation are shown in Table 7. Only for the first test case do we have experimental results to assess verifications. The input data required for these sample calculations are listed in Tables 7.1 through 7.8. These tables would serve a user of the computer program. The documentation in Section III together with the program listing are needed to fully understand the tables.

Table 7.0 Typical conditions of sample calculations

	Source	Fuel Input Rate (g/s)*1)	Number of Floors	Size of a Room (w x d x h) (m)	Shaft size (w x d x h) (m)	Openings (w x h) External (m)	Openings (w x h) Internal (m)	Others
1	Polyurethane foam slab	(*2)	1	2.4 x 3.6 x 2.4	-	0.775 x 1	-	
2	Propane	200	1	4 x 6 x 3	-	1 x 1	1 x 2	
3	Propane	200	2	4 x 6 x 3	3 x 6 x 6.5	1 x 1	1 x 2	
4	Propane	100	2	4 x 6 x 3	3 x 6 x 6.5	1 x 1	1 x 2	
5	Propane	200	2	4 x 6 x 3	3 x 6 x 6.5	1 x 1	1 x 2	3 m/s wind
6	Propane	200	2	4 x 6 x 3	3 x 6 x 6.5	0.1 x 1	1 x 2	
7	Propane	300	5	4 x 6 x 3	4 x 6 x 22.5 4 x 6 x 18.5	1 x 1(1 Fl) 0.1 x 2(others)	1 x 2	
8	Propane	300	10	4 x 6 x 3	4 x 6 x 42.5 4 x 6 x 38.5	1 x 1(1 Fl) 0.1 x 2(others)	1 x 2	

*1) In the samples No. 2-8, fuel input linearly increases from 0 to the indicated value in 1 minute, holds the value for 3 minutes, and then linearly decreases to 0 in a minute.

*2) Input data were obtained from FMRC Test 6 data [9].

Table 7.1

```
SAMPLE1 : FMRC 6-TH EXPERIMENT
 300.
    1    0    0
    1 2.39
BR(N) 2.39
DR(N) 3.62
HR(N) 2.44
OPENS    1    2    1 .775 2.04 1.04
       999
  999
IPR,N    2
IRE,N    1
   10
 0.100E-03
 0.250E+00
 0.800E+03
 0.500E-01
 0.800E+00
 0.100E-03
 0.250E+00
 0.800E+03
 0.500E-01
 0.800E-00
    1    1    1 12.5   40
      .635      .101      .223      .041
     7382.      528.      524.
      0.00     0.050      0.00     0.080
 0.000E-03 0.001E-03 0.001E-03 0.001E-03 0.001E-03
 0.005E-03 0.010E-03 0.200E-03 0.400E-03 0.500E-3
 0.600E-03 1.000E-03 1.200E-03 2.000E-03 2.500E-03
 3.200E-03 4.500E-03 6.200E-03 8.500E-03 11.50E-03
 13.50E-03 23.50E-03 32.50E-03 36.00E-03 46.70E-03
 47.00E-03 48.00E-03 47.10E-03 43.50E-03 38.80E-03
 36.20E-03 42.20E-03 31.70E-03 29.50E-03 9.500E-03
 4.500E-03 4.500E-03 4.500E-03 4.500E-03 4.500E-03
       0.0       0.0       0.0       0.0       0.0
       0.0       0.0       0.0       0.0       0.0
       0.0       0.0       0.0       0.0       0.0
       0.0       0.0       0.0       0.0       0.0
       0.0       0.0       0.0       0.0       0.0
       0.0       0.0       0.0       0.0       0.0
       0.0       0.0       0.0       0.0       0.0
       0.0       0.0       0.0       0.0       0.0
       0.6       0.6       0.6       0.6       0.6
       0.6       0.6       0.6       0.6       0.6
       0.6       0.6       0.6       0.6       0.6
       0.6       0.6       0.6       0.6       0.6
       0.6       0.6       0.6       0.6       0.6
       0.6       0.6       0.6       0.6       0.6
       0.6       0.6       0.6       0.6       0.6
       0.6       0.6       0.6       0.6       0.6
    2 240.
  0.0  0.0
  0.0  0.0  0.0  0.0
```

Table 7.2

```
SAMPLE 2 : 1 STORY, FUEL RICH CASE
 300.
    1    0    0
    4  3.5
BR(N)  4.0  4.0  4.0  4.0
DR(N)  6.0  6.0  6.0  6.0
HR(N)  3.0  3.0  3.0  3.0
OPENS    1    2    1  1.0  2.0  0.0
         1    5    1  1.0  2.0  1.0
         2    3    1  1.0  2.0  0.0
         3    4    1  1.0  2.0  0.0
         4    6    1  1.0  2.0  1.0
       999
  999
IPR,N    2    4    5    3
IRE,N    1    1    2    4
   10
 0.287E-03 0.287E-03 0.287E-03 0.287E-03
 0.200E+00 0.200E+00 0.200E+00 0.200E+00
 0.200E+04 0.200E+04 0.200E+04 0.200E+04
 0.500E-01 0.500E-01 0.500E-01 0.500E-01
 0.800E+00 0.800E+00 0.800E+00 0.800E+00
 0.287E-03 0.287E-03 0.287E-03 0.287E-03
 0.200E+00 0.200E+00 0.200E+00 0.200E+00
 0.200E+04 0.200E+04 0.200E+04 0.200E+04
 0.500E-01 0.500E-01 0.500E-01 0.500E-01
 0.800E+00 0.800E+00 0.800E+00 0.800E+00
    1    2    1  60.    6
      .818      .182      .000      .000
    12027.      300.                32.
      0.00      0.01      0.00      0.05
 0.000E-03 200.0E-03 200.0E-03 200.0E-03 200.0E-03
 0.000E-03
      0.00      0.00      0.00      0.00      0.00
      0.00
      0.00      0.00      0.00      0.00      0.00
      0.00
    2 300.
  0.0  0.0
  0.0  0.0  0.0  0.0
```

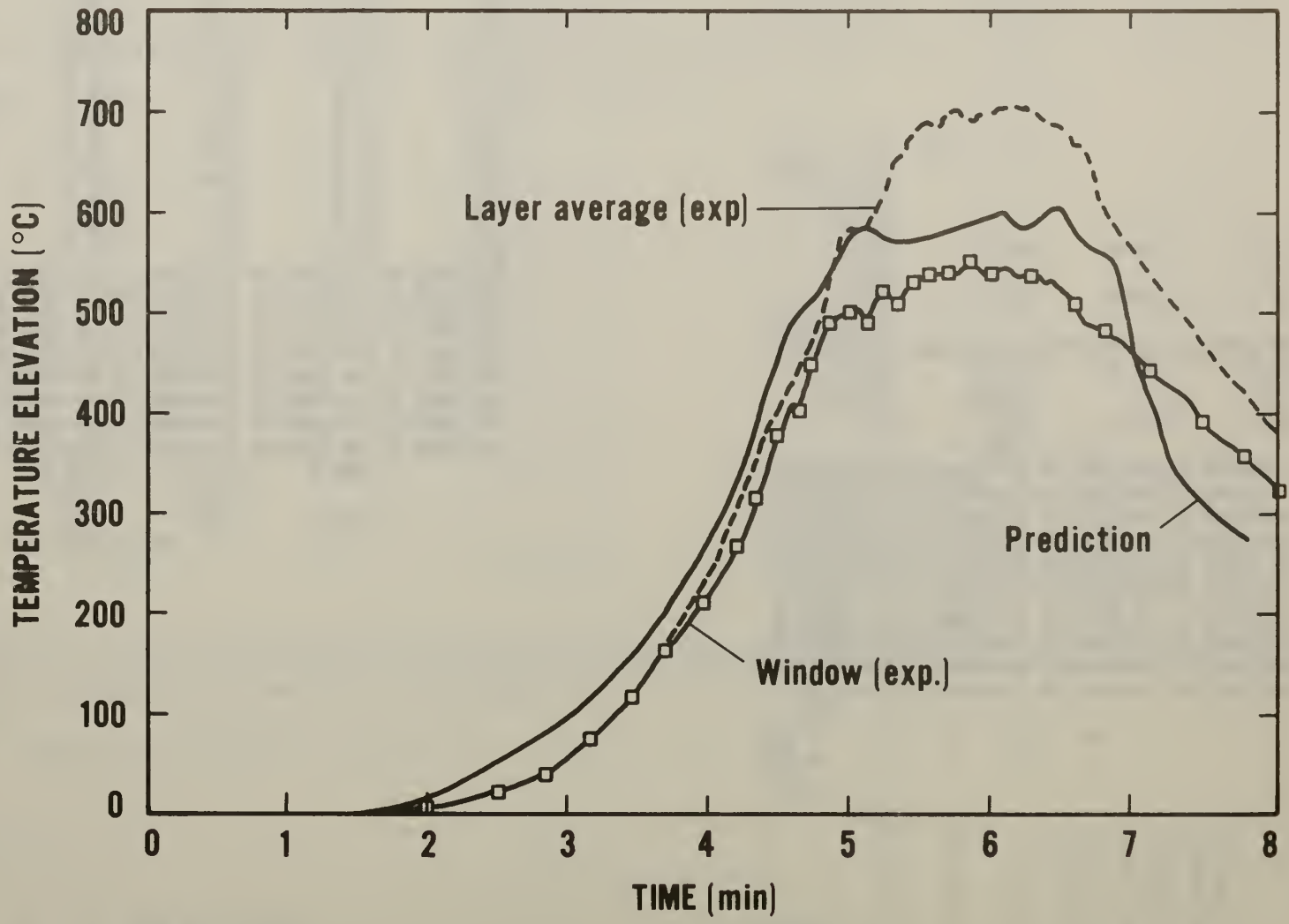

Fig. 7.1(a) Predicted and Tested Temperature Elevation (Sample 1: Comparison with FMRC Test 6)

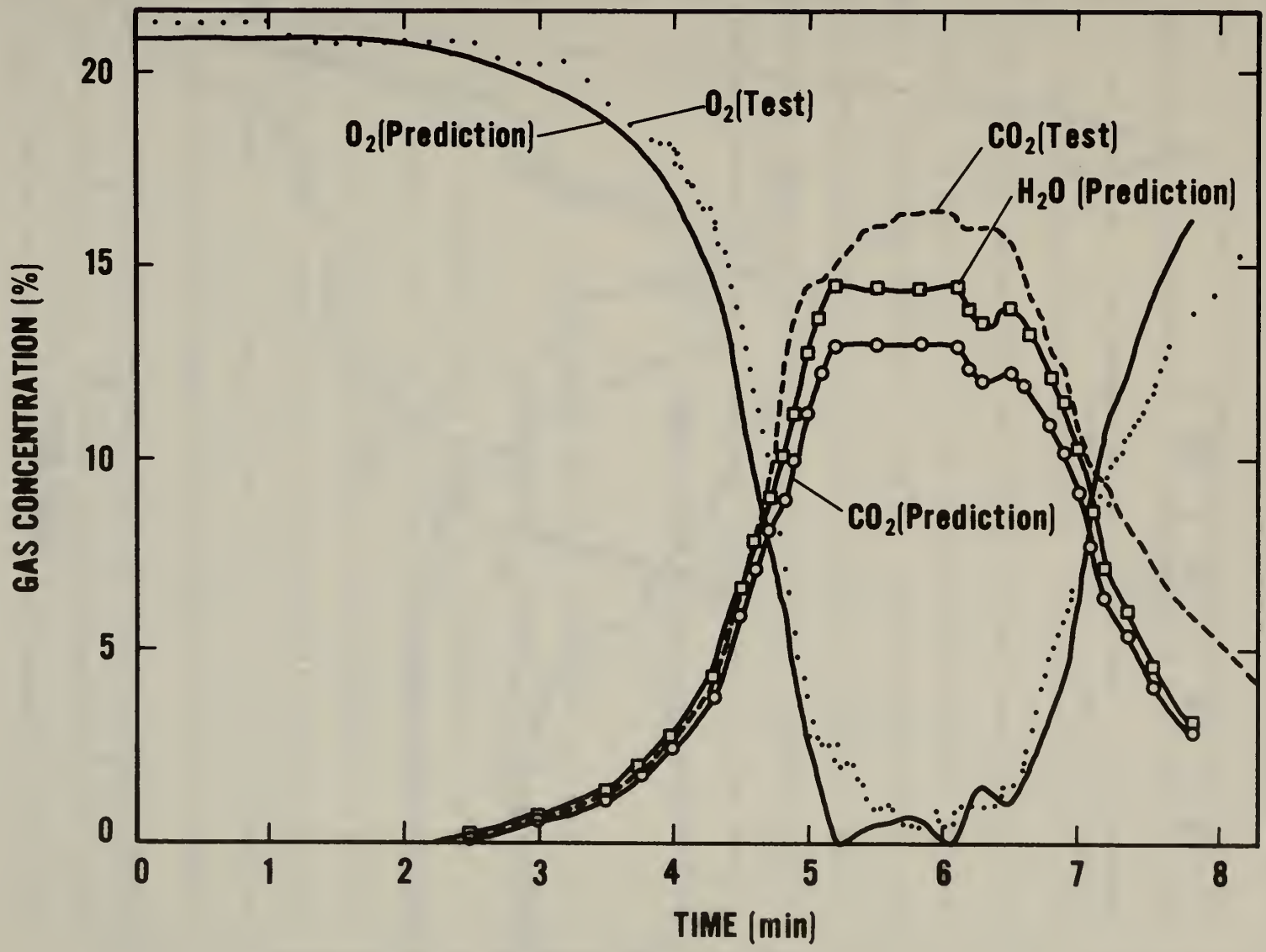

Fig. 7.1(b) Comparison Between Predicted and Tested Gas Concentration

7.1 Sample 1: Comparison with FMRC Test 6 (Figure 7.1)

This sample is an attempt to compare the prediction with the FMRC Test 6 [9]. The experimental configuration is a spreading fire on a horizontal surface within a room with an open window. The predicted temperature is closer to the window temperature of the test than to the layer average temperature. The predicted gas concentrations are not in excellent agreement with the test data. Differences may stem from the fact that the predicted concentrations are the values under the presence of H_2O whereas the measured values are based on dry gas analysis. It is difficult to fully identify the causes of the discrepancies between the predictions and the measurements. Some of them may have to be attributed to the model itself, but some must be attributed to measurements and the inconsistencies of comparing local results with average predictions.

7.2 Sample 2: One story fuel rich (Figure 7.2)

This is an example of a fire in 1 story structure. The fuel input to the 2nd room linearly increases up to 1 min. after the start of the fire, remains at a constant value of 200 g/s until 4 min., and then linearly decreases so that it becomes zero at five minutes. The results are presented in Figures 7.2 a-d. The arrangement of the rooms are displayed schematically in the figures with the rooms labeled as R1, R2, etc. In Figure 7.2 (d), the flow rates are given in kg/s at the arrows and the upper layer gas temperatures are given in °C. This notation will be repeated in subsequent examples. A striking feature of the upper layer temperature is that each of them has a sharp peak in their histories, and

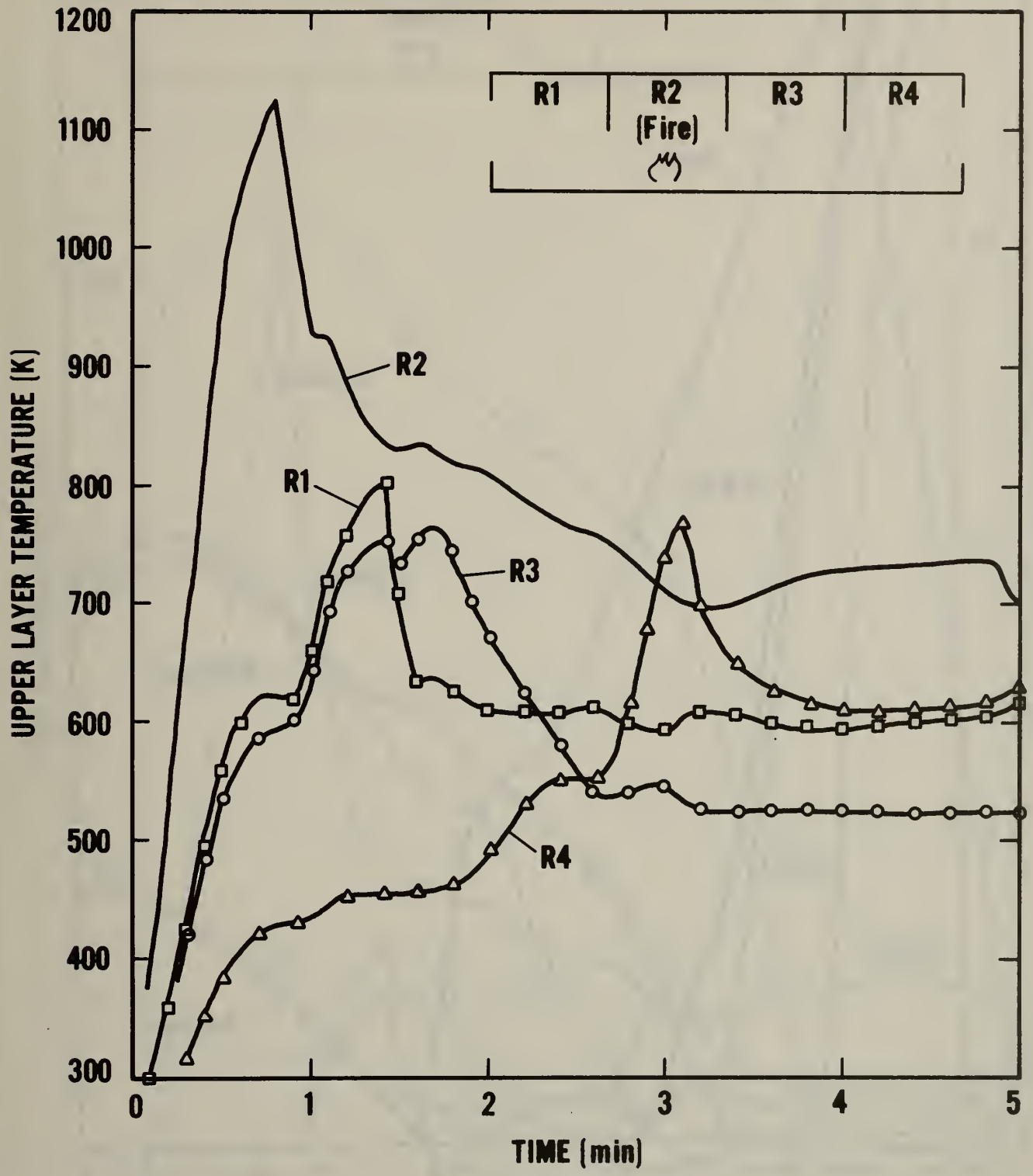

Fig. 7.2(a) Upper Layer Temperatures (Sample 2: One Story, fuel rich fire)

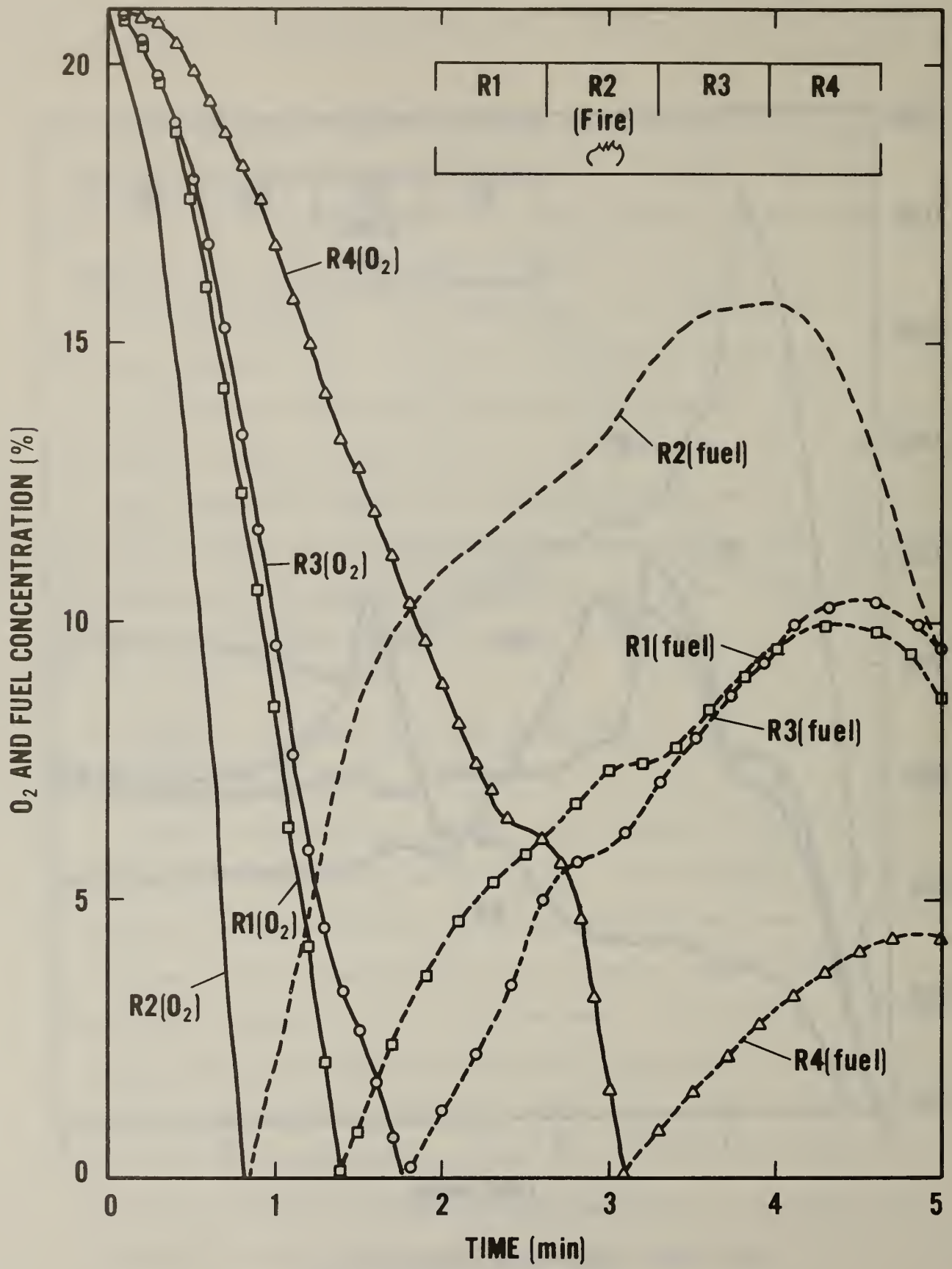

Fig. 7.2(b) O_2 and Fuel Concentrations of the Upper Layers

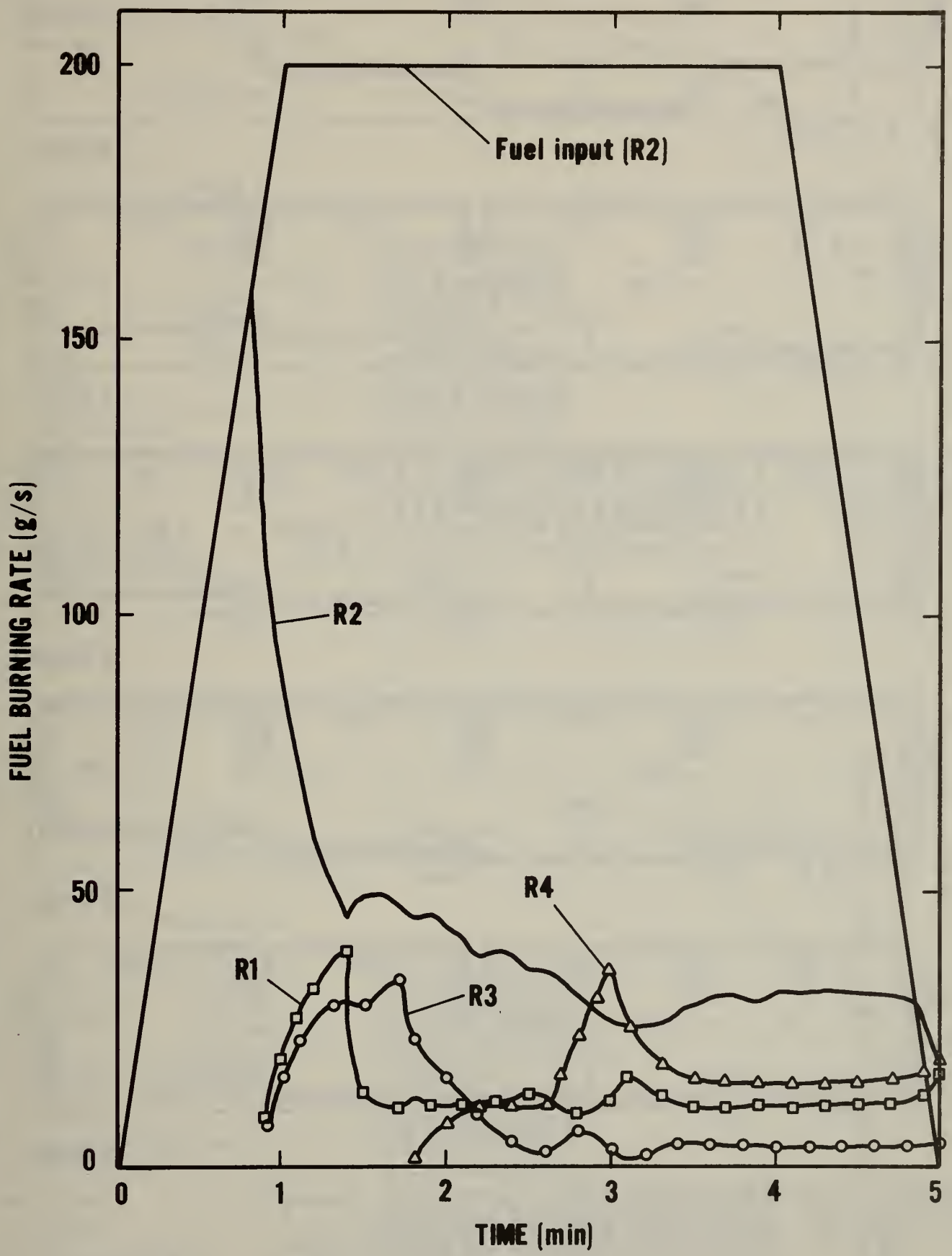

Fig. 7.2(c) Fuel Burning Rate in the Rooms

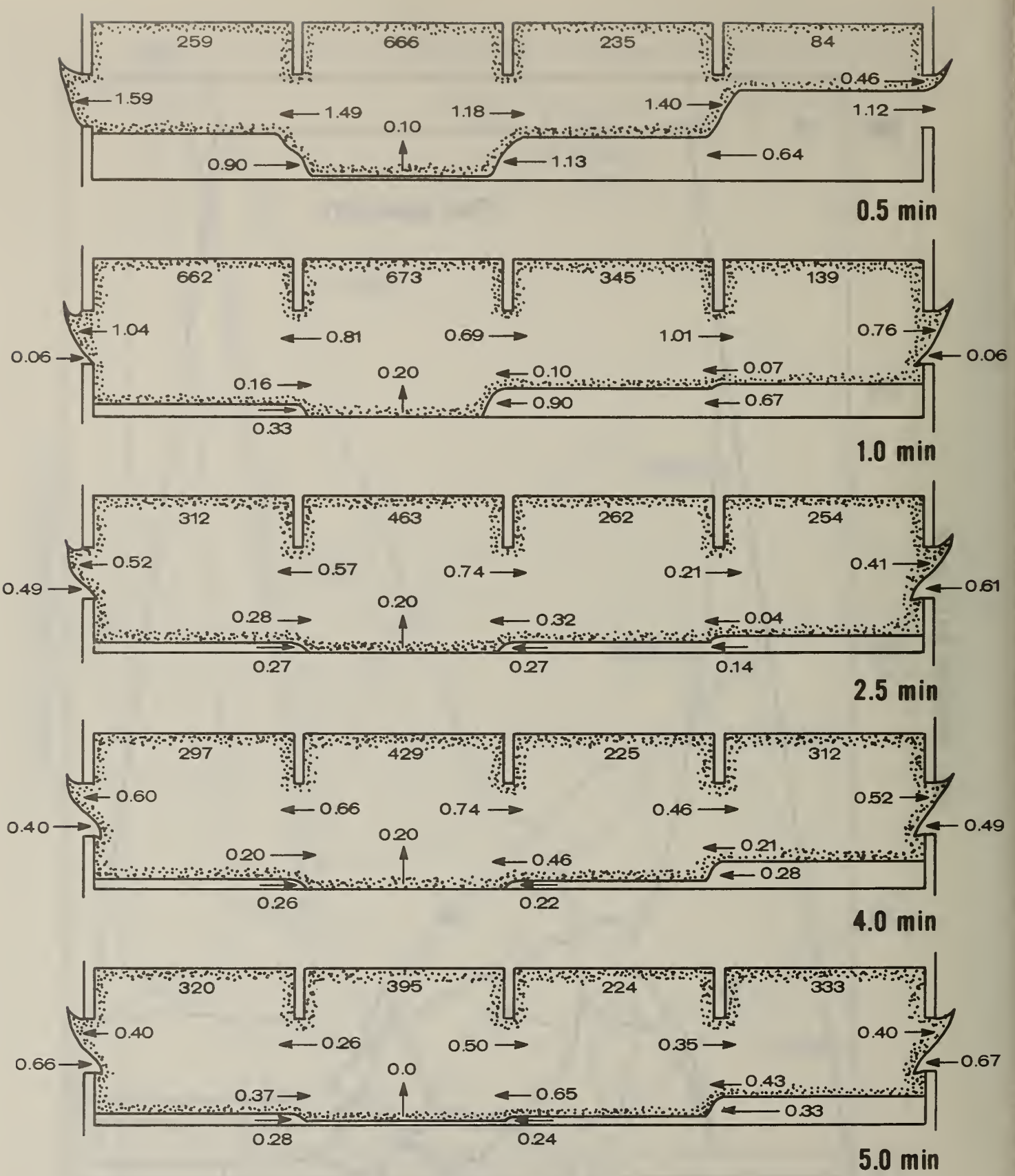

Fig. 7.2(d) Upper Layer and Flow Through Openings (Number under a ceiling with no arrow: temp. elevation; Number at a doorway with arrow: flow rate (kg/s))

Table 7.3

```
SAMPLE 3 : 2 STORY, FUEL RICH CASE
 300.
    2    0    1
    3  3.5
BR(N)  4.0  4.0  4.0
DR(N)  6.0  6.0  6.0
HR(N)  3.0  3.0  3.0
BR(S)       3.0
DR(S)       6.0
HRSTP       6.5
HRSBM       0.0
OPENS    1    4    1  1.0  2.0  0.0
         1    5    1  1.0  2.0  1.0
         2    3    1  1.0  2.0  0.0
         2    4    1  1.0  2.0  0.0
         3    6    1  1.0  2.0  1.0
       999
  999
IPR,N    3    4    2    5
IRE,N    1    3    3    1
   10
 0.287E-03 0.287E-03 0.287E-03
 0.200E+00 0.200E+00 0.200E+00
 0.200E+04 0.200E+04 0.200E+04
 0.500E-01 0.500E-01 0.500E-01
 0.800E+00 0.800E+00 0.800E+00
 0.287E-03 0.287E-03 0.287E-03
 0.200E+00 0.200E+00 0.200E+00
 0.200E+04 0.200E+04 0.200E+04
 0.500E-01 0.500E-01 0.500E-01
 0.800E+00 0.800E+00 0.800E+00
 0.287E-03
 0.200E+00
 0.200E+04
 0.500E-01
 0.800E+00
 0.287E-03
 0.200E+00
 0.200E+04
 0.500E-01
 0.800E+00
    1    2    1  60.    6
      .818       .182       .000       .000
   12027.        300.                  44.
     0.00       0.01       0.00       0.05
 0.000E-03 200.0E-03 200.0E-03 200.0E-03 200.0E-03
 0.000E-03
     0.00       0.00       0.00       0.00       0.00
     0.00
     0.00       0.00       0.00       0.00       0.00
     0.00
   2 300.
  0.0  0.0
  0.0  0.0  0.0  0.0
```

Table 7.4

```
SAMPLE 4 : 2 STORY FUEL LEAN CASE
 300.
    2    0    1
    3  3.5
BR(N)  4.0  4.0  4.0
DR(N)  6.0  6.0  6.0
HR(N)  3.0  3.0  3.0
BR(S)       3.0
DR(S)       6.0
HRSTP       6.5
HRSBM       0.0
OPENS    1    4    1  1.0  2.0  0.0
         1    5    1  1.0  2.0  1.0
         2    3    1  1.0  2.0  0.0
         2    4    1  1.0  2.0  0.0
         3    6    1  1.0  2.0  1.0
       999
  999
IPR,N    3    4    2    5
IRE,N    1    3    3    1
   10
 0.287E-03 0.287E-03 0.287E-03
 0.200E+00 0.200E+00 0.200E+00
 0.200E+04 0.200E+04 0.200E+04
 0.500E-01 0.500E-01 0.500E-01
 0.800E+00 0.800E+00 0.800E+00
 0.287E-03 0.287E-03 0.287E-03
 0.200E+00 0.200E+00 0.200E+00
 0.200E+04 0.200E+04 0.200E+04
 0.500E-01 0.500E-01 0.500E-01
 0.800E+00 0.800E+00 0.800E+00
 0.287E-03
 0.200E+00
 0.200E+04
 0.500E-01
 0.800E+00
 0.287E-03
 0.200E+00
 0.200E+04
 0.500E-01
 0.800E+00
    1    2    1  60.    6
      .818       .182       .000       .000
   12027.        300.                  44.
     0.00       0.01       0.00       0.05
 0.000E-03 100.0E-03 100.0E-03 100.0E-03 100.0E-03
 0.000E-03
     0.00       0.00       0.00       0.00       0.00
     0.00
     0.00       0.00       0.00       0.00       0.00
     0.00
   2 300.
  0.0  0.0
  0.0  0.0  0.0  0.0
```

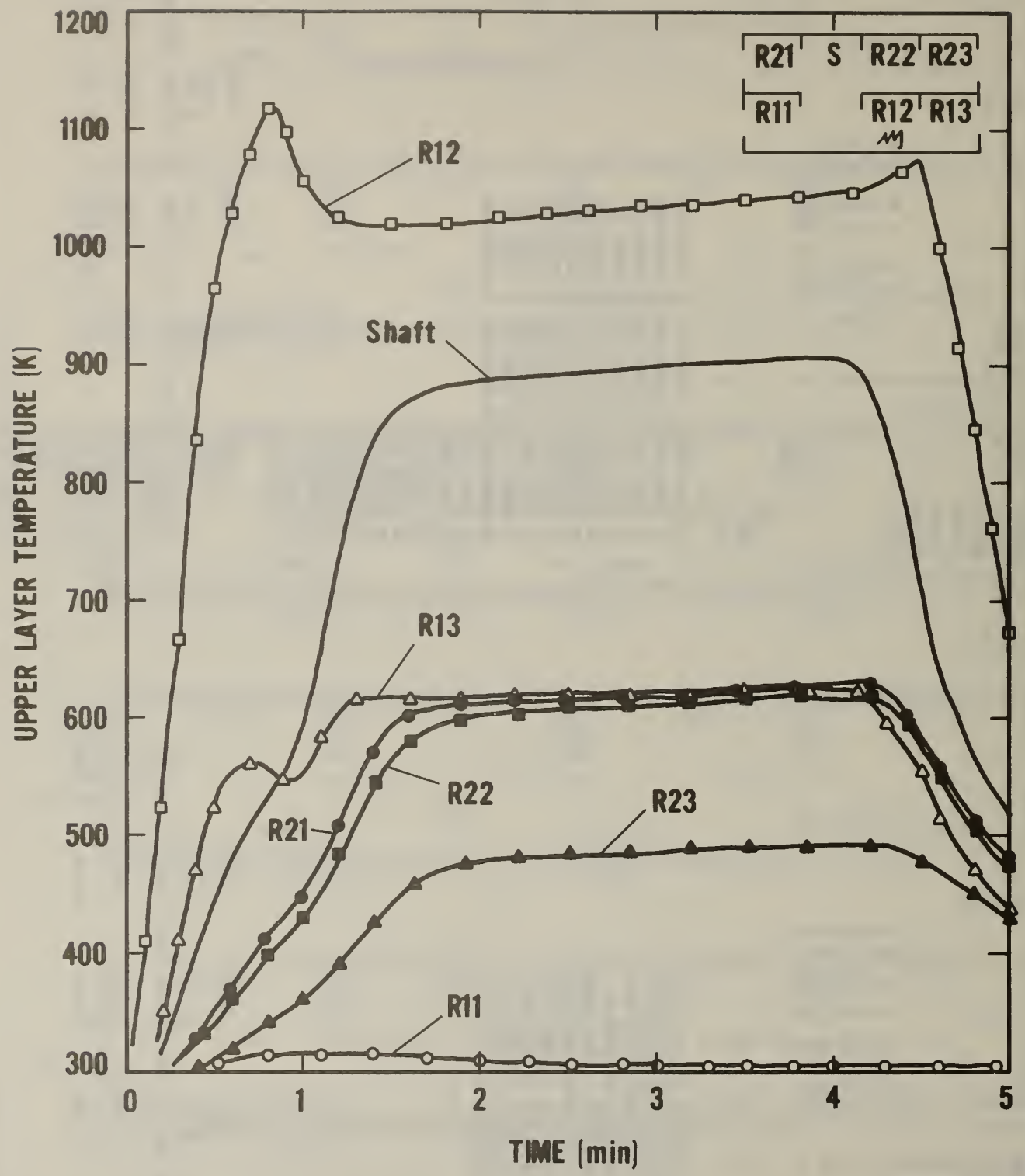

Fig. 7.3(a) Upper Layer Temperatures (Sample 3: Two Story, fuel rich case)

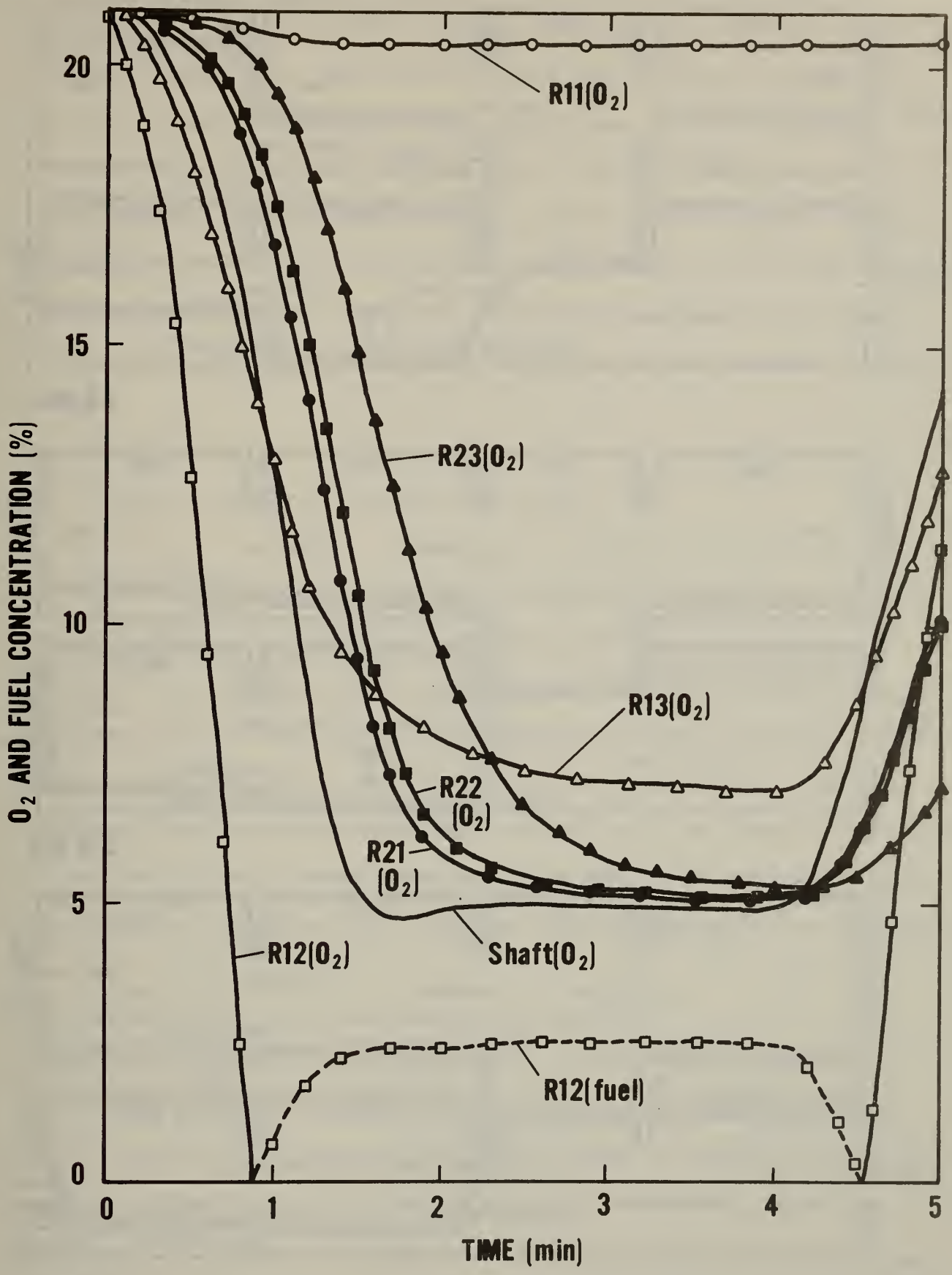

Fig. 7.3(b) O_2 and Fuel Concentration of the Upper Layers

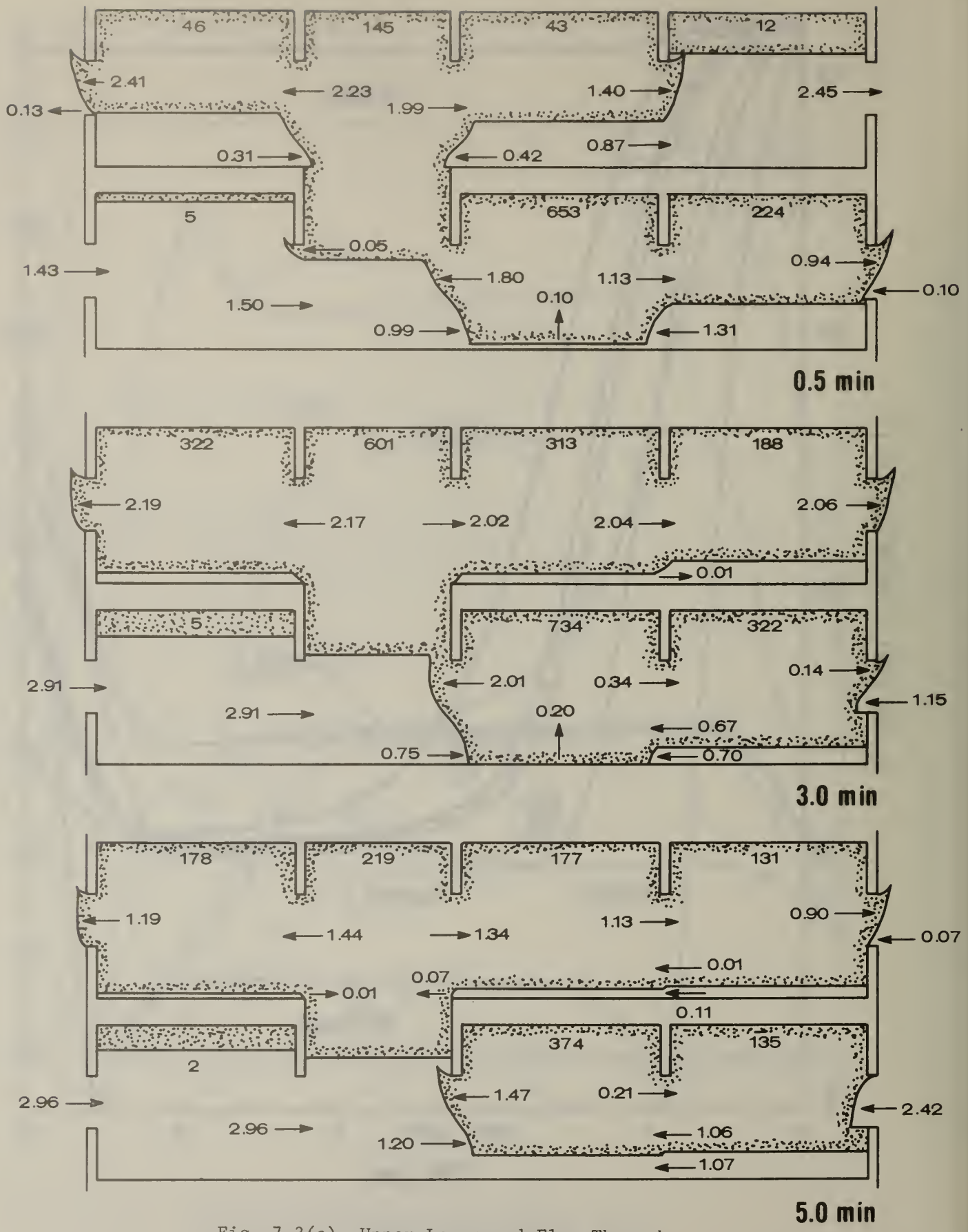

Fig. 7.3(c) Upper Layer and Flow Through Openings (Number under a ceiling with no arrow: temp. elevation; Number at a doorway with arrow: flow rate (kg/s))

the peak time coincides with the time when the oxygen concentration of that room becomes zero. And after the time at the temperature peak in the room of origin, the burning rate of fuel becomes far less than the fuel input rate. This means that some of the input fuel has flowed out through external openings and the rest is accumulated in the rooms. Theoretically, these phenomena are understandable, but it should be noted that this fuel input has been arbitrarily specified. A real fire, in which the fuel input and the thermal conditions are closely coupled, might yield somewhat different results.

7.3 Sample 3: Two story, fuel rich fire (Figure 7.3)

This is a case where the room of fire origin is located in 2nd room on the 1st floor of 2 story structure. The fuel input rate is the same as in sample 2. The point addressed in this example is that the same fuel input may cause very different results for a different structural conditions. As can be seen in Fig. 7.3(a), the temperature of the room of origin remains at considerably high values unlike the preceding case. The reason is that in this 2-story case stronger flows are induced than in the preceding 1-story case because of the presence of a shaft and external openings on the 2nd floor.

7.4 Sample 4: Two story, fuel lean fire (Figure 7.4)

In this example, all the conditions are the same as in sample 3 except that one half of the fuel input is specified. There is a striking different between the shaft temperatures for the two cases, whereas the temperature differences are not very substantial in the room of origin. This example may help to recognize the importance of excess fuel transport on fire spread.

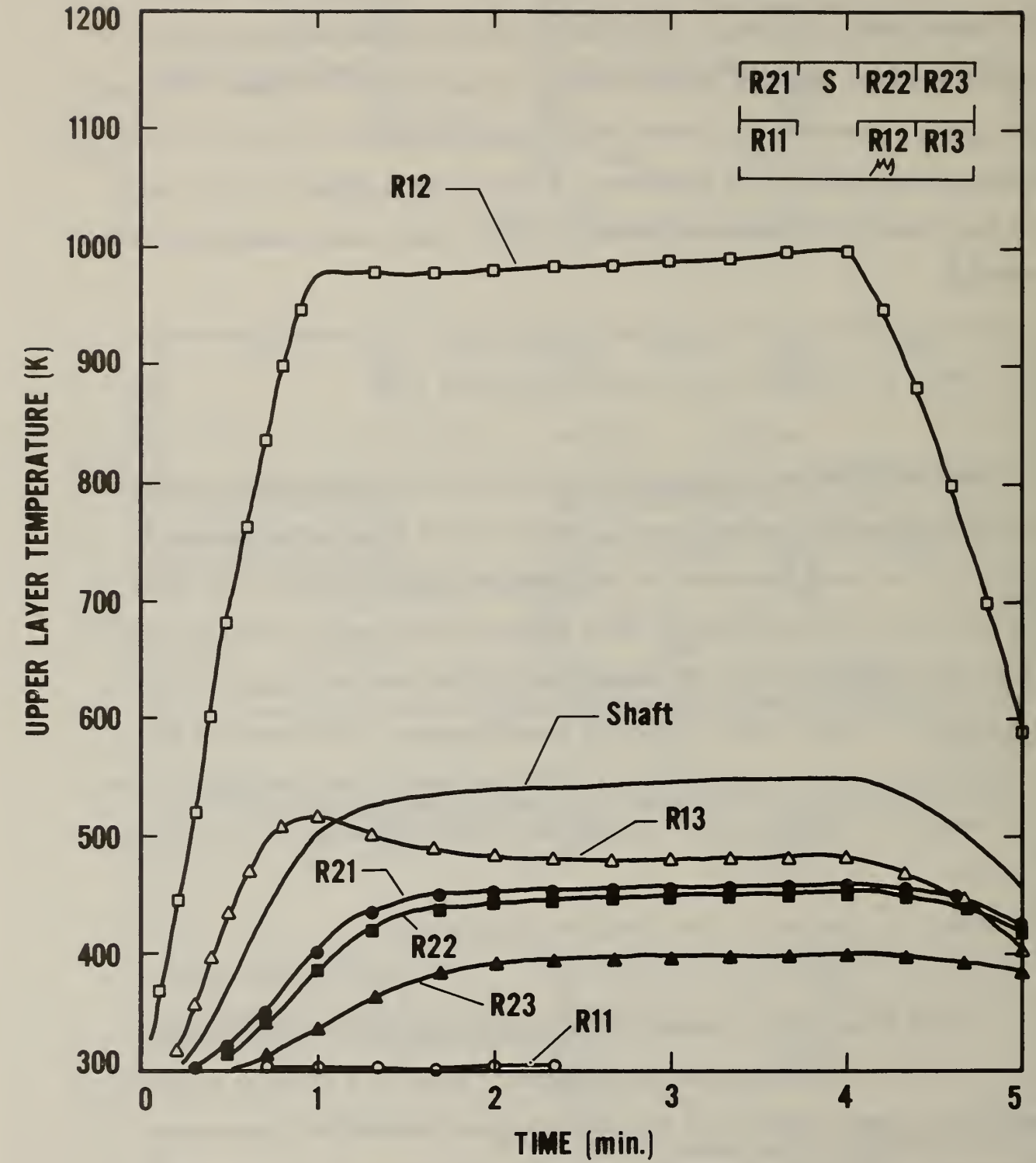

Fig. 7.4 Upper Layer Temperatures (Sample 4: Two Story, fuel lean fire)

Table 7.5

```
SAMPLE 5 : 2 STORY, FUEL RICH, OUTDOOR WIND CASE
 300.
    2    0    1
    3  3.5
BR(N)  4.0  4.0  4.0
DR(N)  6.0  6.0  6.0
HR(N)  3.0  3.0  3.0
BR(S)       3.0
DR(S)       6.0
HRSTP       6.5
HRSBM       0.0
OPENS     1    4    1  1.0  2.0  0.0
          1    5    1  1.0  2.0  1.0
          2    3    1  1.0  2.0  0.0
          2    4    1  1.0  2.0  0.0
          3    6    1  1.0  2.0  1.0
        999
  999
IPR,N    3    4    2    5
IRE,N    1    3    3    1
   10
 0.287E-03 0.287E-03 0.287E-03
 0.200E+00 0.200E+00 0.200E+00
 0.200E+04 0.200E+04 0.200E+04
 0.500E-01 0.500E-01 0.500E-01
 0.800E+00 0.800E+00 0.800E+00
 0.287E-03 0.287E-03 0.287E-03
 0.200E+00 0.200E+00 0.200E+00
 0.200E+04 0.200E+04 0.200E+04
 0.500E-01 0.500E-01 0.500E-01
 0.800E+00 0.800E+00 0.800E+00
 0.287E-03
 0.200E+00
 0.200E+04
 0.500E-01
 0.800E+00
 0.287E-03
 0.200E+00
 0.200E+04
 0.500E-01
 0.800E+00
    1    2    1  60.    6
      .818       .182       .000       .000
    12027.       300.                  44.
      0.00       0.01       0.00       0.05
 0.000E-03 200.0E-03 200.0E-03 200.0E-03 200.0E-03
 0.000E-03
      0.00       0.00       0.00       0.00       0.00
      0.00
      0.00       0.00       0.00       0.00       0.00
      0.00
   2 300.
  3.0  3.0
 -0.8  1.0  0.0 0.0
```

Table 7.6

```
SAMPLE 6 : 2 STORY, FUEL RICH, CLOSED WINDOW
 300.
    2    0    1
    3  3.5
BR(N)  4.0  4.0  4.0
DR(N)  6.0  6.0  6.0
HR(N)  3.0  3.0  3.0
BR(S)       3.0
DR(S)       6.0
HRSTP       6.5
HRSBM       0.0
OPENS     1    4    1  1.0  2.0  0.0
          1    5    1  0.1  2.0  1.0
          2    3    1  1.0  2.0  0.0
          2    4    1  1.0  2.0  0.0
          3    6    1  0.1  2.0  1.0
        999
  999
IPR,N    3    4    2    5
IRE,N    1    3    3    1
   10
 0.287E-03 0.287E-03 0.287E-03
 0.200E+00 0.200E+00 0.200E+00
 0.200E+04 0.200E+04 0.200E+04
 0.500E-01 0.500E-01 0.500E-01
 0.800E+00 0.800E+00 0.800E+00
 0.287E-03 0.287E-03 0.287E-03
 0.200E+00 0.200E+00 0.200E+00
 0.200E+04 0.200E+04 0.200E+04
 0.500E-01 0.500E-01 0.500E-01
 0.800E+00 0.800E+00 0.800E+00
 0.287E-03
 0.200E+00
 0.200E+04
 0.500E-01
 0.800E+00
 0.287E-03
 0.200E+00
 0.200E+04
 0.500E-01
 0.800E+00
    1    2    1  60.    6
      .818       .182       .000       .000
    12027.       300.                  44.
      0.00       0.01       0.00       0.05
 0.000E-03 200.0E-03 200.0E-03 200.0E-03 200.0E-03
 0.000E-03
      0.00       0.00       0.00       0.00       0.00
      0.00
      0.00       0.00       0.00       0.00       0.00
      0.00
   2 300.
  0.0  0.0
  0.0  0.0  0.0  0.0
```

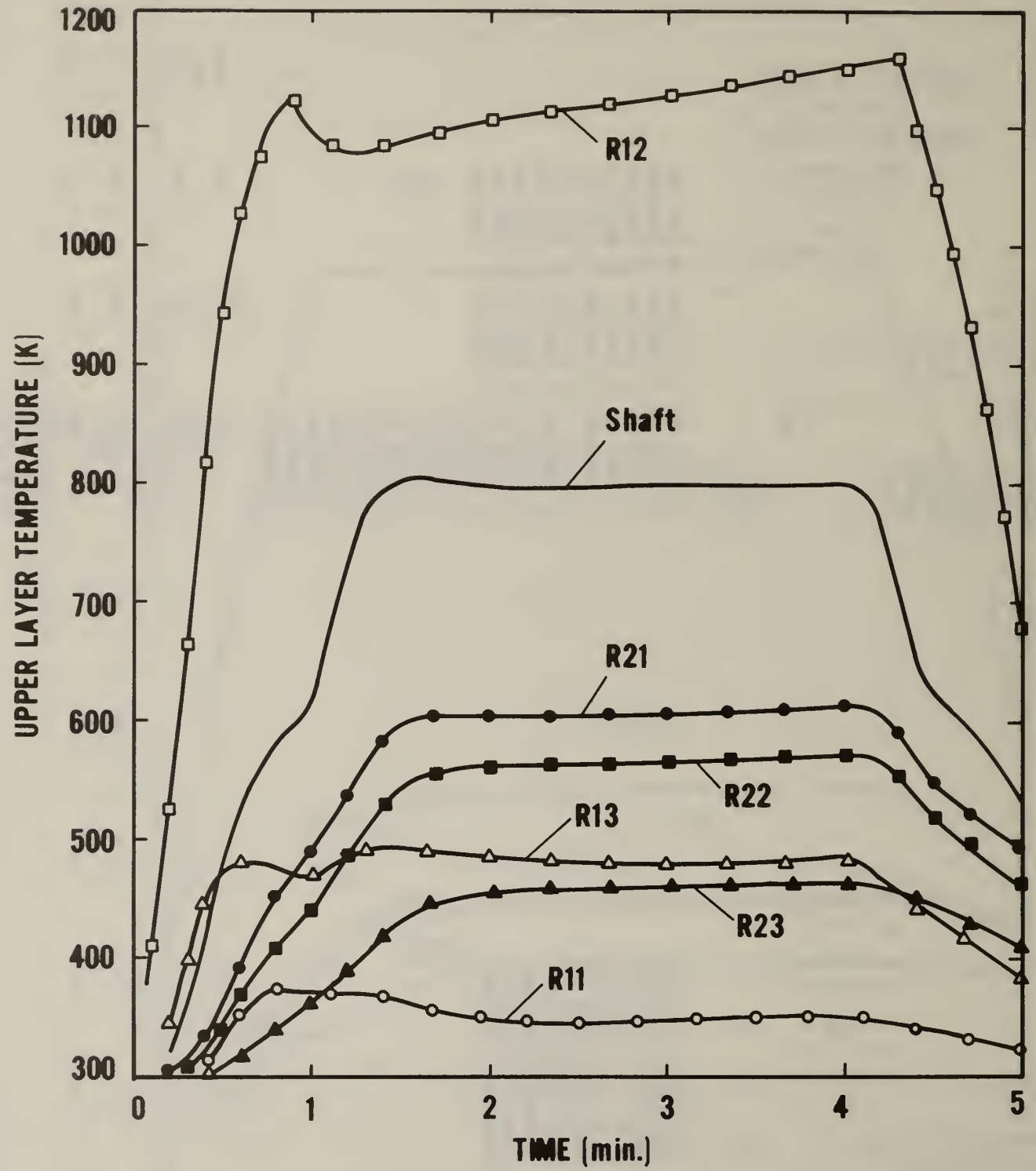

Fig. 7.5(a) Upper Layer Temperatures
(Sample 5: Two Story, fuel
rich fire without door wind)

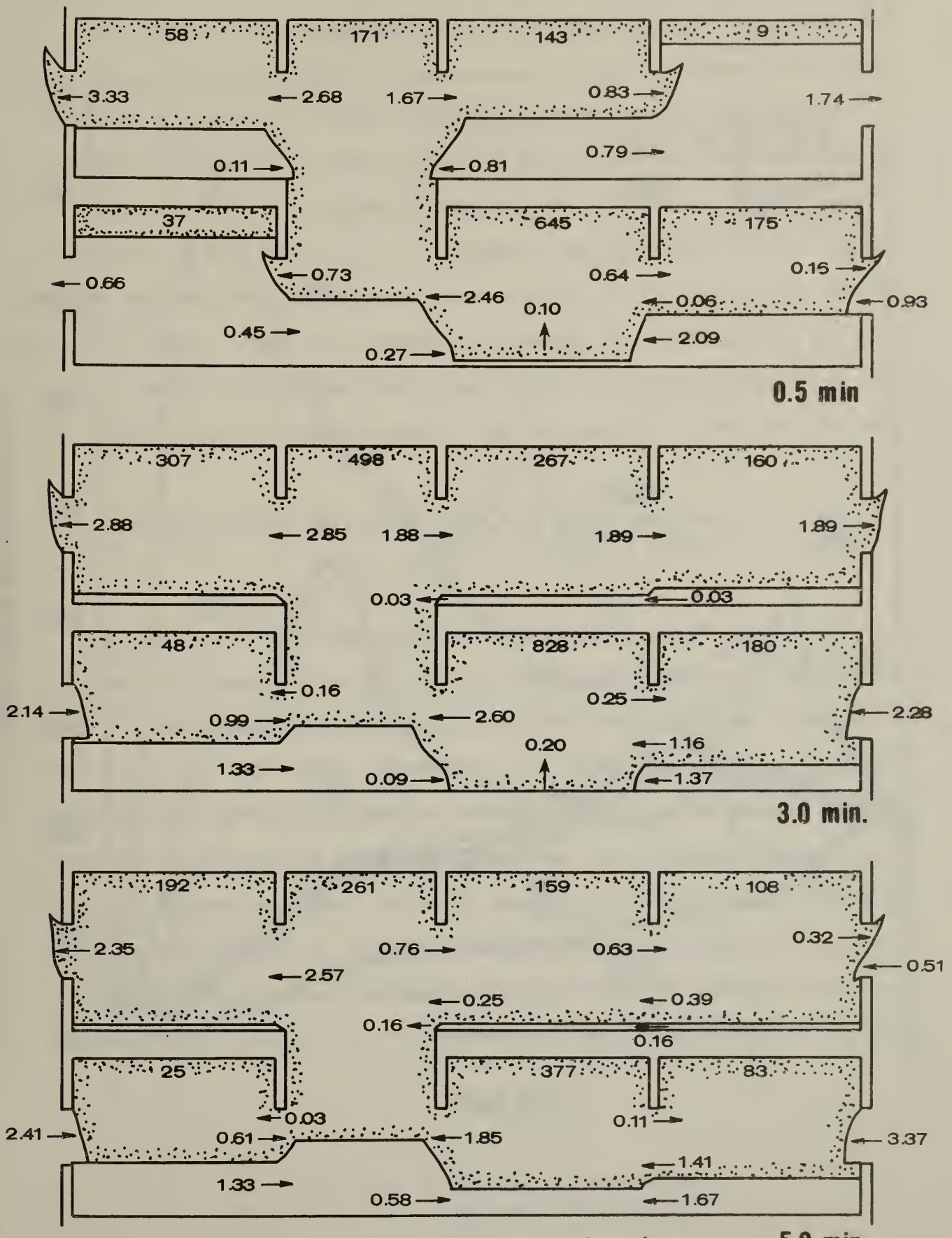

Fig. 7.5(b) Upper Layer and Flow Through Openings (Number under ceiling with no arrow: temp. elevation; Number at an opening with an arrow: flow rate (kg/s))

7.5 Sample 5: Two story, fuel rich fire with outdoor wind (Figure 7.5)

In this example, the outside wind with constant velocity of 3 m/s blows against the right hand side of the structure, and exerts a positive pressure on the right of the building and a negative pressure on the opposite side. The fuel input is specified as in example 7.3. As can be seen by referring to Figs. 7.3(a) and 7.5(a), the wind results in raising the fire room temperature and lowering the shaft temperature compared with sample 3. The wind causes more air to be blown into the fire room, by which more fuel is burned in the room and less fuel is transported into the shaft than the case of sample 3.

7.6 Sample 6: Two story, fuel rich fire with narrow external openings (Figure 7.6)

This is an example in which the width of every external opening is narrowed to 0.1 m. The temperature of each room again behaves in a complex manner as in sample 2. The flows through external openings are, as expected, generally weak except at early stages. Even under the very narrow external opening condition, the temperatures behave nearly the same as under wide opening condition at the very beginning, where the burning in the room of origin is not obstructed by oxygen vitiation. But this results at the cost of an extreme pressure elevation in the structure. In Fig. 7.6(d), in which the shaft pressures are compared between samples 3 and 6, a very different behavior of the pressures can be observed.

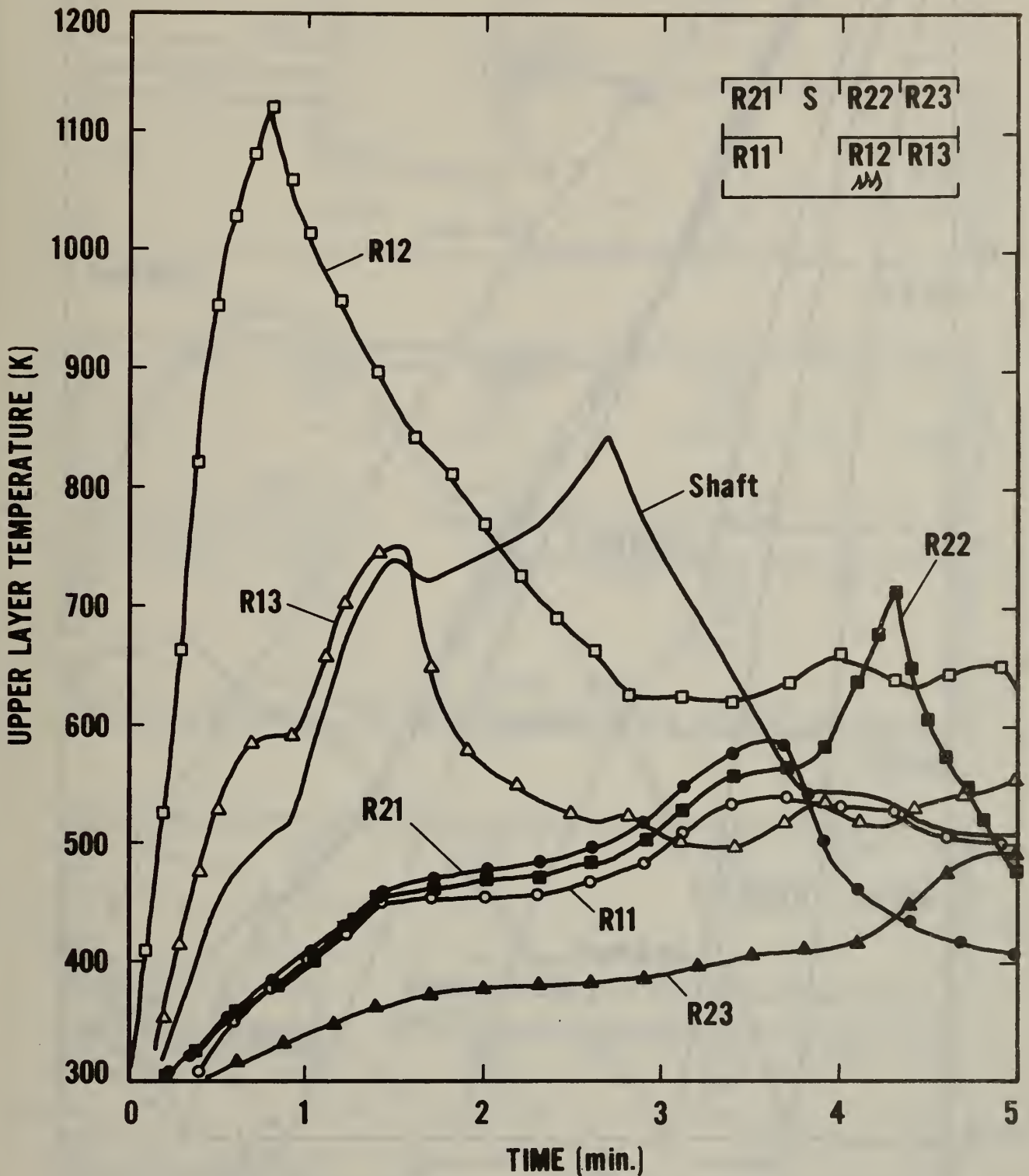

Fig. 7.6(a) Upper Layer Temperatures (Sample 6: Two Story, fuel rich fire with narrow external openings)

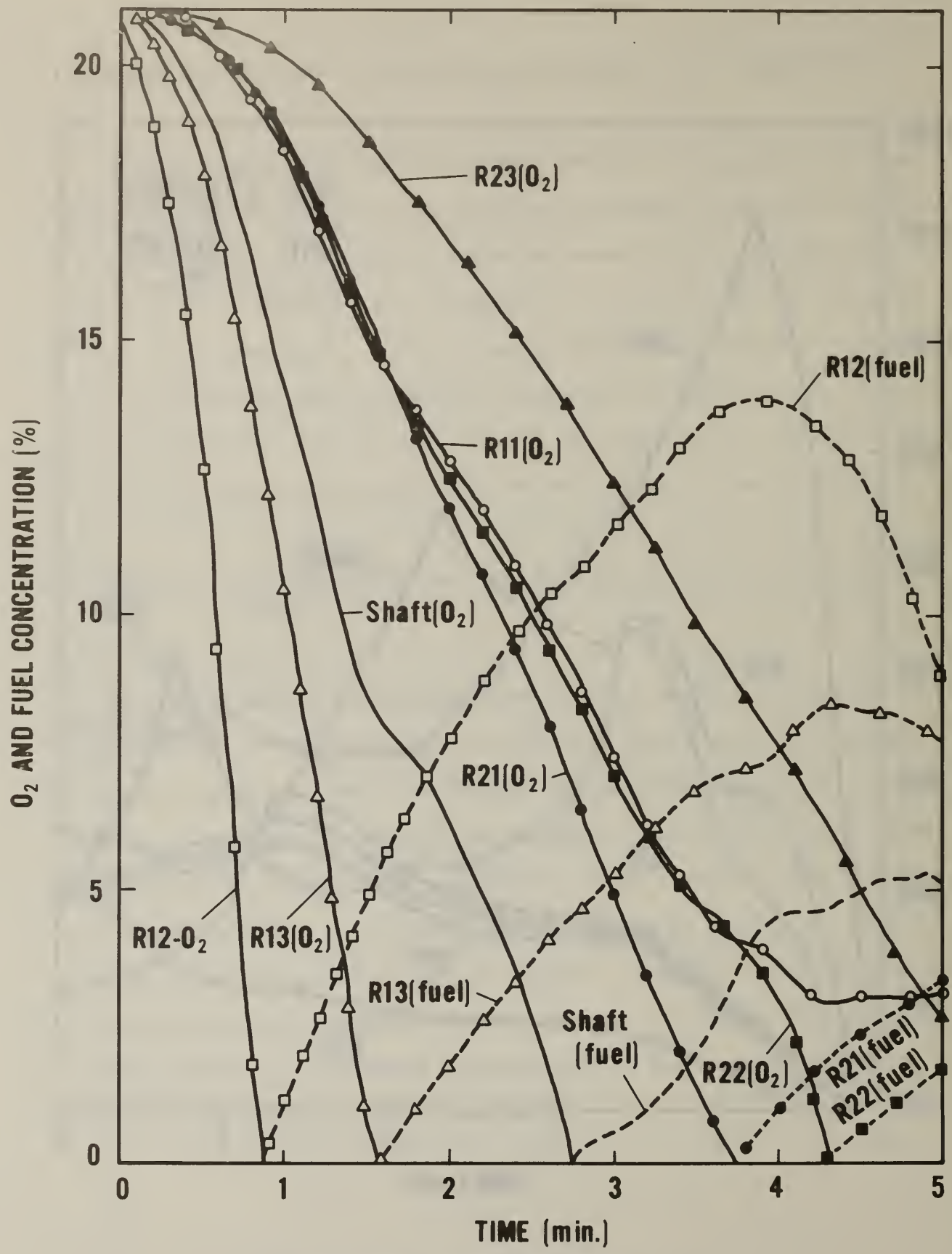

Fig. 7.6(b) O_2 and Fuel Concentrations of Upper Layers

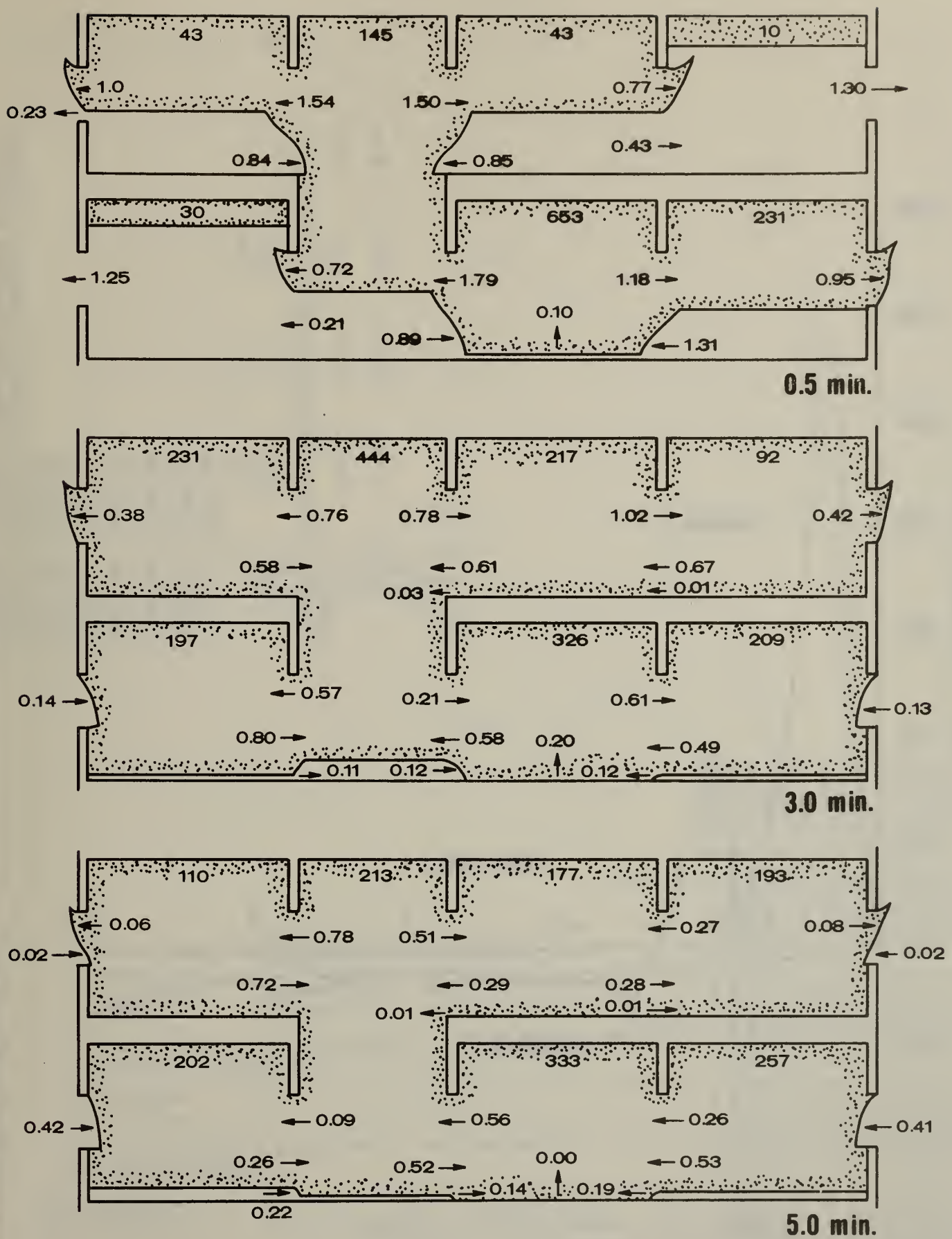

Fig. 7.6(c) Upper Layer and Flow Through Openings (Number under a ceiling with no arrow: temp. elevation; Number at an opening with an arrow: flow rate (kg/s)

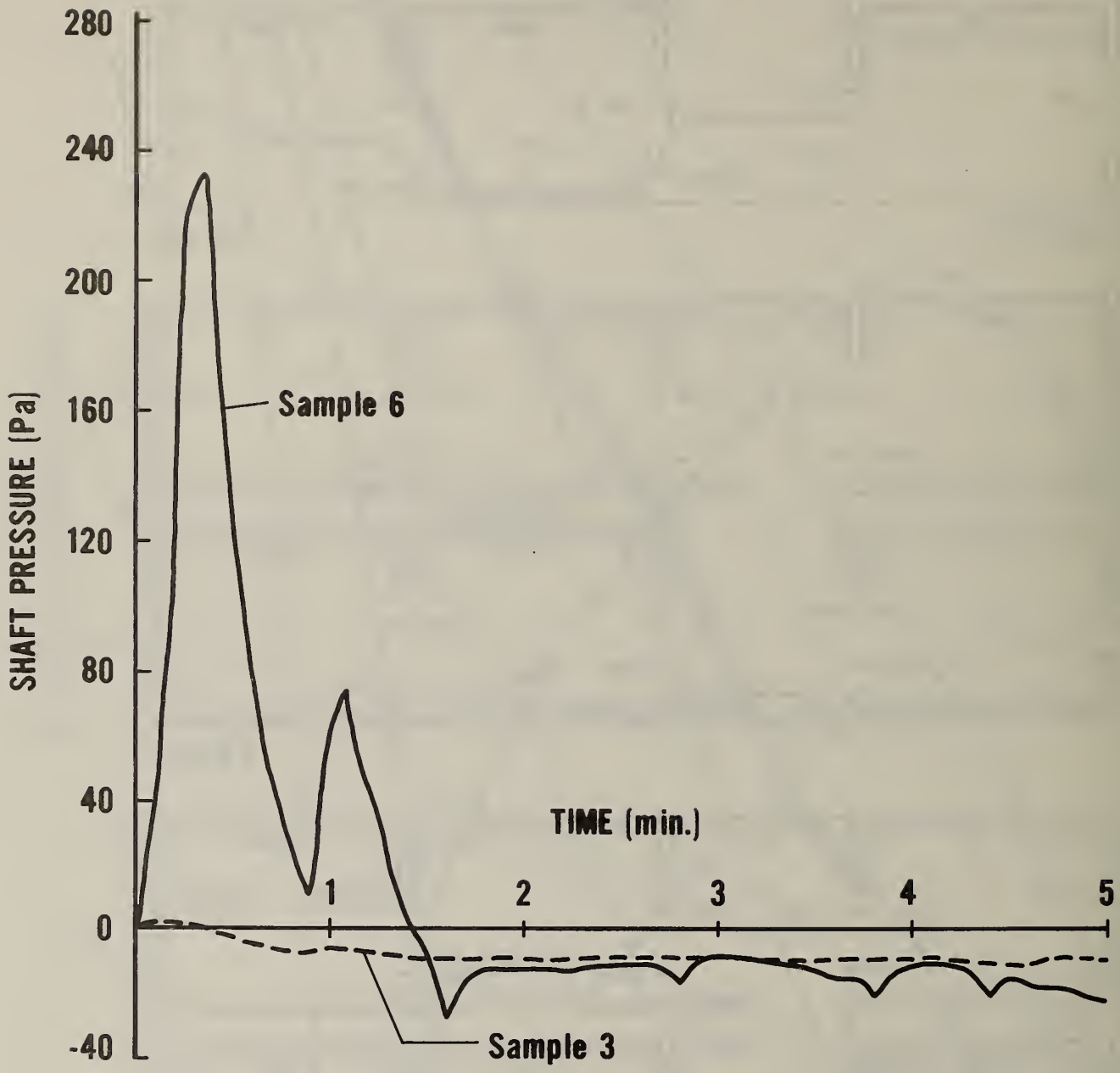

Fig. 7.6(d) Shaft Pressure (at ground level)

Table 7.7

```
SAMPLE 7 : 5 STORY, FUEL RICH CASE
 300.
    5    1    2
    5  4.0
    1    5  4.0
BR(N)  4.0  4.0  4.0  4.0  4.0
DR(N)  6.0  6.0  6.0  6.0  6.0
HR(N)  3.0  3.0  3.0  3.0  3.0
BR(1)  4.0  4.0  4.0  4.0  8.0
DR(1)  6.0  6.0  6.0  6.0  6.0
HR(1)  3.5  3.5  3.5  3.5  3.5
BR(S)       4.0       4.0
DR(S)       6.0       6.0
HRST       22.5      22.5
HRSB        0.0       4.0
OPEN      1    2    1  1.0  2.0  0.0
          1    8    1  0.1  2.6  0.6
          2    3    1  1.0  2.0  0.0
          3    6    1  1.0  2.0  0.0
          4    5    1  1.0  2.0  0.0
          4    6    1  1.0  2.0  0.0
          5    7    1  1.0  2.0  0.0
       999
     1    1    2    1  1.0  2.0  0.0
     1    1    8    1  1.0  2.0  1.0
     1    2    3    1  1.0  2.0  0.0
     1    3    6    1  1.0  2.0  0.0
     1    4    5    1  1.0  2.0  0.0
     1    4    6    1  1.0  2.0  0.0
     1    5    9    1  1.0  2.0  1.0
     6    6    8    1  0.1  2.0  0.0
     6    7    8    1  0.1  2.0  0.0
   999
 IPR,N    3    4    2    5    7    8    6
 IRE,N    1    1    3    4    4    1    1
 IPR,1    3    4    2    5    7    8    6
 IRE,1    1    1    3    4    4    1    1
   10
 0.287E-03 0.287E-03 0.287E-03 0.287E-03 0.287E-03
 0.200E+00 0.200E+00 0.200E+00 0.200E+00 0.200E+00
 0.200E+04 0.200E+04 0.200E+04 0.200E+04 0.200E+04
 0.500E-01 0.500E-01 0.500E-01 0.500E-01 0.500E-01
 0.800E+00 0.800E+00 0.800E+00 0.800E+00 0.800E+00
 0.287E-03 0.287E-03 0.287E-03 0.287E-03 0.287E-03
 0.200E+00 0.200E+00 0.200E+00 0.200E+00 0.200E+00
 0.200E+04 0.200E+04 0.200E+04 0.200E+04 0.200E+04
 0.500E-01 0.500E-01 0.500E-01 0.500E-01 0.500E-01
 0.800E+00 0.800E+00 0.800E+00 0.800E+00 0.800E+00
 0.287E-03 0.287E-03 0.287E-03 0.287E-03 0.287E-03
 0.200E+00 0.200E+00 0.200E+00 0.200E+00 0.200E+00
 0.200E+04 0.200E+04 0.200E+04 0.200E+04 0.200E+04
 0.500E-01 0.500E-01 0.500E-01 0.500E-01 0.500E-01
 0.800E+00 0.800E+00 0.800E+00 0.800E+00 0.800E+00
 0.287E-03 0.287E-03 0.287E-03 0.287E-03 0.287E-03
 0.200E+00 0.200E+00 0.200E+00 0.200E+00 0.200E+00
0.200E+04 0.200E+04 0.200E+04 0.200E+04 0.200E+04
0.500E-01 0.500E-01 0.500E-01 0.500E-01 0.500E-01
0.800E+00 0.800E+00 0.800E+00 0.800E+00 0.800E+00
0.287E-03 0.287E-03
0.200E+00 0.200E+00
0.200E+04 0.200E+04
0.500E-01 0.500E-01
0.800E+00 0.800E+00
0.287E-03 0.287E-03
0.200E+00 0.200E+00
0.200E+04 0.200E+04
0.500E-01 0.500E-01
0.800E+00 0.800E+00
   2    3    1  60.    6
    .818      .182      .000      .000
  12027.      300.                 44.
    0.00      0.01      0.00      0.00
0.000E-03 300.0E-03 300.0E-03 300.0E-03 300.0E-03
0.000E-03
    0.00      0.00      0.00      0.00      0.00
    0.00
    0.00      0.00      0.00      0.00      0.00
    0.00
   2 300.
 0.0  0.0
 0.0  0.0  0.0  0.0
```

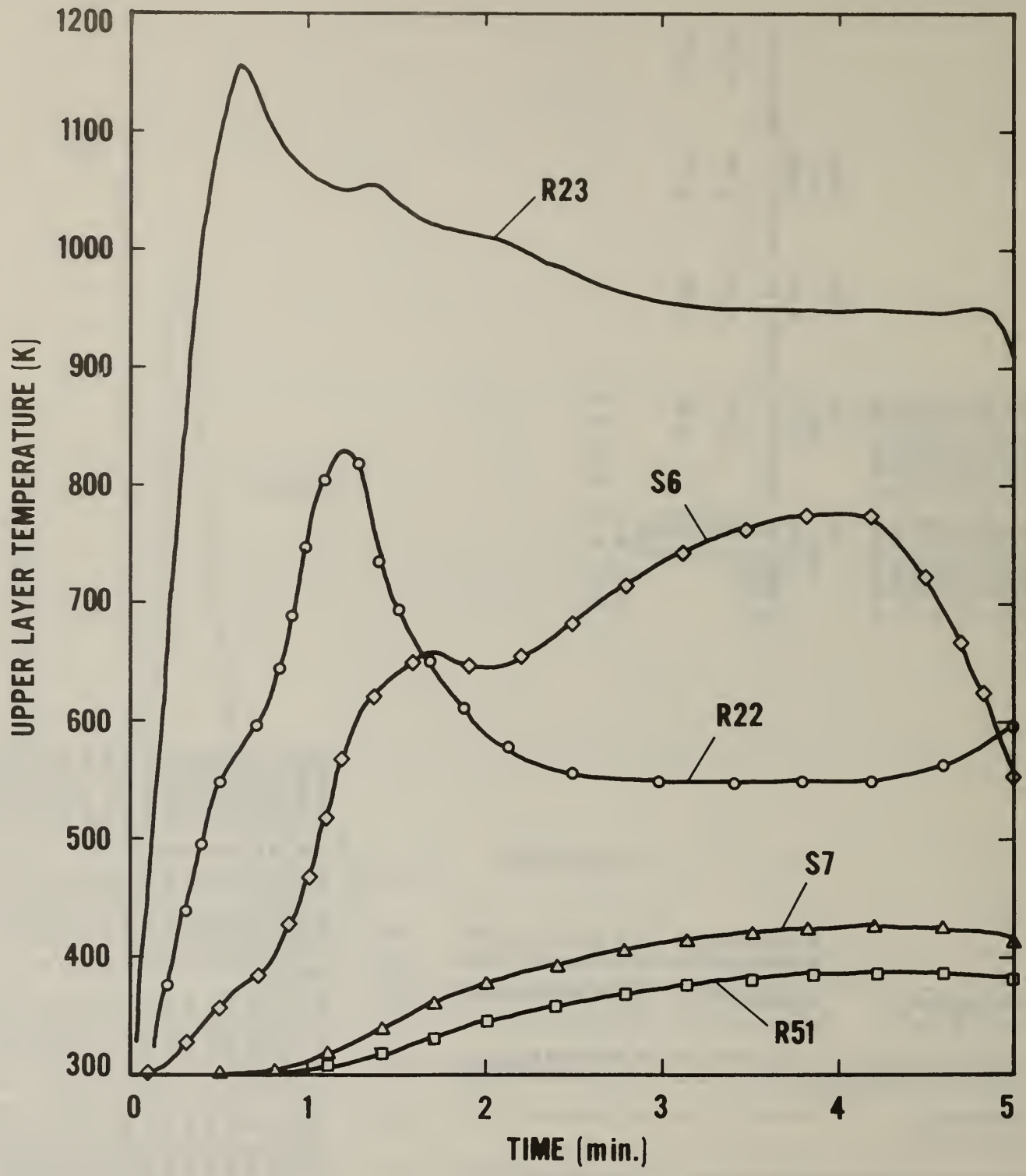

Fig. 7.7(a) Upper Layer Temperatures (Sample 7: Five Story, fuel rich fire with narrow external openings; Note: Rni denotes i-th room on n-th floor)

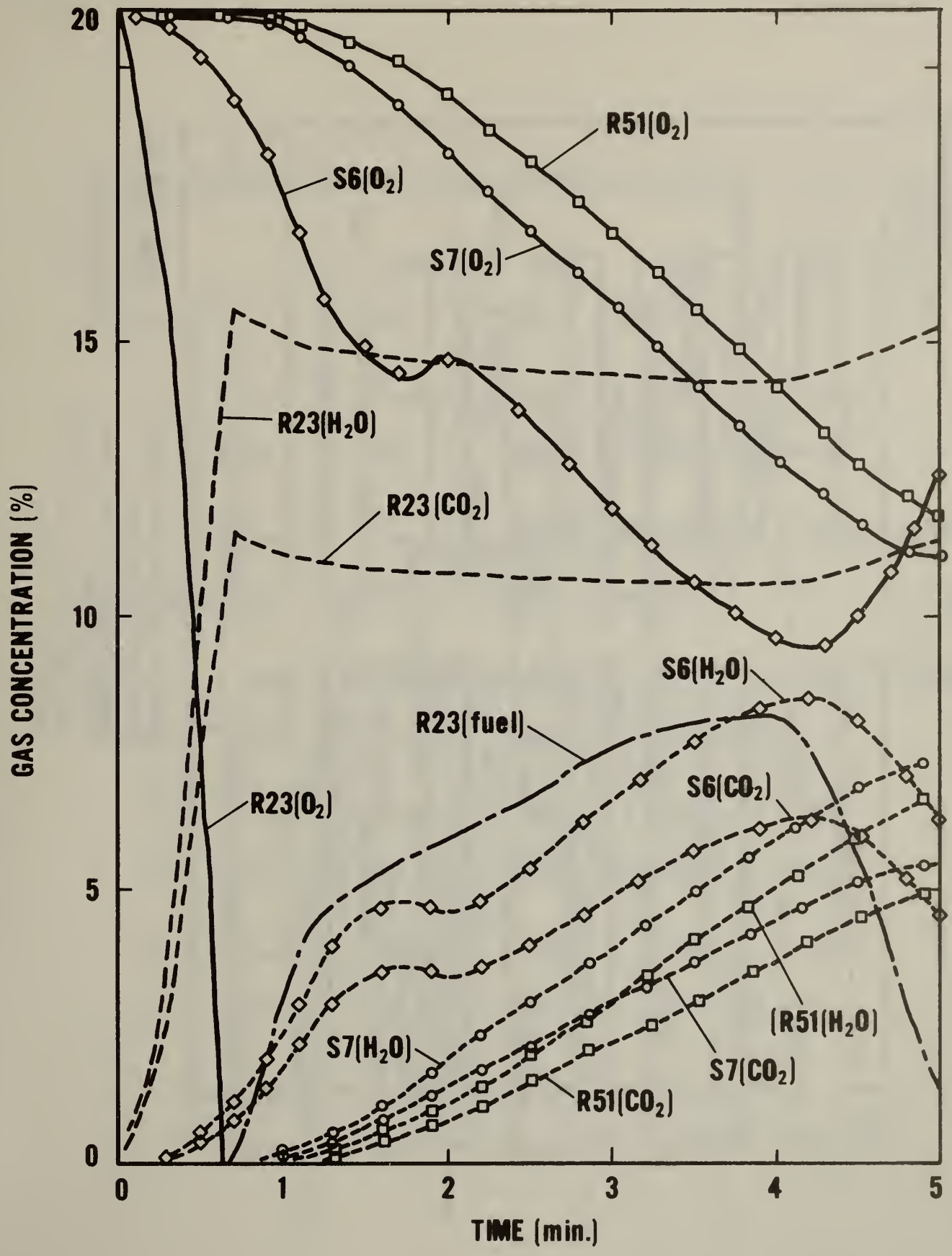

Fig. 7.7(b) Upper Layer Gas Concentrations

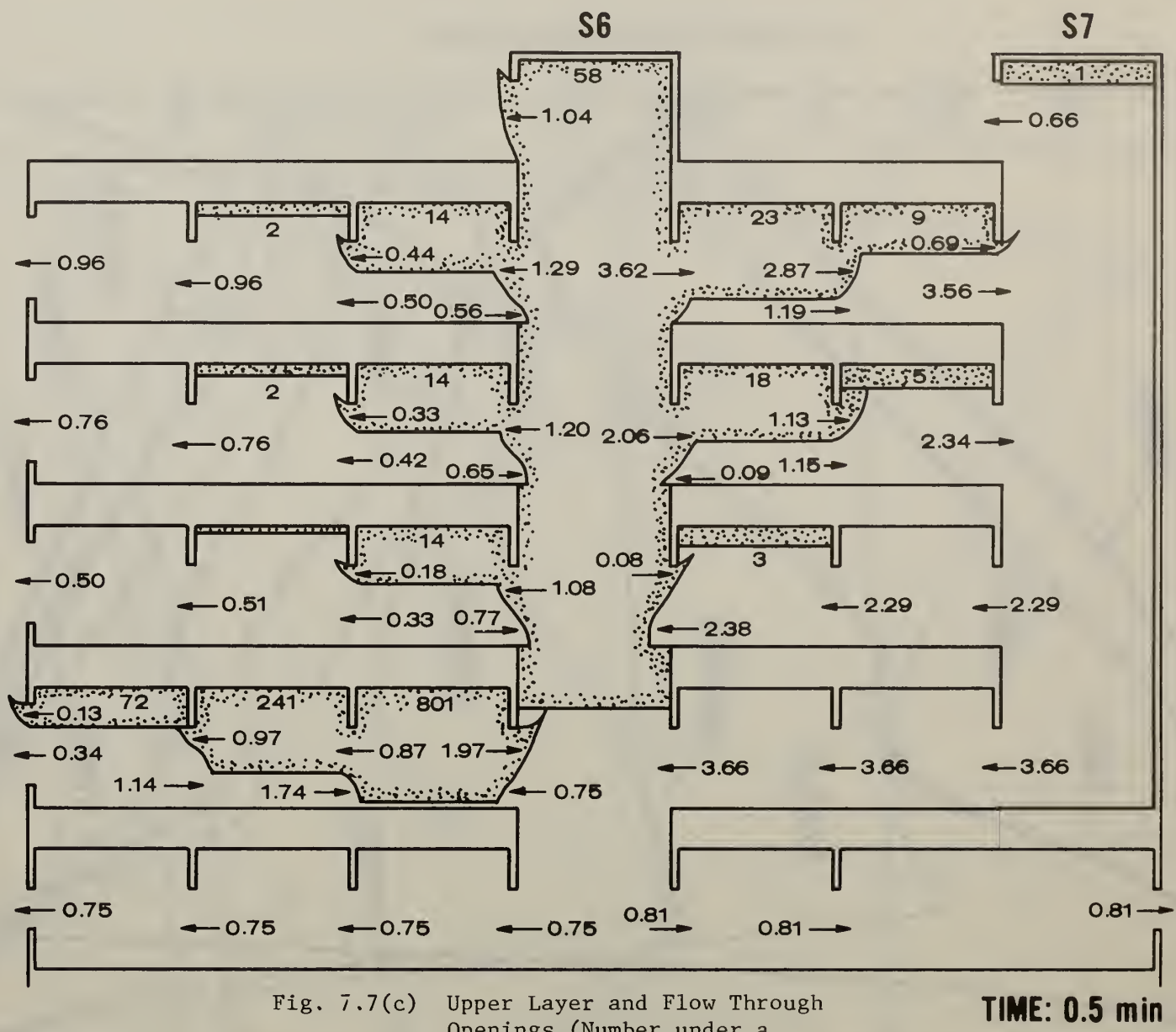

Fig. 7.7(c) Upper Layer and Flow Through Openings (Number under a ceiling with no arrow: temp. elevation; Number at an opening with an arrow: flow rate (kg/s)) 0.5 - 5.0 min.

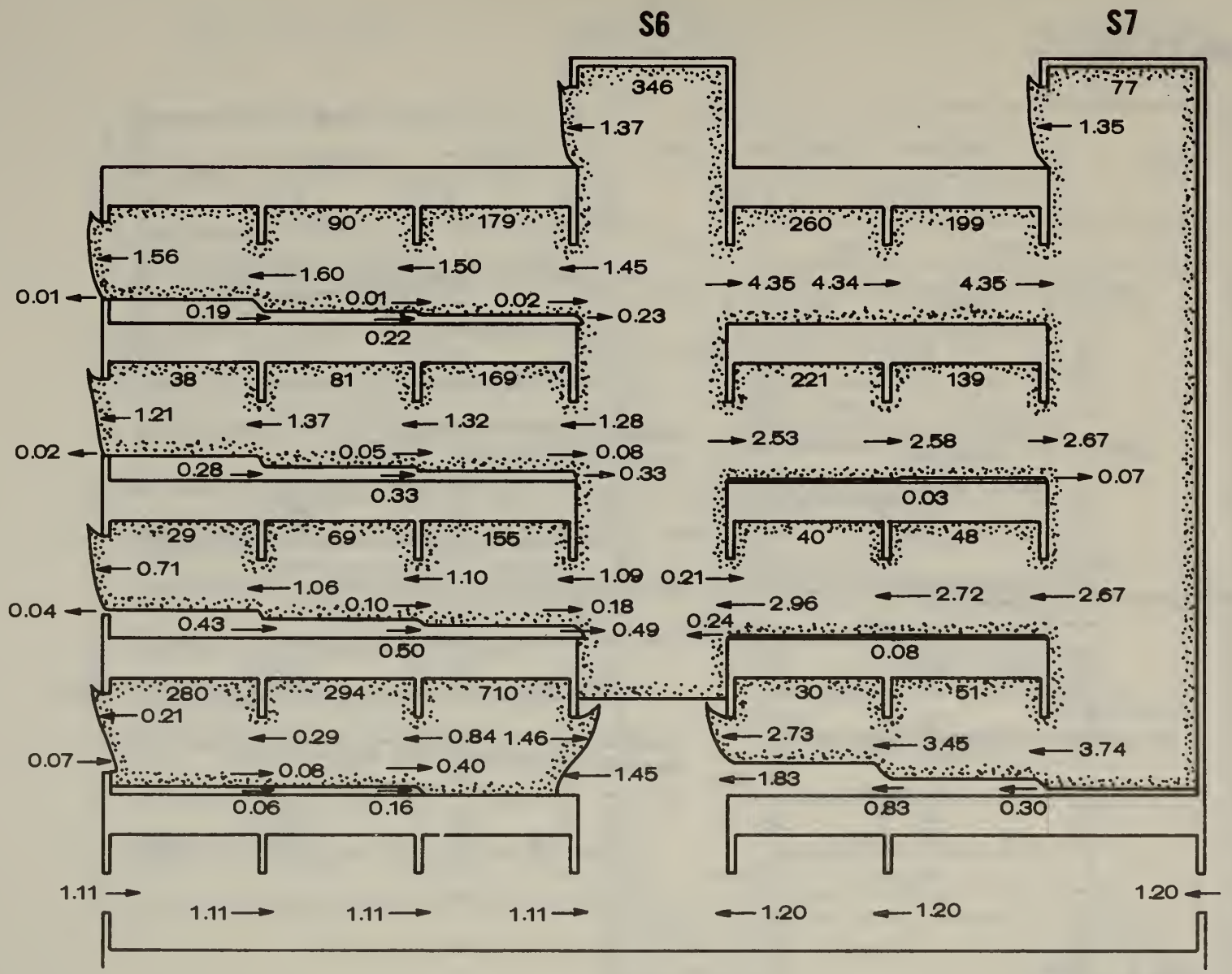

Fig. 7.7(c) cont'd

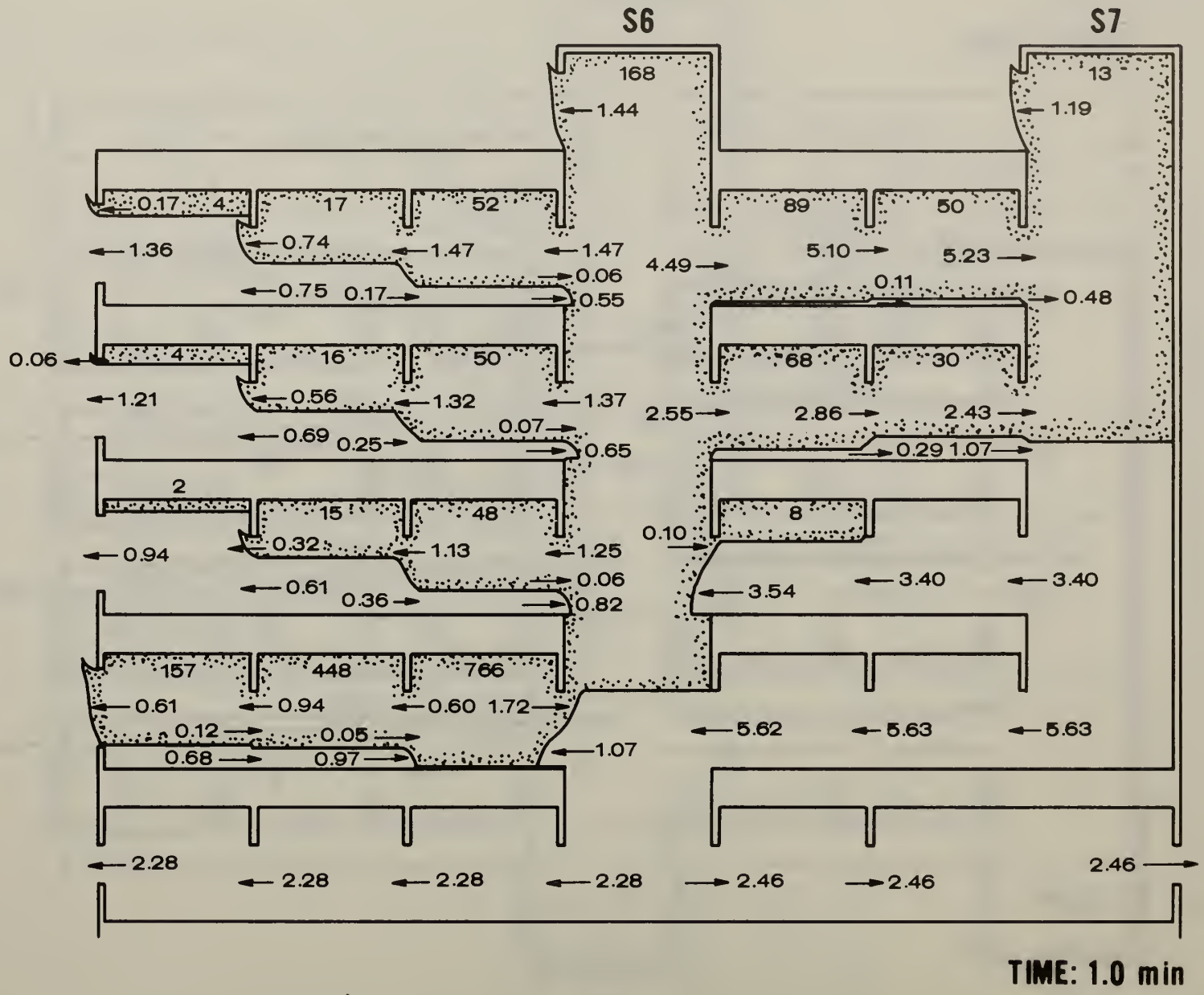

Fig. 7.7(c) cont'd

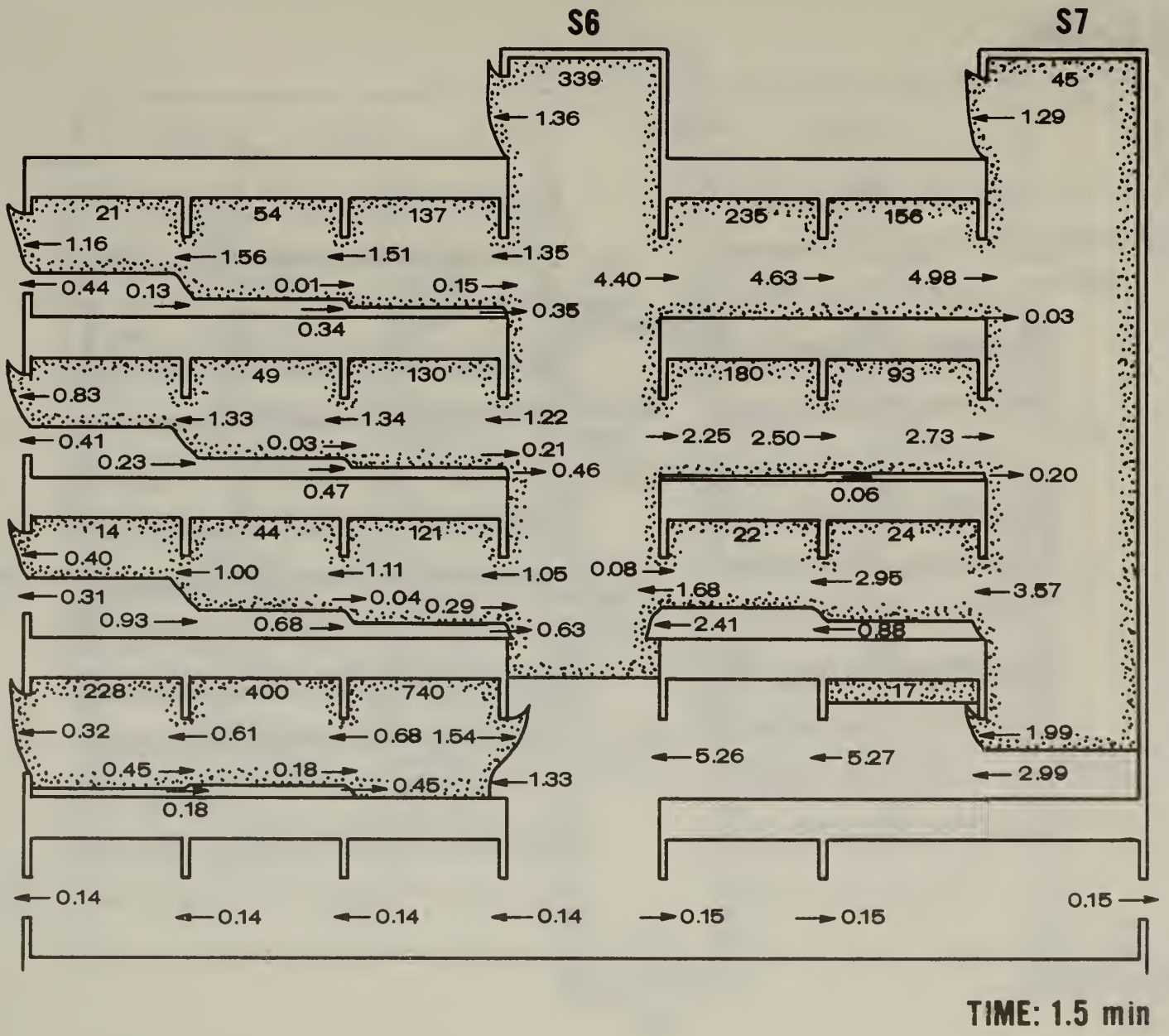

Fig. 7.7(c) cont'd

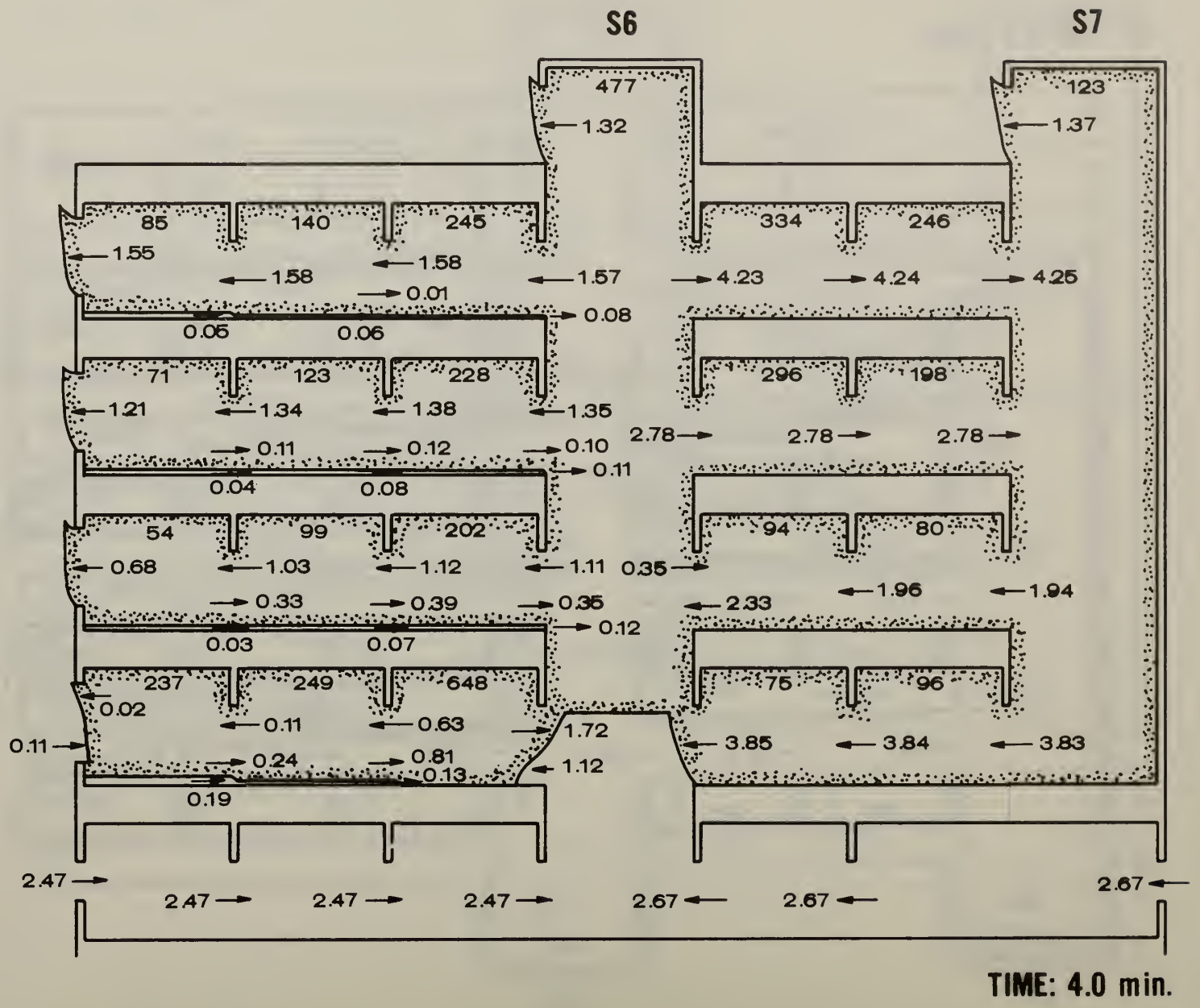

Fig. 7.7(c) cont'd

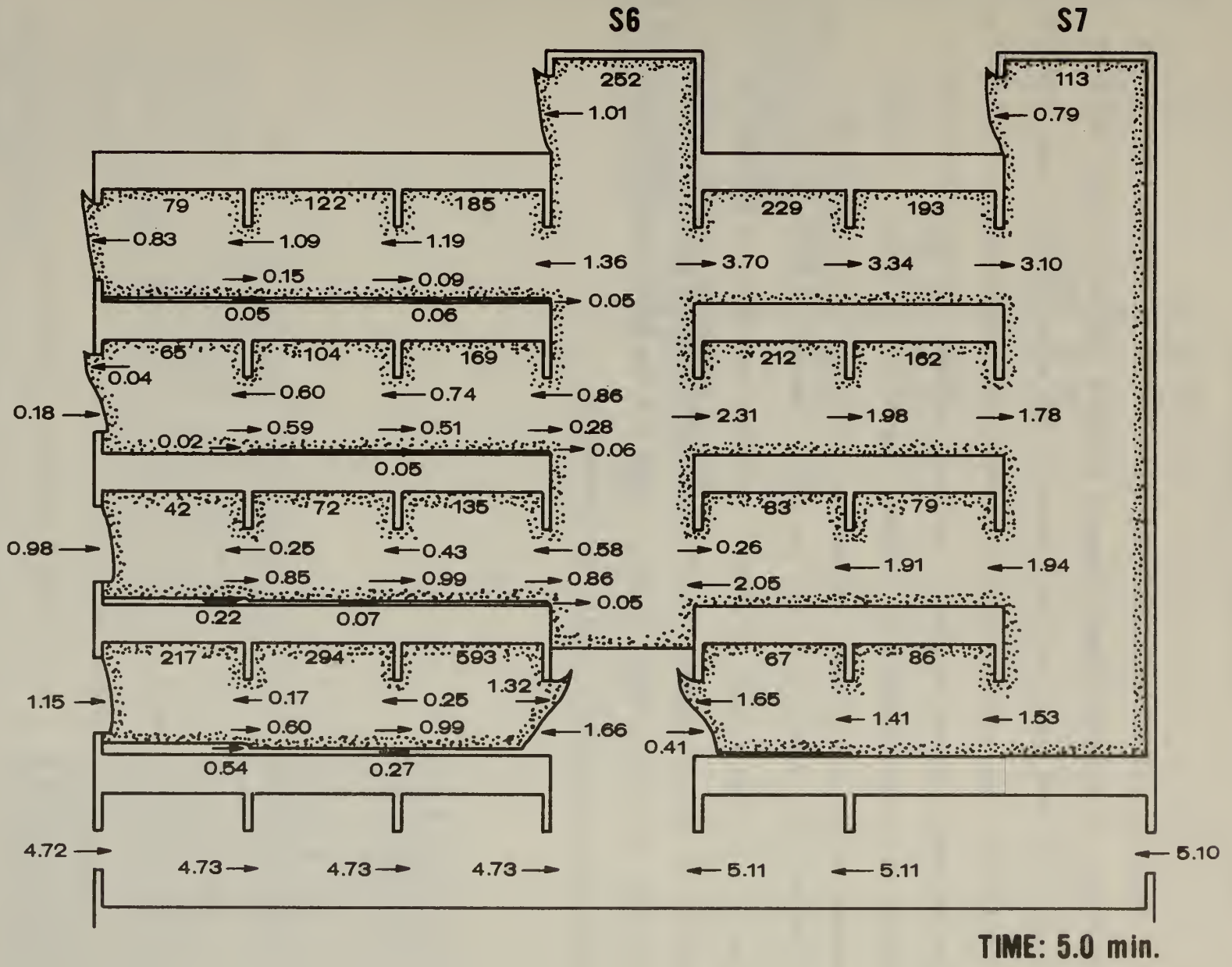

Fig. 7.7(c) cont'd

7.7 Sample 7 and 8: Fire in tall buildings (Figures 7.7 and 7.8)

These are the cases to which the present model is applied to very tall buildings. It has been almost commonly accepted that the hot gas, which is contaminated with smoke and toxic gases, is the major cause of human fatality in buidling fires, especially in the case of highrise buildings. Therefore, some reasonable method to predict the smoke movement will greatly help to develop the countermeasures to alleviate the hazard of smoke. Of course, several efforts are already underway for this purpose, for example by Wakamatsu [12], Tamura [13], and Klote [14], however, I believe this is the first attempt in which a two layer zone modeling approach is applied to tall buildings. By now there is no adequate experimental data by which the results shown in Fig. 7.7 and 7.8 can be validated, but it seems that the computed results are plausible.

Table 7.8

```
SAMPLE 8 : 10 STORY, FUEL RICH CASE
 300.
   10    1    2
    5  4.0
    1    5  4.0
BR(N)  4.0  4.0  4.0  4.0  4.0
DR(N)  6.0  6.0  6.0  6.0  6.0
HR(N)  3.0  3.0  3.0  3.0  3.0
BR(1)  4.0  4.0  4.0  4.0  8.0
DR(1)  6.0  6.0  6.0  6.0  6.0
HR(1)  3.5  3.5  3.5  3.5  3.5
BR(S)       4.0       4.0
DR(S)       6.0       6.0
HRST       42.5      42.5
HRSB        0.0       4.0
OPEN     1    2    1  1.0  2.0  0.0
         1    8    1  0.1  2.6  0.6
         2    3    1  1.0  2.0  0.0
         3    6    1  1.0  2.0  0.0
         4    5    1  1.0  2.0  0.0
         4    6    1  1.0  2.0  0.0
         5    7    1  1.0  2.0  0.0
       999
    1    1    2    1  1.0  2.0  0.0
    1    1    8    1  1.0  2.0  1.0
    1    2    3    1  1.0  2.0  0.0
    1    3    6    1  1.0  2.0  0.0
    1    4    5    1  1.0  2.0  0.0
    1    4    6    1  1.0  2.0  0.0
    1    5    9    1  1.0  2.0  1.0
   11    6    8    1  0.1  2.0  0.0
   11    7    8    1  0.1  2.0  0.0
  999
IPR,N    3    4    2    5    7    8    6
IRE,N    1    1    3    4    4    1    1
IPR,1    3    4    2    5    7    8    6
IRE,1    1    1    3    4    4    1    1
   10
 0.287E-03 0.287E-03 0.287E-03 0.287E-03 0.287E-03
 0.200E+00 0.200E+00 0.200E+00 0.200E+00 0.200E+00
 0.200E+04 0.200E+04 0.200E+04 0.200E+04 0.200E+04
 0.500E-01 0.500E-01 0.500E-01 0.500E-01 0.500E-01
 0.800E+00 0.800E+00 0.800E+00 0.800E+00 0.800E+00
 0.287E-03 0.287E-03 0.287E-03 0.287E-03 0.287E-03
 0.200E+00 0.200E+00 0.200E+00 0.200E+00 0.200E+00
 0.200E+04 0.200E+04 0.200E+04 0.200E+04 0.200E+04
 0.500E-01 0.500E-01 0.500E-01 0.500E-01 0.500E-01
 0.800E+00 0.800E+00 0.800E+00 0.800E+00 0.800E+00
 0.287E-03 0.287E-03 0.287E-03 0.287E-03 0.287E-03
 0.200E+00 0.200E+00 0.200E+00 0.200E+00 0.200E+00
 0.200E+04 0.200E+04 0.200E+04 0.200E+04 0.200E+04
 0.500E-01 0.500E-01 0.500E-01 0.500E-01 0.500E-01
 0.800E+00 0.800E+00 0.800E+00 0.800E+00 0.800E+00
 0.287E-03 0.287E-03 0.287E-03 0.287E-03 0.287E-03
 0.200E+00 0.200E+00 0.200E+00 0.200E+00 0.200E+00
0.200E+04 0.200E+04 0.200E+04 0.200E+04 0.200E+04
0.500E-01 0.500E-01 0.500E-01 0.500E-01 0.500E-01
0.800E+00 0.800E+00 0.800E+00 0.800E+00 0.800E+00
0.287E-03 0.287E-03
0.200E+00 0.200E+00
0.200E+04 0.200E+04
0.500E-01 0.500E-01
0.800E+00 0.800E+00
0.287E-03 0.287E-03
0.200E+00 0.200E+00
0.200E+04 0.200E+04
0.500E-01 0.500E-01
0.800E+00 0.800E+00
   2    4    1  60.    6
    .818      .182      .000      .000
  12027.      300.                 44.
    0.00      0.01      0.00      0.00
0.000E-03 300.0E-03 300.0E-03 300.0E-03 300.0E-03
0.000E-03
    0.00      0.00      0.00      0.00      0.00
    0.00
    0.00      0.00      0.00      0.00      0.00
    0.00
   2 300.
 0.0  0.0
 0.0  0.0  0.0  0.0
```

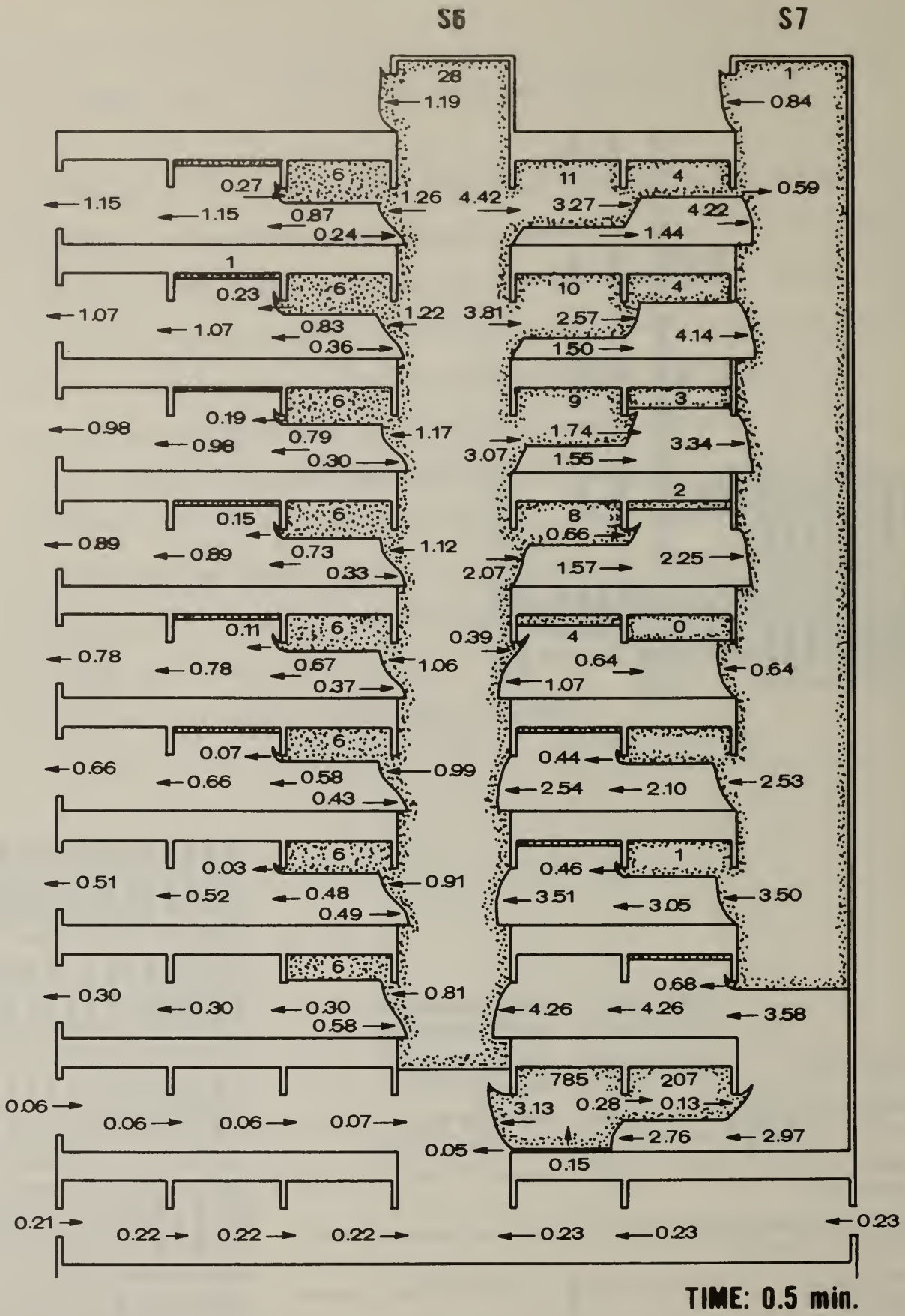

Fig. 7.8 Upper Layer and Flow Through Openings (Sample 8: Ten Story, fuel rich fire with narrow external openings) 0.5 - 4.5 min.

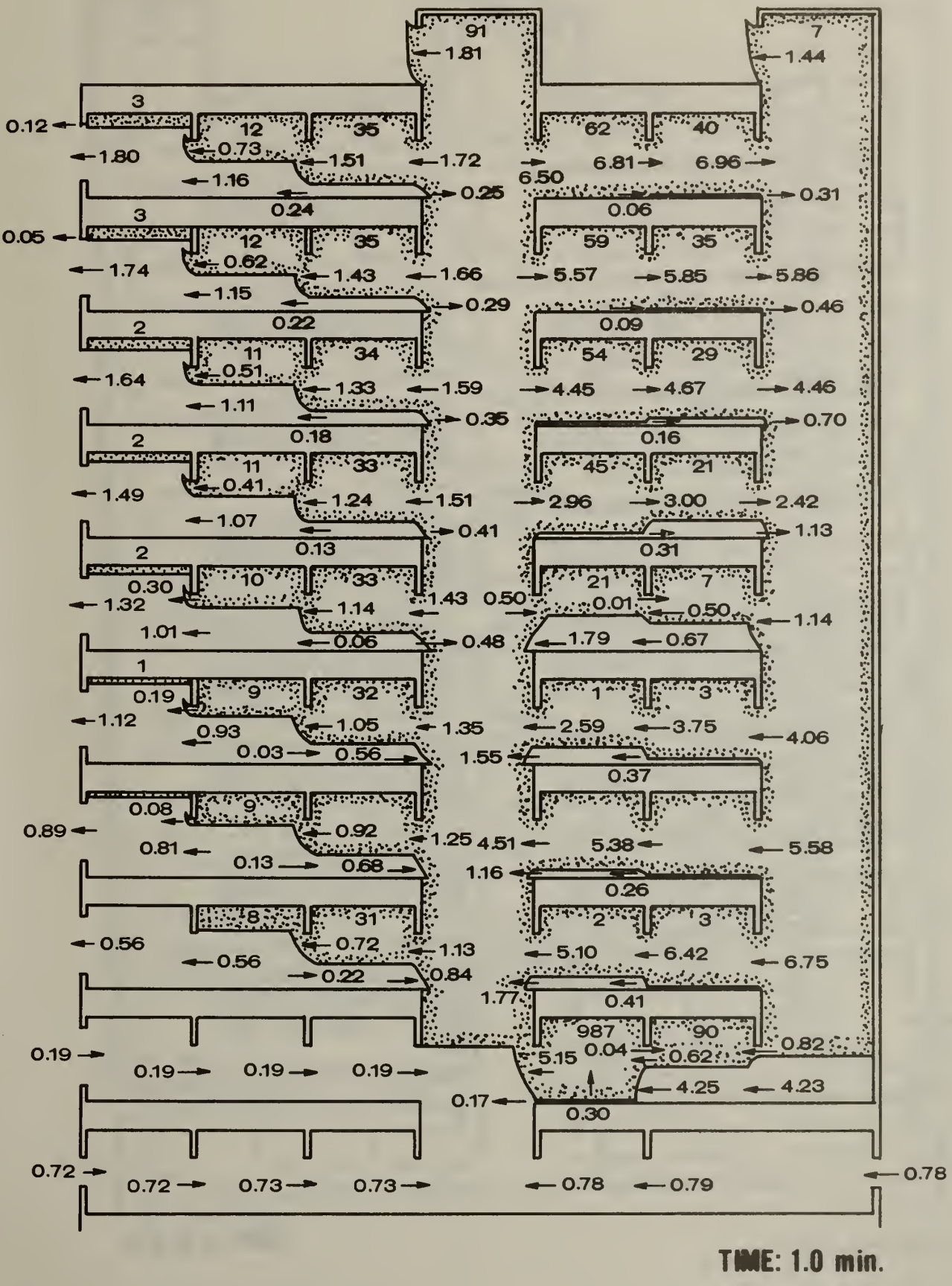
91
1.81
7
1.44
3
0.12
12
35
62
40
0.73
1.80
1.51
1.72
6.81
6.96
6.50
1.16
0.25
0.31
0.24
0.06
3
0.05
12
35
59
35
0.62
1.74
1.43
1.66
5.57
5.85
5.86
1.15
0.29
0.46
0.22
0.09
2
11
34
54
29
0.51
1.64
1.33
1.59
4.45
4.67
4.46
1.11
0.35
0.70
0.18
0.16
2
11
33
45
21
0.41
1.49
1.24
1.51
2.96
3.00
2.42
1.07
0.41
1.13
0.13
0.31
2
10
33
21
7
0.30
1.32
1.14
1.43
0.50
0.01
0.50
1.14
1.01
0.06
0.48
1.79
0.67
1
0.19
9
32
1
3
1.12
0.93
1.05
1.35
2.59
3.75
4.06
0.03
0.56
1.55
0.37
0.08
9
0.89
0.92
1.25
4.51
5.38
5.58
0.81
0.13
0.68
1.16
0.26
8
31
2
3
0.56
0.72
1.13
5.10
6.42
6.75
0.56
0.22
0.84
1.77
0.41
987
90
0.19
0.82
0.04
0.62
5.15
0.19
0.19
0.19
4.25
4.23
0.17
0.30
0.72
0.72
0.73
0.73
0.78
0.79
0.78
TIME: 1.0 min.

Fig. 7.8 cont'd

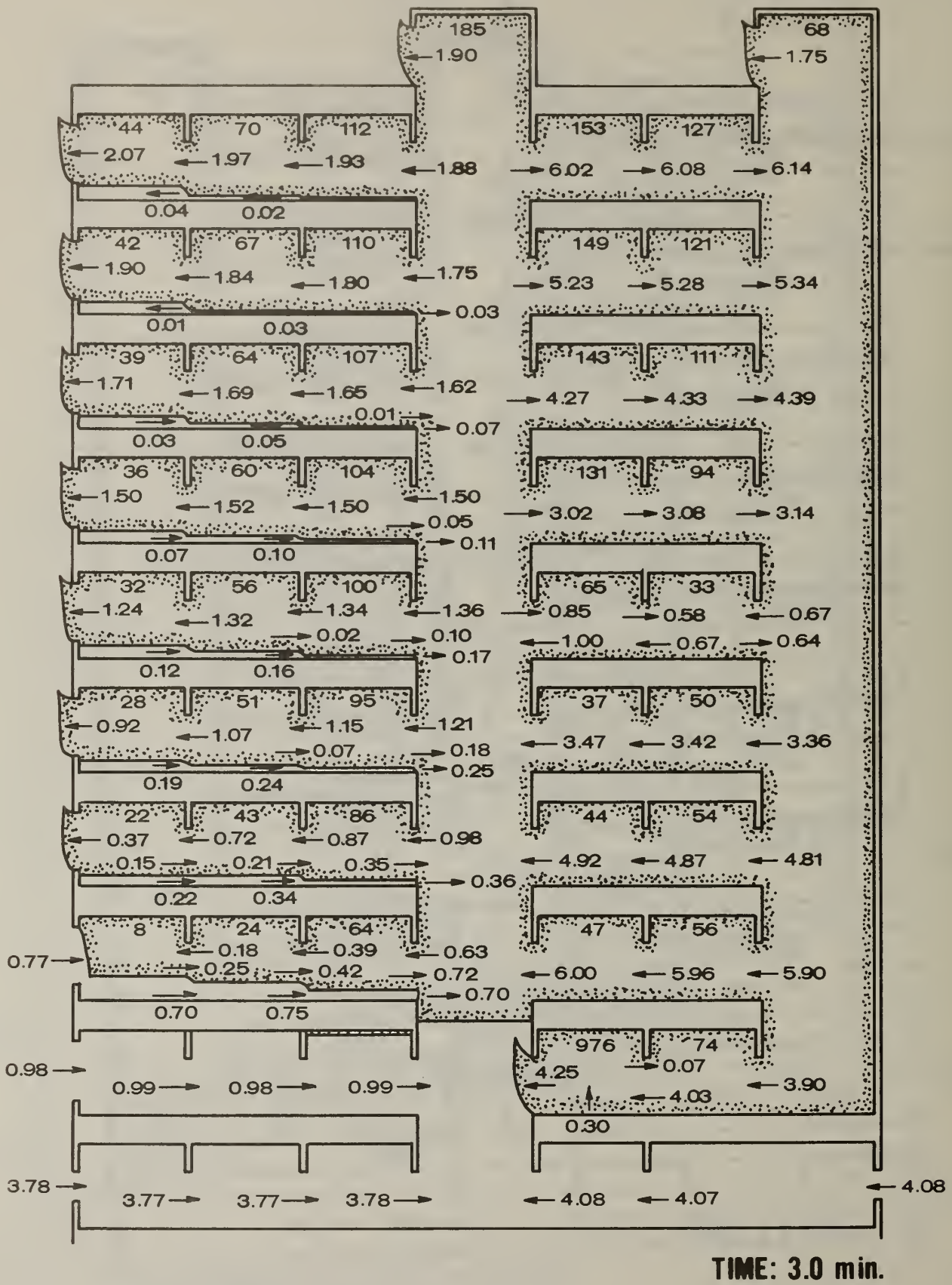
185
1.90
68
1.75
44 70 112
2.07 1.97 1.93 1.88
153 127
6.02 6.08 6.14
0.04 0.02
42 67 110
1.90 1.84 1.80 1.75
149 121
5.23 5.28 5.34
0.01 0.03 0.03
39 64 107
1.71 1.69 1.65 1.62
143 111
4.27 4.33 4.39
0.03 0.05 0.01 0.07
36 60 104
1.50 1.52 1.50 1.50
131 94
3.02 3.08 3.14
0.07 0.10 0.05 0.11
32 56 100
1.24 1.32 1.34 1.36
65 33
0.85 0.58 0.67
0.12 0.16 0.02 0.10 0.17
1.00 0.67 0.64
28 51 95
0.92 1.07 1.15 1.21
37 50
3.47 3.42 3.36
0.19 0.24 0.07 0.18 0.25
22 43 86
0.37 0.72 0.87 0.98
44 54
4.92 4.87 4.81
0.15 0.21 0.35
0.22 0.34 0.36
8 24 64
0.18 0.39 0.63
47 56
0.77
0.25 0.42 0.72
6.00 5.96 5.90
0.70 0.75 0.70
976 74
0.98
0.07
4.25
3.90
0.99 0.98 0.99
4.03
0.30
3.78
3.77 3.77 3.78
4.08 4.07
4.08
TIME: 3.0 min.

Fig. 7.8 cont'd

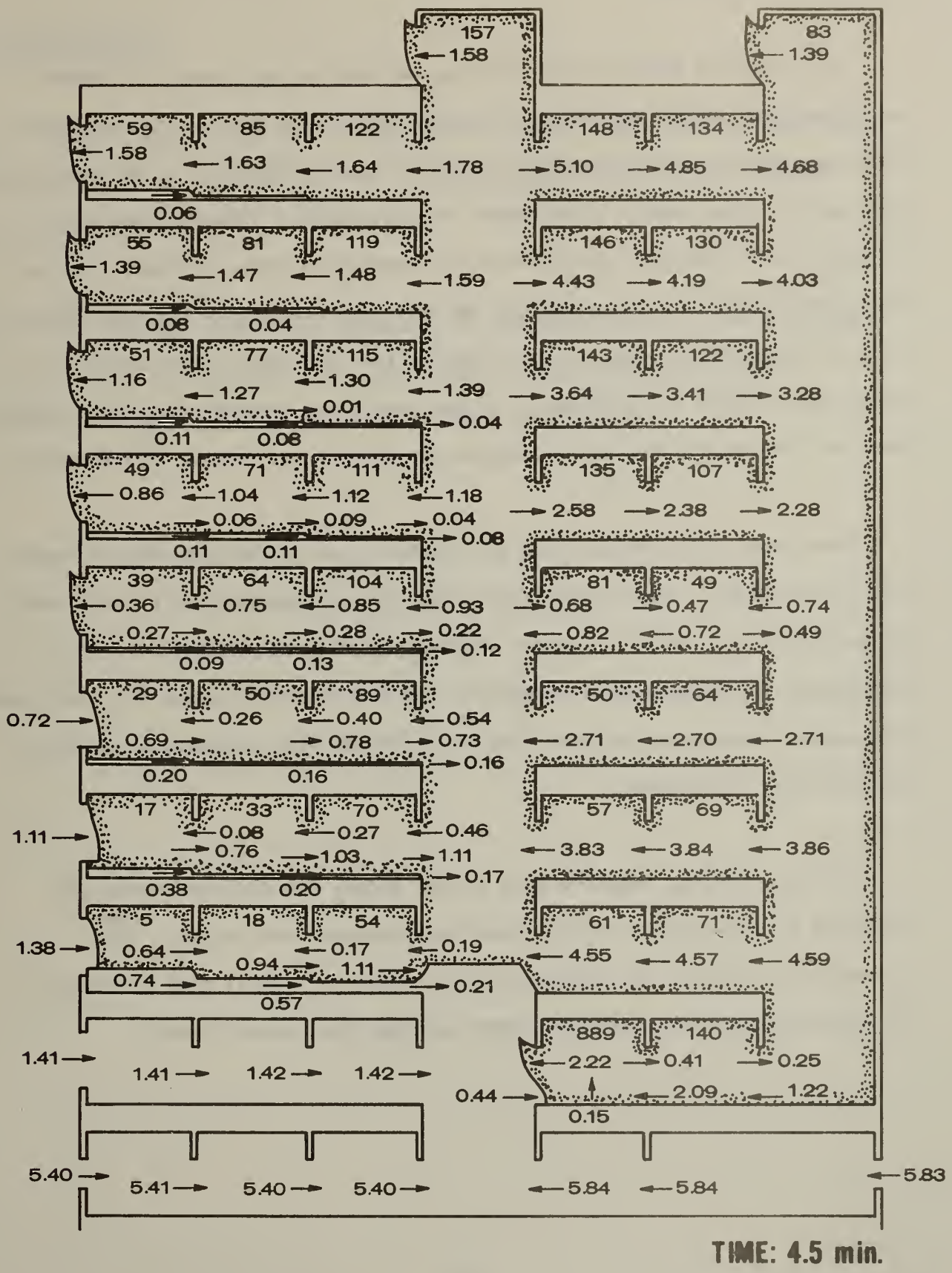
157
1.58
83
1.39
59
85
122
148
134
1.58
1.63
1.64
1.78
5.10
4.85
4.68
0.06
55
81
119
146
130
1.39
1.47
1.48
1.59
4.43
4.19
4.03
0.08
0.04
51
77
115
143
122
1.16
1.27
1.30
1.39
3.64
3.41
3.28
0.01
0.04
0.11
0.08
49
71
111
135
107
0.86
1.04
1.12
1.18
2.58
2.38
2.28
0.06
0.09
0.04
0.08
0.11
0.11
39
64
104
81
49
0.36
0.75
0.85
0.93
0.68
0.47
0.74
0.27
0.28
0.22
0.82
0.72
0.49
0.09
0.13
0.12
29
50
89
50
64
0.72
0.26
0.40
0.54
0.69
0.78
0.73
2.71
2.70
2.71
0.20
0.16
0.16
17
33
70
57
69
1.11
0.08
0.27
0.46
0.76
1.03
1.11
3.83
3.84
3.86
0.38
0.20
0.17
5
18
54
61
71
1.38
0.64
0.17
0.19
4.55
4.57
4.59
0.94
1.11
0.74
0.21
0.57
889
140
1.41
2.22
0.41
0.25
1.41
1.41
1.42
1.42
0.44
2.09
1.22
0.15
5.40
5.41
5.40
5.40
5.84
5.84
5.83
TIME: 4.5 min.

Fig. 7.8 cont'd

V. CONCLUDING REMARKS

The preceding model, which had been devised in an attempt to predict multiroom fire spread has advanced a step toward that goal. The refinements have been made so that excess fuel transport and combustion can be predicted. As a result, some sample calculations with large fuel inputs dramatically display predictions with characteristic temperature peaks for each room as excess fuel departs. These results may have been caused by the specification of an arbitrary fuel input rate, or may in fact be truely characteristic of actual fire growth in buildings. In any case, some properly designed experiments will be needed for the validation or further refinement of the model.

Some trial calculations were also made of the prediction smoke movement in tall buildings. The results seem to be fairly encouraging for utilizing the two layer zone model for smoke movement in highrise buildings. But substantial refinements must be made in the calculation schemes for this purpose. Eventually, ventilation effects need to be added, and experimental studies conducted for validation.

Finally, for any complete fire spread model, the fuel input must be predicted in the context of the local environmental conditions. The current model has not yet addressed this, and is a logical next step which can be developed consistent with other current fire growth models.

ACKNOWLEDGEMENT

I would like to express my gratitude to many people of the Center for Fire Research, at the National Bureau of Standards, who helped me work comfortably.

Also special thanks are addressed to the people of the Fire Modeling Group, headed by Quintiere, and some other people such as McCaffrey for much valuable advice, discussions and encouragement.

REFERENCES

[1] Quintiere, J.G. and McCafferey, B.J., "The Burning of Wood and Plastic Cribs in an Enclosure", Vol. 1, Nat. Bur. of Stand. (U.S.), NBSIR 80-2054 (1980).

[2] Rockett, J.A., "Modeling of NBS Mattress Tests with the Harvard Mark V Fire Simulation", Nat. Bur. of Stand. (U.S.), NBSIR 81-2440 (1982).

[3] Rehm, R.G. and Baum, H.R., "The Equation of Motion for Thermally Driven, Buoyant Flows", J. Res. Nat. Bur. of Stand., Vol. 83 (3), May-June (1978).

[4] Quintiere, J.G., "An Approach to Modeling Wall Fire Spread in a Room", Fire Safety Journal (3), (1981).

[5] Zukoski, E.E. and Kubota, T., "A Computer Model for Fluid Dynamic Aspects of a Transient Fire in a Two Room Structure", Daniel and Florence Gruggenheim Jet Propulsion Center, California Inst. of Tech., Jan. (1978).

[6] McCaffrey, B.J., "Momentum Implication for Buoyant Diffusion Flame", Vol. 52, Combustion and Flame Journal, 1983.

[7] Modak, A.T., "Radiation from Products of Combustion", Fire Research, 1 (1978/79).

[8] Mitler, H.E. and Emmons, H.W., "Documentation for CFC, the Fifth Harvard Computer Fire Code", NBS-GCR-81-344, (1981), National Bureau of Standards.

[9] Alpert, A.L., J. de Ris, et al., "Influence of Enclosure on Fire Growth Volume I: TEST DATA, Test 6: Window and No Doorway", FMRC Tech. Rep. No. OAOR2.BU-6, (1977).

[10] Tanaka, T., "A Model on Fire Spread in Small Scale Buildings", BRI Res. Paper No. 79 (1978), Building Research Institute (Japan).

[11] Tanaka, T., "A Model on Fire Spread in Small Scale Buildings (2nd Report)", BRI Res. Paper No. 84 (1980), Building Research Institute (Japan).

[12] Wakamatsu, T., "Calculation Methods for Predicting Smoke Movement in Building Fires and Designing Smoke Control System", Fire Standard and Safety, ASTM STP 614 (1977), Amer. Soc. of Testing and Materials.

[13] Yoshida, H., Shaw, C.Y. and Tamura, G.T., "A FORTRAN Program to Calculate Smoke Concentration in Multi-story Buildings", NRCC, DBR Computer Program No. 45 (1979), National Research Council (Canada)

[14] Klote, J. H., "A Computer Program for Analysis of Pressurized Stairwells and Pressurized Elevator Shafts", NBSIR 80-2157 (1980), Nat. Bur. of Standards.

NBS-114A (REV. 2-8C)

U.S. DEPT. OF COMM. **BIBLIOGRAPHIC DATA SHEET** *(See instructions)*	1. PUBLICATION OR REPORT NO. NBSIR 83- 2718	2. Performing Organ. Report No.	3. Publication Date July 1983

4. TITLE AND SUBTITLE

A Model of Multiroom Fire Spread

5. AUTHOR(S)

T. Tanaka

6. PERFORMING ORGANIZATION *(If joint or other than NBS, see instructions)*

NATIONAL BUREAU OF STANDARDS
DEPARTMENT OF COMMERCE
WASHINGTON, D.C. 20234

7. Contract/Grant No.

8. Type of Report & Period Covered

9. SPONSORING ORGANIZATION NAME AND COMPLETE ADDRESS *(Street, City, State, ZIP)*

10. SUPPLEMENTARY NOTES

☐ Document describes a computer program; SF-185, FIPS Software Summary, is attached.

11. ABSTRACT *(A 200-word or less factual summary of most significant information. If document includes a significant bibliography or literature survey, mention it here)*

Some refinements have been made on a multi-room fire spread model. The primary improvements are: (a) that a model on excess fuel burning in arbitrary room has been introduced; (b) that a model for the prediction of gas concentrations has been added; (c) that subroutine ABSORB, which was created by Modak, has been introduced to predict the upper layer emissivity; (d) that a new fire plume model developed by McCaffrey has been included to remove the inaccuracy and inplausibility of a vertical point heat source plume model; and (e) that the code has been revised so that it can deal with tall buildings with somewhat less computer memory size.

Also, some sample calculation results with the new code and a documentation of the code have been included.

12. KEY WORDS *(Six to twelve entries; alphabetical order; capitalize only proper names; and separate key words by semicolons)*

compartment fires; computer programs; fire models; fire plumes; fire spread; high rise buildings

13. AVAILABILITY

☒ Unlimited

☐ For Official Distribution. Do Not Release to NTIS

☐ Order From Superintendent of Documents, U.S. Government Printing Office, Washington, D.C. 20402.

☒ Order From National Technical Information Service (NTIS), Springfield, VA. 22161

14. NO. OF PRINTED PAGES 178

15. Price